Modeling the Behaviour of New Zealand Steel Connections in Fire

Submitted By

Hao Yang (Raymond) Qiu

Supervised by:

Dr Anthony K. Abu

Associate Professor G. Charles Clifton

This thesis is submitted in partial fulfillment of the requirements for the degree of Master of Engineering in Fire Engineering

Department of Civil and Natural Resources Engineering
University of Canterbury
Private Bag 4800
Christchurch, New Zealand

Abstract

The performance of steel connections are critical in the overall survivability of a building in the event of a fire, as highlighted by previous accidental fires in multistorey buildings and also by large scale tests. Although studies on the behavior of steel connections have been conducted overseas, particularly in Europe and the U.K., a lack of understanding on the behavior of New Zealand connections currently exists. At present, the New Zealand connections are expected to perform better in fire conditions than their European equivalents due to their design for ductility in severe earthquakes.

The researched reported herein investigates this assumption through the use of the non-linear finite element analysis, using a software called ABAQUS. The analytical packages within the program were firstly explored and validated through modelling of previously conducted experimental tests, in particular an isolated web side plate (also known as fin plate) connection and a flexible endplate connection.

Following the modelling of previously conducted experimental tests, one of the connections of the large scale test at the Cardington laboratories in 2001 was redesigned using flexible endplate and web side plate connections in accordance with current design recommendations from New Zealand and the U.K. The behavior of these connections were then analyzed and compared to determine their differences in performance.

The finite element models of the designed flexible endplate connections indicate although that they are both able to largely maintain structural integrity when exposed to extreme fire conditions, the New Zealand design performed comparatively better as a result of its increased ductility provisions through the differences in detailing.

On the other hand, the web side plate connections designed using the recommendations of the New Zealand and U.K. design guides resulted in largely similar designs. Based on this, the performance between the two web side plate connections are expected to be largely similar in an event of a fire.

Acknowledgements

I would like to express my most sincere gratitude to my supervisors, Dr. Anthony Abu and Associate Professor G. Charles Clifton for their encouragement, guidance and countless hours of support during this study. Their passion and insight in structural fire engineering have played a significant role in helping me undertake this research within the allocated timeframe for which I am truly grateful. Being able to have them as supervisors has been a privilege.

I would like to extend my gratitude to Kinglsey Ukanwa for his invaluable help with the use of the finite element software ABAQUS at the initial stages of my study which was instrumental in the development of the models presented herein.

A special thanks to the Department of Civil Engineering at the University of Canterbury which has provided me with a suitable environment to carry out this research. In particular, I would like to acknowledge Olive Dalton and Leigh Davidson for their endless commitment to helping students such as myself with the set-up of computer systems and administrative tasks.

I would like to thank Fire and Emergency NZ, Arup, SFPE and Olsson Fire and Risk for their financial support throughout my Master's degree, and their continued support of the Fire Engineering program at the University of Canterbury.

Finally, I would like to thank my parents, brother, and friends for their patience, encouragement, and support without which this study would not be possible. They have been my inspiration to undertake my Masters' degree, and I dedicate this work to them.

Table of Contents

List of Figures

List of Tables

1 Introduction

1.1 Background

Due to having structural properties including high strength and ductility, steel is widely accepted as a globally popular construction material for high rise buildings. Compared to concrete, steel has significant advantages such as quicker erection time, long spans, adaptability, and is generally more aesthetically pleasing (Al-Jabri, 1999). However the structural properties of steel are highly affected by exposure to fire which causes a reduction in strength and stiffness, leading to deformation and potential collapse (Buchanan and Abu, 2017). This phenomenon has resulted in a need to understand the behaviour of structural steel elements, providing the motivation of research into this particular field which began in the late nineteenth century (Lin, 2014). At that time, research was focused on inventing new methods and materials which could be used to protect steel members from fire in order to delay its rise in temperature and decrease in strength for particular periods of time. This led to the development of different forms of applied steel protection including the use of: concrete encasement, gypsum boards, sprayed concrete and intumescent paint (Buchanan and Abu, 2017). Although these protection methods have proven to be effective against fire, they often neutralize the advantages of steel construction as they have been reported to increase construction costs by up to 30% (El-Rimawi, 1989) as well as causing time delays due to their installation (Dowling, 1997). More significantly, some aspects of the unprotected structure such as the composite floor systems may have high inherent resistance to fire and need not to be protected.

To combat the negative aspects of using protection materials, the recent approach for structural fire engineering design in buildings has been to design as many unprotected structural steel members as possible to be able to withstand loads under both ambient and elevated temperatures,

rather than protecting all exposed steel members which would typically have only been designed for ambient temperature loads. As a result, steel framed buildings are commonly designed to comprise of a mix between protected and unprotected members, decreasing the costs associated with applying the necessary protection mechanisms to steel by approximately half since the early 1980's (Robinson, 1998). To accommodate this approach effectively, a deeper understanding of the behaviour and strength limits of steel is required, expediting the research and development of new methods for engineering analysis and design of steel members in fire. To date, although the current knowledge on the performance of steel framing members in fire is well documented for Standard Fire test conditions and reasonably well documented for performance in a structural system, there has been much less research into the performance of steel connections in fire.

The historic lack of research in the field of the performance of connections in fire may be a result of its relative complexity and the assumption that that current connection designs are robust enough to withstand elevated temperatures, due to the consideration that they are fixed and are only designed to withstand comparatively simple bending and shear forces (Wang et al., 2010). Another significant reason lies in the Standard Fire Testing basis of establishing structural element performance; these tests cover beams, columns and walls but not connections. However, the importance of understanding the performance of steel connections in fire was demonstrated through the observed damage of the Broadgate Phase 8 fire and the structural collapse of the World Trade Center disaster (WTC 1), where it was exemplified that the ability of the connections in redistributing forces has a large impact on the survival duration of the overall structure in fire conditions (Al-Jabri, 1999; Steel Construction Institute, 1991). This was contradictory to the earlier belief that steel connections need not be considered in structural fire design due to an

expectation of their ability to sustain structural integrity under elevated temperature conditions, resulting in research being undertaken in order to better understand the phenomenon.

Although some research has been conducted in recent years to better understand the performance of beam-to-column connections in fire, the studies undertaken on this topic have been undertaken in areas of low seismic activity – namely in Europe and the United Kingdom. Thus, the studies focus on steel connections designed and detailed to resist moment, shear, and axial forces which were not required to be designed to structurally sustain earthquake-induced loading in accordance with the local structural design standards (Booth et al., 1998). In New Zealand, steel beam-to-column connections are designed and detailed to be able to resist seismic loads due to earthquakes as required by local structural design standards (New Zealand Standards Institute, 1997).

Based on this, it is expected that the design and detailing of connections to resist seismic forces leads to an improved robustness in fire conditions. However, it is currently unknown at this stage whether the New Zealand connections are able to perform sufficiently in a real fire due to the current lack of research surrounding this particular topic. In accordance with the current steel structures standard, NZS3404 (New Zealand Standards Institute, 1997), there is a lack of guidance for the specific design of steel connections in fire, where Clause 11.10.1.1 attempts to addresses this by stating that connections are to be protected with the maximum thickness of fire protection material used for other members in the frame. Although this method will be for use in limiting the temperature of the components in the connection, it does not account of the effects of additional rotation as well as tension and compression forces which are applied as a result of the expansion and contraction of connecting members during a fire as explained in Section 2 of this study. As a result, this highlights the lack of guidance on the structural fire design for connections in current New Zealand design approaches.

This study examines the viability of current New Zealand design standards for simple steel connections through modelling their performance in fire conditions using the Finite-Element-Modelling software ABAQUS. In particular, the study examines the performance of New Zealand web side plate connections and flexible end plate connections - otherwise known as fin plate and partial depth endplate connections in the U.K., due to their common use and differences in withstanding forces induced by shear and moment.

Therefore, the research described herein is intended to provide information and knowledge about the performance of these connections in fire and will be the first step in developing a distinct new area of research in New Zealand on steel connections in fire which will ultimately provide specific design provisions for these connections in fire conditions.

1.2 Behaviour of Steel Connections in Fires

In the Broadgate Phase 8 incident on June 23rd 1990, a major fire occurred on the ground floor of a 14th storey building during its final stages of construction, causing structural damage to the steel frame (Al-Jabri, 1999). Despite the steel beams and connections being protected by intumescent paint, two steel flexible end plate connections above the fire failed as a result of tensile forces exerted by the connecting beam upon cooling, where two bolts fractured in one connection while the end plate fractured in the other. The failure modes encompassing fracture of the endplate were also observed in the Cardington fire tests shown in Figure 1-1.

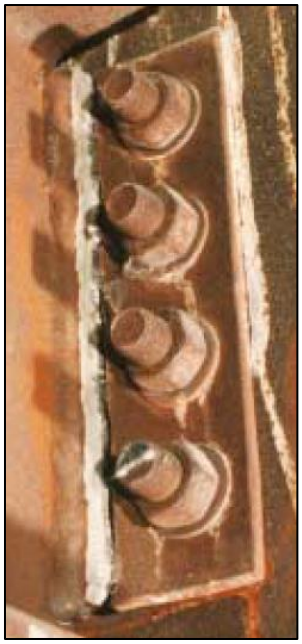

Figure 1-1 Fracture of an end plate in the Cardington test (Al-Jabri, 1999)

On the other hand, the World Trade Center 5 (WTC 5) was a 9-storey office and retail building which experienced structural collapse as a result of failure due to fire conditions. The incident occurred on September 11, 2001 in New York City, where the 9-storey office and retail building was subjected to a fire caused by flaming debris falling from WTC 1, ultimately causing it to undergo a progressive collapse from the 8th floor to the 4th floor (LaMalva, 2007). As opposed to the connections in the Broadgate Phase 8 incident which failed during cooling, it was determined that plate connections in WTC 5 were reported to have failed during the heating phase where stresses caused by thermal expansion and deflection of connecting girders causes them to deflect and place large amounts of stress onto the top bolt holes in a central beam to girder connection (LaMalva, 2007). Approximately two hours after the fire started, the top bolts ruptured under the increased stress and failed as a result, leading to progressive collapse of the building. A recovered connection sample and the locations of connection failure from the incident are shown in Figure 1-2 and Figure 1-3 respectively.

Figure 1-2 Recovered connection sample from WTC5 (LaMalva, 2007)

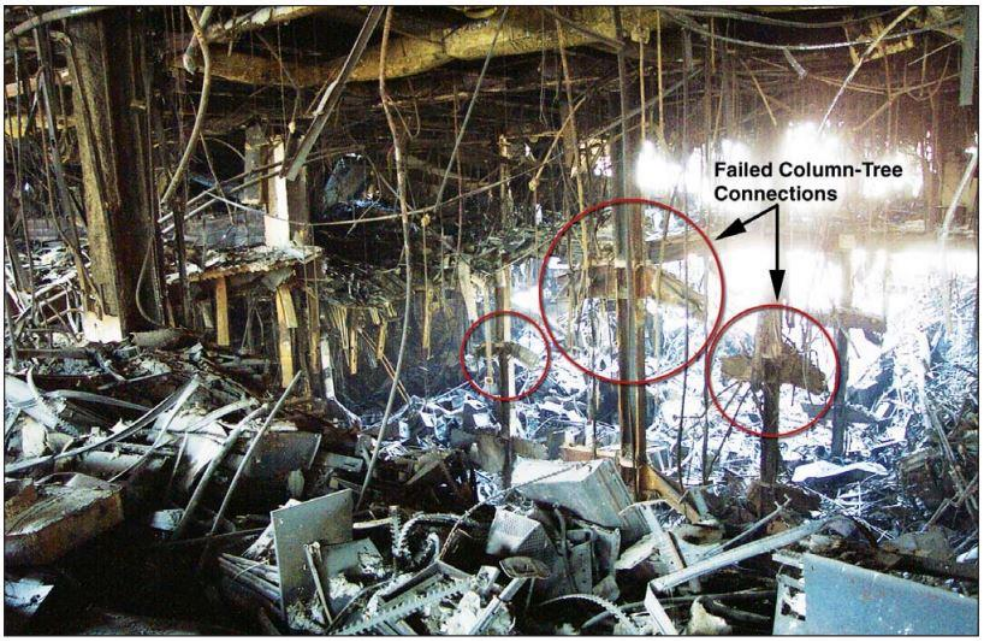

Figure 1-3 Failed connections in WTC5 (FEMA, 2002)

Similarly, World Trade Centre 7 (WTC 7) – a 47 story office building adjacent to the main World Trade Center complex had also undergone structural collapse due to fire conditions on September 11, 2001 in New York City. In WTC 7, fires ignited on over 10 floors in the building by falling

debris from WTC, with fires in the lower floors (7 to 9 and 11 to 13) burning out of control due to failure in the water supply for the automatic sprinkler system that was installed in the building, eventually leading to collapse approximately 7 hours after the collapse of the neighboring WTC 1 (NIST, 2008). From the investigation undertaken by NIST, it was reported that the collapse sequence of the structural frame was initiated as a result of the thermal expansion of steel beams and girders. Due to extended spans of heated 15 m beams on the north and east sides of the structure, they experienced considerably large thermal elongations and axial compressive forces, the simple shear connection used between a column and key girder on the 13th floor failed, which, along with other structural components damaged by the fire led to the collapse of the 13th floor – subsequently leading to the progressive collapse of floors below until the 5th floor (NIST, 2008). Consequentially, the collapse of the floors resulted in the column being unsupported laterally which eventually buckled and led to the global collapse of the structure. Thus, given the danger of steel connections failing in fire scenarios, it is important to be able to understand the behaviour of such connections under elevated temperatures in order to develop design methods and models which can be used in structural design for fire exposure.

However, accounts of steel connections performing substantially well in fire have been observed in real instances. This is exemplified by the Broadgate Phase 8 fire involving unprotected steel beams with composite steel deck/concrete floor, where despite columns being shortened up to 100 mm due to plastic deformation, as well as the floor deflecting up to 600 mm, structural integrity was able to be maintained throughout the heating and cooling phases (SCI, 1991). Similarly in the 1991 Churchill Plaza fire, a steel frame protected with a 90 minute fire resistance rating supporting composite steel and concrete flooring was exposed to a fire for a sufficient period before being extinguished by the building's sprinkler system, where it was reported that the structure was able

to sustain loads up to 50% greater than the design as a result of tensile membrane action. Overall, these events demonstrate the lack of a full understanding of the behaviour of steel connections under elevated temperatures which currently exists, as the notation of their observed behaviour in real fires has provided a large range of possibilities.

1.3 Objectives

The proposed research project described herein will aim to provide knowledge on the behaviour of common New Zealand steel connections in fires and address the lack of guidance on their design. As a result of this work, the following information will be provided to practicing structural fire engineers in New Zealand:

- A deeper understanding of the behaviour of common steel connections in fire during both the heating and cooling phases
- Assessment of the performance of commonly used New Zealand steel connections under elevated temperatures. As steel connections in New Zealand are designed to be ductile to withstand seismic loading in accordance with NZS3404, this research will aim to determine how they perform under elevated temperatures
- A set of finite element models for common steel connections

This work will ultimately aim to assess the current state of guidance for the design of steel connections under elevated temperatures and recommend ways in which it can be improved for robustness, as well as detail methods in which component models may be used for structural fire analysis.

2 Literature Review

In accordance with local and international guidelines for the structural requirements of buildings (IStructE, 2002; MBIE, 2016), buildings are designed to ensure safety of occupants against structural failure as a result of loads that are likely to be experienced throughout their lifetime, including those from disasters such as earthquakes and fires. Hence, buildings are required to be designed against catastrophes due to failure of connections in fire such as the progressive collapse mechanism which occurred in the WTC5 and WTC7 incidents, as discussed in Chapter 1. The term *progressive collapse* is defined by the occurrence of large scale failure of components within a structure as a consequence of failure in local components (Starossek, 2007). This is exemplified by the danger caused by structural steel being heated in fires due to its property of high thermal conductivity and loss of strength with increasing temperatures. This will impose significant demands on the connections, with these demands differing between the heating and the cooling phases. The loss of strength in the connection may lead to the supported floor collapsing onto the structural components below, inducing sudden dynamic loads and potentially causing the failure of floors below.

With traditional steel structural fire safety design in which steel is protected against elevated temperatures by the coverage of all exposed steel beams and columns with materials, there is a lack of quantifiable guidance on the protection of steel beam-to-column connections based on the belief that protected connections would conduct less heat due to having comparatively large masses of steel relative to that of connecting members (Block, 2006) and the lack of suitable fire testing facilities for connection testing. This approach is effective in limiting the temperature increase in the protected components and hence the temperature induced member deformations, however the deformations that still occur are sufficient to generate considerable additional axial

and tensile forces in the connections as well as local plastic buckling of beams and columns as a result of thermal expansion/contraction of the connecting members (Wang et. al, 2012). The application of these forces may induce supplementary moments to the connection, even in simple shear connections which are initially designed as hinges. Figure 2-1 highlights how these additional forces may occur, where it can be seen that initially compressive forces develop in the connecting beam due to thermal expansion, and this force is transferred to the connecting column through the connection assembly and also through contact of the bottom flange of the beam due to increased rotation. Upon additional heating, the beam may undergo buckling and catenary action which leads to tensile forces acting on the connection (Wang et al., 2010). Additional tensile forces then form upon cooling of the beam due to contraction of the heated element.

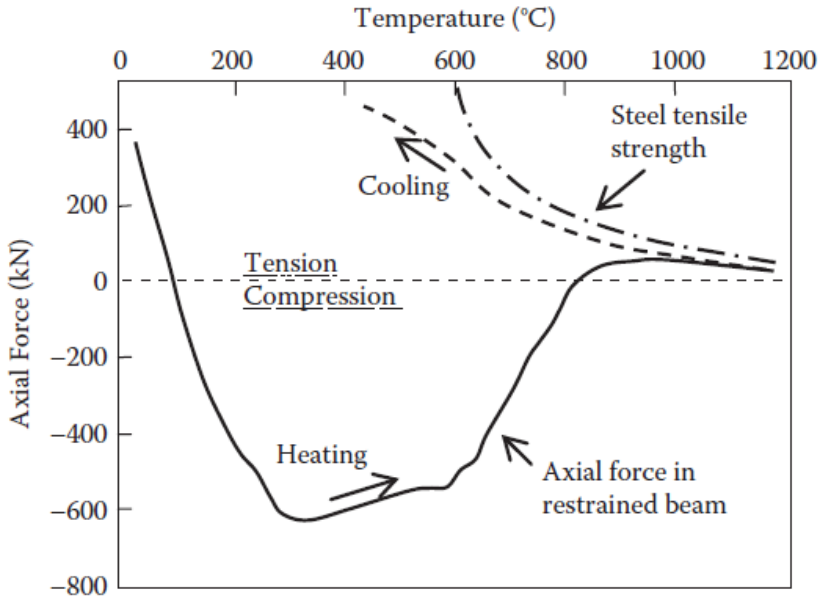

Figure 2-1 Axial force in axially restrained composite beam (Wang et al., 2012)

The current fire engineering design approach for connections does not require these additional forces to be considered and this can lead to localized complete connection failure as seen in the World Trade Center Collapse. Furthermore, the properties of the components within steel

connections under elevated temperatures must also be understood as they weaken under the influence of fire induced heating at different rates to the structural steel members. Nonetheless, in order to study the performance of connection behaviour in fire, it is important to first understand the philosophies supporting their design.

2.1 Design of Steel Connections in New Zealand

Connections play a very significant role in providing building stability and integrity for structural frames during ambient and elevated temperatures. As defined by Eurocode 3 and NZS 3404, a connection is a location at which two or more elements meet and is required to be capable of transmitting design action effects including ductility demands (eg from severe earthquake or severe fire). In both standards, steel connections can be classified into one of three forms: rigid, semi-rigid or simple, depending on the requirements of the structure. Traditionally, connections are designed to be either rigid or simple, where rigid connections are designed to transfer the full moment of the beam end into the column as a result of a high rotational stiffness and therefore the angles between members remains unchanged up to the attainment of the capacity of the weakest connecting member, while simple connections transfer shear and axial forces, with negligible rotational stiffness (Feeney and Clifton, 1995) limiting the moments generated.. The classification of semi-rigid connections lies between the two extremes and is designed to provide a limited rotational stiffness under the design loading.

As simple connections provide a number of benefits over semi-rigid or rigid connections, including lower fabrication and erection costs, they are more commonly used in practice (Hu, 2009), and have therefore been chosen as the focus of this study. In particular, two simple connection designs – web side plates and flexible endplates - have been outlined based on the availability of comparable experimental data of the connections under elevated temperatures, and their

widespread use throughout- the two regions. While the behaviour of connections designed to European standards have been examined in previous studies (Dai et al, 2010; Hu, 2009; Selamet and Garlock, 2014; Yu et al, 2009a; Yu et. al, 2008) a lack of understanding of the fire performance of connections designed to New Zealand standards and detailing requirements currently exists. Although the simple connections designed to the two standards are similar based on appearance, there are significant differences in detailing due to differences in the grade of materials and demand capacity requirements between the regions which may influence the connection behaviour under elevated temperatures as a result.

2.1.1 New Zealand Design Philosophy

Geographically, New Zealand is situated on a plate boundary between the India-Australian plate and the Pacific plate. This plate boundary includes the Alpine Fault, with over 800 kilometers of measured fault movement making it the largest known fault displacement worldwide. Many parts of New Zealand are subjected to high seismic demands and seismic design and detailing requirements to accommodate the deformation demands. These underpin connection design and detailing requirements as a result (Robinson, 2014) . Notably, the destruction of buildings as a result of the M7.8 Hawke's Bay earthquake in 1931 first highlighted the need for buildings to be able to sustain lateral forces and dissipate energy in earthquakes (Ingham and Griffith, 2011). In response to the Hawke's bay earthquake, the New Zealand Standards Institute published a by-law (NZSS No. 95), which requires buildings to be designed to be able to sustain a horizontal acceleration of 0.1g, and includes a suggestion that buildings used as spaces for public gatherings should be constructed using steel or reinforced concrete (New Zealand Standards Institute, 1935). It was not until 1965, then 1976 where research was incorporated into the national design standard

(NZS 4203) and in major advancement to allow seismic design with other materials, including timber and reinforced masonry (New Zealand Standards Institute, 1976).

Due to the increased use of steel in New Zealand, significant research and design documents for the material have undergone rapid development in recent years, most notably the first publication of NZS3404 - Steel Structures Standard in 1989 (New Zealand Standards Institute, 1989) and design guides by HERA (Heavy Engineering Research Association) (Clifton, 1994; Feeney and Clifton, 1995). These documents include applications and principles of the developments in research to date at the time, in turn recognizing the importance of the design and detailing of steel connections in order to resist seismic forces. As a basis of comparison, following the observations of the extensively damaged steel beam-to-column moment resisting connections caused by the 1994 Northridge earthquake in California (Sabol and Engelhardt, 1994), Clifton (1995) conducted a study to determine the effectiveness of the New Zealand design procedures of steel connections. Clifton (1995) created a model of the connection using standard New Zealand design procedures and determined that the beam flange to column flange failure modes of the American connection are able to be dependably suppressed by the New Zealand connection as a result of differences in steel strength and design for ductility (Feeney and Clifton, 1995).

The most recent documentation for the design principles of structural steel is outlined in the latest revision of NZS3404 (New Zealand Standards Institute, 1997), with an adherence to the Steel Connect design guidance documents developed by Steel Construction New Zealand as design guide - formulated to increase the robustness steel connections (SCNZ, 2008a, 2008b). These documents bring updated and improved design philosophies to the design of New Zealand connections by incorporating the requirement of increased ductility and strength capacity in

comparison with their overseas counterparts, with the major differences arising from the focus in their ability to sustain earthquake induced forces.

In the later revisions of the New Zealand Standards, beam-to-column connections are required to be designed and detailed in accordance with pre-determined overstrength factors for moment and shear capacities of the connecting beam, as documented in NZS 3404. This requirement is to ensure that the ductility of the structural frame can be realized through the formation of plastic hinges in the connecting beam prior to the failure of the connection which may result in catastrophic failure of the overall structure (Feeney and Clifton, 1995). Additionally, the minimum yield strength of steel used for connections in New Zealand has been increased to 300 MPa, compared to the lower grade steels used in Europe, with the UK often using steel with the minimum yield strength of 275 MPa. Hence, as a result of the increased capacity of New Zealand connections designed against seismic forces, it is expected that they have a higher inherent resistance to the effects of elevated temperatures despite the lack of research to date.

2.2 Design of New Zealand Connections in Fire

Traditionally in New Zealand, there has been no specific guidance on the design of connections in fire. The conventional approach has been to determine the temperatures at the connection using simple calculation methods, then to subsequently calculate the capacity of each component in the connection based on reduced strengths. On the contrary, in local practice, the current version of the New Zealand standard for structural steel conservatively requires the steel connection to be fire rated to at least the equivalent level of fire rating applied to the connecting elements. However as previously discussed, simply fire rating the connection or calculating the residual capacities of each component does not take into account the additional forces which occur as a result of thermal effects such as expansion and catenary action of the connecting beam.

In recent times, New Zealand standards have begun to progressively recognize and utilize the design methodologies adopted by the Eurocodes inclusion of modern research. Particularly, the new revision for the Composite Structures Standard – AS/NZS 2327 (New Zealand Standards Institute, 2017) incorporates the use of the "Component Method" for the design of connections at ambient temperatures. The component method allows for a relatively simple approach in predicting the stiffness and resistance of connections by modelling the joint as an accumulation of its components. The Component Method has also been developed for steel connections to be used in fire scenarios, and has proven to be able to recreate results determined from experimental testing provided that the stiffness and properties of the components are determined accurately (Block, 2006b; Simões da Silva et. al, 2001; Spyrou, 2002; Yu et al., 2009). Although the component method has been developed to show credible results under elevated temperatures, is has not been validated for use on New Zealand connection designs due to the lack of available experimental data. Therefore, the research conducted herein aims to provide some information in terms of better understanding the performance and differences in New Zealand connections in comparison with those used abroad. However, to understand the performance of New Zealand connections in fire, it is important to first understand the basic properties of steel under the influence of elevated temperatures.

2.3 Properties of Steel at Elevated Temperature

The structural properties of steel at elevated temperatures have been extensively studied in recent years as this knowledge is fundamental to fire engineering design. Steel undergoes a significant decrease in stiffness and strength with increasing temperatures, which may ultimately lead to structural failure due to excessive levels of deflection depending on the application of loads (Sarraj, 2007).

The strength properties of steel are defined by stress strain relationships, with typical ambient temperature behaviour of steel being well established. However upon heating, the stress strain relationship changes significantly depending on the temperature. Different elevated temperature mechanical properties have been considered by different countries in the past, although this is now becoming more standardised on the Eurocode specified mechanical properties.

2.3.1 Eurocode 3: Part 1-2 and BS 5950 Part 8

The properties of structural steel adopted in EN 1993-1-2: Structural Fire Design (European Committee for Standardization, 2005a) and BS 5950 Part 8: Code of practice for fire resistant design (British Standards Institution, 2003) are largely based on the experimental studies conducted by Kirby and Preston (1988). Their experiments consisted of determining the properties of European carbon steels under transient testing of increasing temperatures with grades 43A and 50B - possessing yield strengths of 275N/mm^2 and 355N/mm^2 respectively, correlating to grades S275 and S355. In their tests, the steel specimens were held under constant loads while temperatures were increased under rates of 2.5, 5, 10 and 20^{o}C/min from temperatures of 20^{o}C to 900^{o}C. From the results generated by the experimental tests, appropriate stress strain curves were developed over varying temperatures for the purpose of structural fire engineering, and have been incorporated into design standards BS 5950 and Eurocode 1993-1-2. Specifically, Eurocode 1993-1-2 determines the curves in accordance with Equations (2-1)

$$
\begin{aligned}
&\varepsilon = 0 \text{ to } \varepsilon_{p,\theta}: && \sigma = \varepsilon E_{a,\theta} \\
&\varepsilon = \varepsilon_{p,\theta,\theta} \text{ to } \varepsilon = \varepsilon_{y,\theta} = 0.02 && \sigma = f_{p,\theta} - c + {}^{b}/_{a}\sqrt{a^2 - (0.02 - \varepsilon)^2} \\
&\varepsilon = \varepsilon_{y,\theta} \text{ to } \varepsilon = \varepsilon_{t,\theta} = 0.15 && \sigma = f_{y,\theta} \\
&\varepsilon = \varepsilon_{t,\theta} \text{ to } \varepsilon = \varepsilon_{u,\theta} = 0.20 && \sigma = f_{y,\theta}[1 - (\varepsilon - 0.15)/0.05)]
\end{aligned}
\qquad (2\text{-}1)
$$

where:

- ε is the strain
- $\varepsilon_{y,\theta}$ is the yield strain
- $\varepsilon_{p,\theta}$ is the strain at the plastic limit
- $\varepsilon_{t,\theta}$ is the limiting strain for yield strength
- $\varepsilon_{u,\theta}$ is the ultimate strain
- $E_{a,\theta}$ is the slope of the linear elastic range
- $f_{p,\theta}$ is the proportional limit
- $f_{y,\theta}$ is the effective yield strength
- $a = \sqrt{(0.02 - \varepsilon_{p,\theta})(0.02 - \varepsilon_{p,\theta} + c/E_{a,\theta}}$
- $b = \sqrt{c(0.02 - \varepsilon_{p,\theta})E_a + c^2}$
- $c = \frac{(f_{y,\theta} - f_{p,\theta})^2}{(\varepsilon_{y,\theta} - \varepsilon_{p,\theta})E_{a,\theta} - 2(f_{y,\theta} - f_{p,\theta})}$

Eurocode 3 couples the above equations with reduced values of yield strength, proportional limit and elastic modulus as functions of temperature based reduction factors illustrated in Figure 2-2, in order to determine modified versions of stress-strain curves for carbon steels at elevated temperatures. Under this approach, strain hardening is only considered for temperatures up to 400^{o}C where the stress-strain curves are able to be enhanced by the ultimate strength of the material. On the other hand for temperatures above 400^{o}C, strain hardening is not significant, and hence generic stress strain curves are able to be formed as shown S275 carbon steel in Figure 2-3.

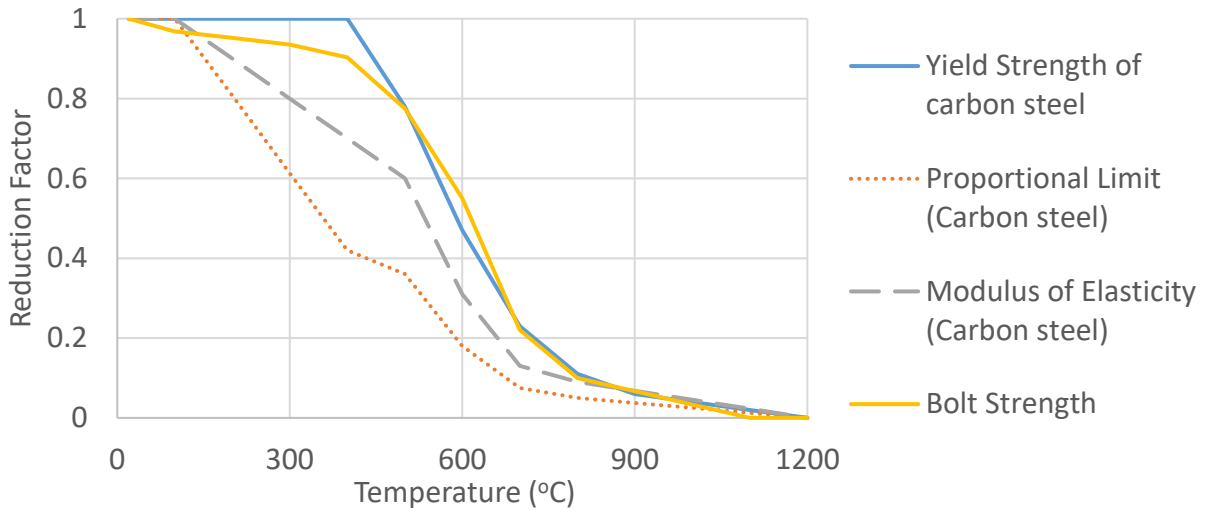

Figure 2-2 Reduction factors for carbon steels and bolts at elevated temperatures in EC3 (European Committee for Standardization, 2005a)

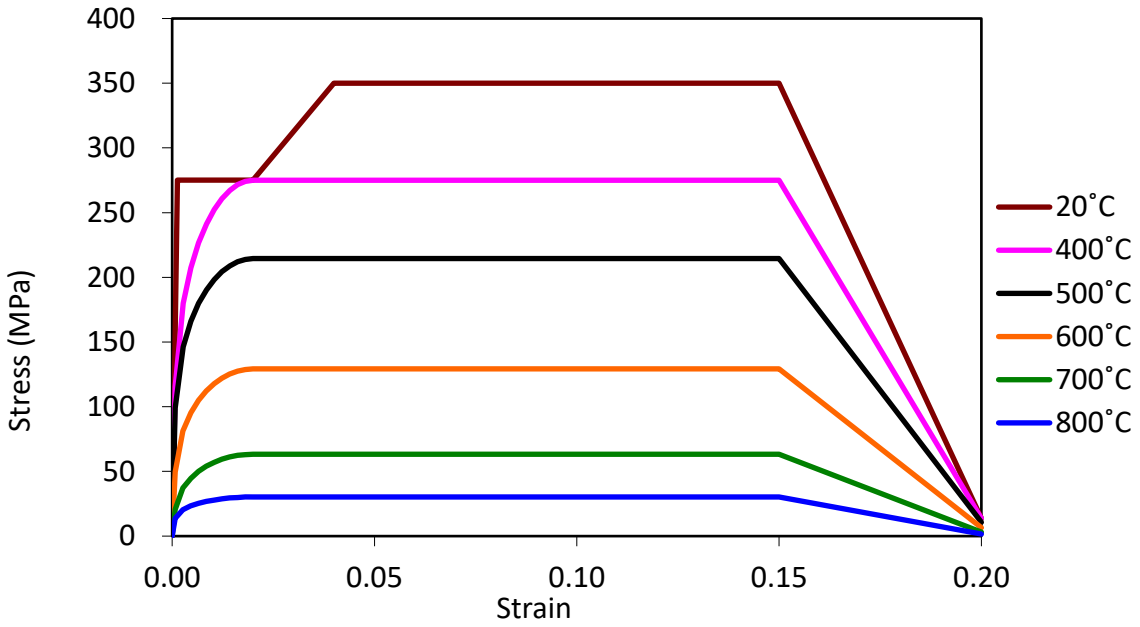

Figure 2-3 Stress-strain curves for S275 steel at elevated temperatures determined by EC3 (European Committee for Standardization, 2005a)

A similar approach of the application of reduction factors for calculating the reduced strength of bolts under elevated temperatures is also applied in Eurocode 3, with the difference being the modulus of elasticity is not considered to be significant. Hence, the reduction factors illustrated in Figure 2-2 are only provided for the strength of bolts which applies for both tension and shear.

In addition to the loss of strength experienced by steel under elevated temperatures, steel also undergoes thermal expansion as a function of temperature when heated. In accordance with Eurocode 3 Part 1.2, the co-efficient of thermal expansion (α) can be determined through Equations (2-2) below, where the constant thermal expansion coefficient between 750^{o}C and 860^{o}C represents the phase change in steel at a molecular level.

$$\textbf{For } 20^{o}C \leq \theta_a < 750^{o}C$$

$$\alpha = (1.2 \times 10^{-5}\, \theta_a + 0.4 \times 10^{-8}\, \theta_a^2 - 2.416 \times 10^{-4})$$

$$\textbf{For } 750^{o}C \leq \theta_a \leq 860\ ^{o}C \qquad (2\text{-}2)$$

$$\alpha = 1.1 \times 10^{-2}$$

$$\textbf{For } 860^{o}C < \theta_a \leq 1200^{o}C$$

$$\alpha = 2.0 \times 10^{-5}\, \theta_a - 6.2 \times 10^{-3}$$

where:

θ_a is the temperature of steel (^{o}C)

α is the co-efficient of thermal expansion

2.3.2 New Zealand Standards

The reduction factors for the yield stress and the modulus of elasticity of structural steel provided in the current revision of NZS 3404: Steel Structures Standard (New Zealand Standards Institute,

1997) are based on the experimental tests conducted by Proe et al. (1986) and the recommendations by CTICM (Centre Technique Industriel de la Construction Métallique, 1982). The calculations for yield stress and modulus of elasticity with respect to temperature is determined by Equations (2-3) and (2-4) respectively.

$$\frac{f_y(T)}{f_y(20)} = 1 \qquad \text{when } 0^oC < T \leq 215^oC$$

$$\frac{f_y(T)}{f_y(20)} = \frac{905 - T}{690} \qquad \text{when } 215\,^oC < T \leq 905^oC \tag{2-3}$$

where:

- $f_y(T)$ = yield stress of steel at temperature T^{o}C
- $f_y(20)$ = yield stress of steel at 20^{o}C
- T = temperature of steel in ^{o}C

$$\frac{E(T)}{E(20)} = 1 + \frac{T}{2000\left[Ln\left(\frac{T}{1100}\right)\right]} \qquad \text{when } 0^oC < T \leq 600^oC$$

$$\frac{E(T)}{E(20)} = \frac{690\ (1 - \frac{T}{1000})}{T - 53.5} \qquad \text{when } 600\,^oC < T \leq 1000^oC \tag{2-4}$$

where:

- $E(T)$ = modulus of elasticity of steel at temperature T^{o}C
- $E(T)$ = modulus of elasticity of steel at 20^{o}C

Relative to the values provided by Eurocode 3 shown in Figure 2-4, NZS 3404 has similar yield strength reduction factors, but is significantly less conservative and simplified for determining the modulus of elasticity based on the having defined two zones of linear interpolation. However, it is worth noting that structural fire aspect of NZS 3404 has not been revised since its release in 1997 and has not been updated unlike the Eurocode 3 which has undergone numerous iterations.

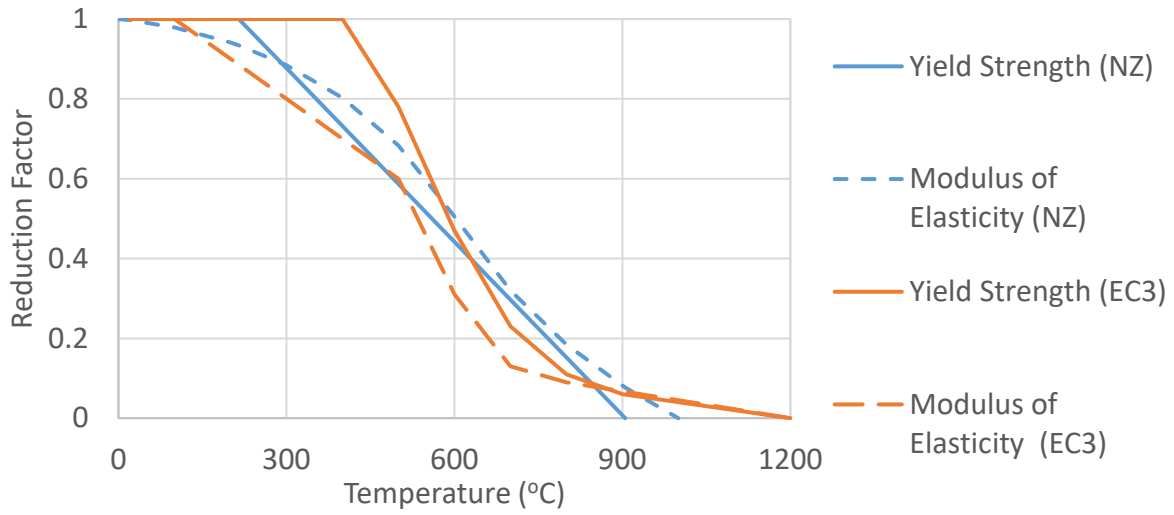

Figure 2-4 Carbon steel reduction factors (European Committee for Standardization, 2005a; New Zealand Standards Institute, 1997)

2.4 Differences in Simple Connection Design between Europe and New Zealand

As documented in the Structural Steelwork Connections Guide (SCNZ, 2008a), specific design parameters and detailing requirements have been developed for the various types of beam-to-column connections used in New Zealand to achieve increased robustness and ductility, with those for web plates and flexible end plates being specifically outlined and compared with connection design guides developed by the Steel Construction Institute (SCI, 2013, 2014) in accordance with Eurocode 3.

Notably, structural design in New Zealand recognizes the distinction in designing a structural system with the capacity to sustain calculated displacements in addition to singularly forced-based designs (Butterworth, 1995; Priestley, 1993). As a response, New Zealand connection design quantitatively requires connections to be able to accommodate gravity load and seismic drift induced rotations of 0.030 radians without collapse (SCNZ, 2008a). This contrasts with Eurocode 3, which although also requires simple connections to have adequate rotation capacity, does not specify a quantitative limitation. Instead, the requirement is assumed to be met if a bolted connection meets a criteria which considers the governing design resistance and thickness of connecting members (European Committee for Standardization, 2004b), ultimately leading to key differences in the detailing of the steel connections.

2.4.1 Web side plate connections

In order to accommodate the governing 0.030 radians of relative rotation in seismic and extreme fire scenarios, the design features of New Zealand web side plate (WSP) connections documented by SCNZ is dependent on the ductile yielding of the connection and the suppression of bolt or weld failure as the weakest link component in the connection.

The design procedures were developed based on research conducted by Murray and Butterworth (1990). The study undertook 14 experimental tests of WSP beam-to-column connections with 6 different detailing configurations; each connection being placed under large relative rotations to simulate the effects of an earthquake. From this study, it was discovered that yielding of bolt holes, particularly in the web of the connecting beam (Figure 2-6) is the desirable outcome during large rotations as it allows for an extremely ductile mechanism, whereas on the contrary, the shearing of bolts or peeling failure of welds was observed to be a significantly brittle failure mode and is to be avoided through structural design. Furthermore, Murray and Butterworth (1990) observed that

the rotational capacity of the WSP connection was dependent on the occurrence of contact between the bottom flange of the beam and the supporting column, which increases the stresses in the connection through prying forces by acting as a lever. To account for these mechanisms, SCNZ (2008a) incorporates the following design features for WSP connections:

- To prevent the possibility of bolt shear under extreme seismic drift induced rotations and fire conditions, the clear plate thickness is limited to half the bolt diameter and the bolt group capacity is greater than the lowest limiting flexural condition of the cleat or beam web
- The beam/column seismic end gap shown in Figure 2-5 is to meet the criteria presented in Equation (2-5):

$$\frac{a_c}{s_{g1} - a_{e1}} \leq 33 \tag{2-5}$$

Where:

- a_c is the end gap distance between the connecting beam and column
- s_{g1} is the bolt gauge distance
- a_{e1} is bolt edge distance

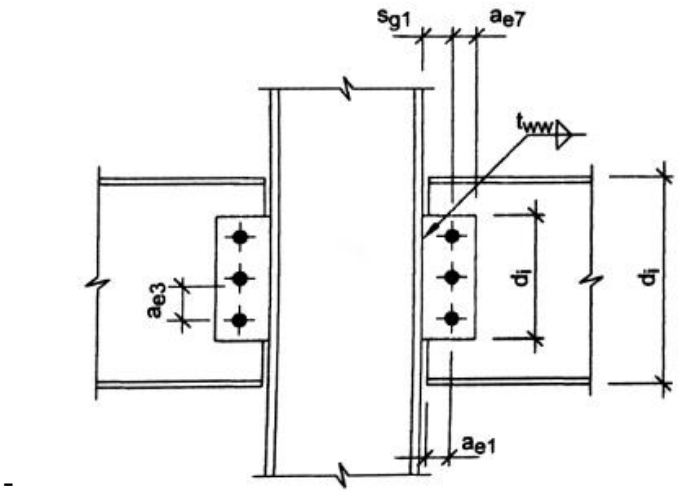

Figure 2-5 Fin plate connection (SCNZ, 2008a)

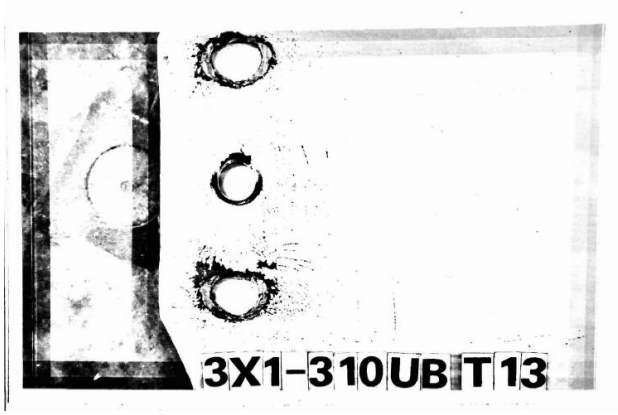

Figure 2-6 Yield of bolt holes (Murray and Butterworth, 1990)

In comparison, the SCI (2014) recommends that the rotational capacity of the web side plate connection is to be achieved through hole distortions of the connecting members, and/or through shear deformation of bolts; a significant contrast to the ductile design philosophy of the New Zealand design which does not permit the yielding of bolts due to the resulting brittle failure which may arise. Hence based on the increased ductility of the New Zealand web side plate connection design as a result of detailing for higher rotation capacity, they are generally assumed to be able to accommodate the high rotations which arise when subjected to elevated temperatures in a fire.

2.4.2 Flexible endplate connections

Similarly, the design of flexible endplate connections in New Zealand has been documented based on the requirements of being able to achieve 0.030 radians of rotation due to seismic drift in addition to thermal strains induced by extreme fire events without collapse. As per the Structural Steelwork Connections Guide (SCNZ, 2008a), the following design features for flexible endplate connections have been incorporated to meet the above requirements:

- Welds of cleats to the beams have a design capacity greater than that of the resultant action due to development of over-strength of 1.2 times the flexural yield of the end plate under tensile load and direct shear.
- The beam web adjacent to the top of the cleat have sufficient capacity to resist combined shear and local longitudinal tension, using a Von Mises based stress criterion.
- The end plate is maintained as flexible by limiting the thickness of the endplate as a function of the bolt gauge in Equation (2-6) below:

$$11 \leq \frac{s_g}{t_i} \leq 14 \qquad (2\text{-}6)$$

  where:

  - s_g is the bolt gauge (mm)

  - t_i is the thickness of the endplate (mm)

- To prevent transverse tensile tearing in the web below the bottom edge of the end plate, block transverse shear and tensile yield capacity is assessed based upon a web block 20 mm wide and as deep as the end plate. Compression yield strength is assessed to develop along the top edge of the web block shear element as long as two local web buckling criteria are satisfied. The first of these is that the top flange is laterally restrained at the location by

a concrete slab or other means. The second criterion is that the clear web depth to web thickness ratio between the top of the cleat and the underside of the flange, is less than or equal to 17.5.

Upon testing 33 samples of flexible end plate connections designed under the recommendations of SCNZ as shown in Figure 2-7, it was demonstrated that the capacity design approach was able to successfully accommodate and surpass the minimum required beam end rotation of 0.030 radians. Additionally, it was confirmed that the design procedures allowed for the plate tensile and shear yielding of the connection under the tested design configurations, where the inelastic yielding and the end plate and beam web were found to be beneficial for a ductile failure mechanism.

Figure 2-7 Capacity testing of flexible end plate connections (Hyland, 2003)

In comparison, the recommendations for flexible end plates in the design guide for steel connections in Europe places significantly higher emphasis on the overall shear capacity of the connection, with relatively less emphasis on the rotational capacity and ductility as a result of differences in design requirements between Europe and New Zealand (SCI, 2014). This is exemplified by differences in the recommended detailing of the connections, where (SCI, 2014)

recommends the use of 10mm or 12mm thick end plates and a bolt gauge of 90mm, compared to (SCNZ, 2008a) which relates the factors to optimise ductility.

Although both design requirements address the importance of achieving sufficient axial tension capacity, there is significant difference in the capacity requirements. In New Zealand, the required capacity is a function of the yield strength of the endplate and bolt gauge (SCNZ, 2008a), whereas the required capacity in Europe is determined by Eurocode 1991-1-7 (European Committee for Standardization, 2006) for accidental actions which incorporates a criteria for required axial capacity based on the risk group of the structure in order to mitigate damage by events such as explosions, impact or consequences of human error.

As a result of the factors described herein, it is expected that the New Zealand connections are designed to be more robust when operating in the plastic range than their European counterparts. This is based on the contrasting capacity requirements for rotation and ductility, from which the assumption of New Zealand connections being adequate under elevated temperatures arose. Whereas the behaviour of European connections under elevated temperatures is relatively well understood through previous experimental and numerical studies, the study reported herein sets the precedence of understanding the behaviour of New Zealand connections and tests their assumed performance in fire by comparing connections designed as per the two regions and numerically modelling their behaviour under fire conditions.

2.5 Investigation of the behaviour of steel connections in fire

2.5.1 Experimental investigations

The earliest recorded experimental studies on the performance of isolated steel connections in fire were undertaken by Kruppa (1976) and British Steel (1982), where a range of connections from

"flexible" to "rigid" were tested under rising temperatures following the standard fire curve (ISO, 1975). The results from these early tests established that both bolts and the connecting members undergo significant deflections and deformations in fire conditions (Simões da Silva and Santiago, 2005).

Lawson (1990) investigated the behaviour of connections in fire which had the benefit of structural continuity by testing specimens of a cruciform set up consisting of a column and two symmetrically connecting beams. In total, eight specimens of various connection types including flush endplate, extended endplate and web cleats (with each beam supporting a concrete slab) were tested under the standard fire curve. Through the eight tests, it was reported that the steel beam experienced significantly higher temperatures than the components within the connection, where temperatures in the lower beam flange reached 650^{o}C to 750^{o}C, meanwhile the temperature of bolts was 150^{o}C to 200^{o}C lower. The results from this experiment suggested that the composite action from the concrete slabs provided an increased performance of steel connections in fire through distributing moments, and it is believed that connections feature a natural robustness in fire, potentially as a result of higher concentrated thermal mass (Sulong, 2005). However due to restrictions on applicable loads by the testing apparatus, insufficient moment and rotation data was obtained from the tests.

Following the Broadgate fire incident in 1990, a proper understanding of the behaviour of complete structures in fire was shown to be critical, leading to full-scale fire tests being conducted at the Cardington Laboratory in Bedforshire, U.K with the aim of assessing the performance of structural elements in a fire under natural constraints (Amer and Moore, 1994; Bailey, Lennon, and Moore, 1999; Y.C. Wang, 2002). Although being significantly more expensive in comparison to experimental tests on isolated steel connections, large scale testing provides an accurate

representation of the behaviour of real steel connections in fire based on its ability to consider the influence of the overall structure.

The full-scale building built for the tests consisted of an eight-storey steel frame with concrete floor slabs on each floor as shown in Figure 2-8. The frame was designed as an office building in accordance with the relevant British Standards and structural Eurocodes, as it featured five bays of 9 m by three bays of 6 m, 9 m and 6 m as shown in Figure 2-9. The structure was constructed as a no-sway frame to sustain gravity and wind loads, with beam-to-column connections being flexible endplates, and beam-to-beam connections being fin plates (otherwise known as web side plates in New Zealand), both of which were designed to resist vertical shear from a combined dead and live load of 7.15 kN/m^2 to replicate a real commercial office floor load.

Figure 2-8 Test building in the Cardington test (Moss and Charles Clifton, 2004)

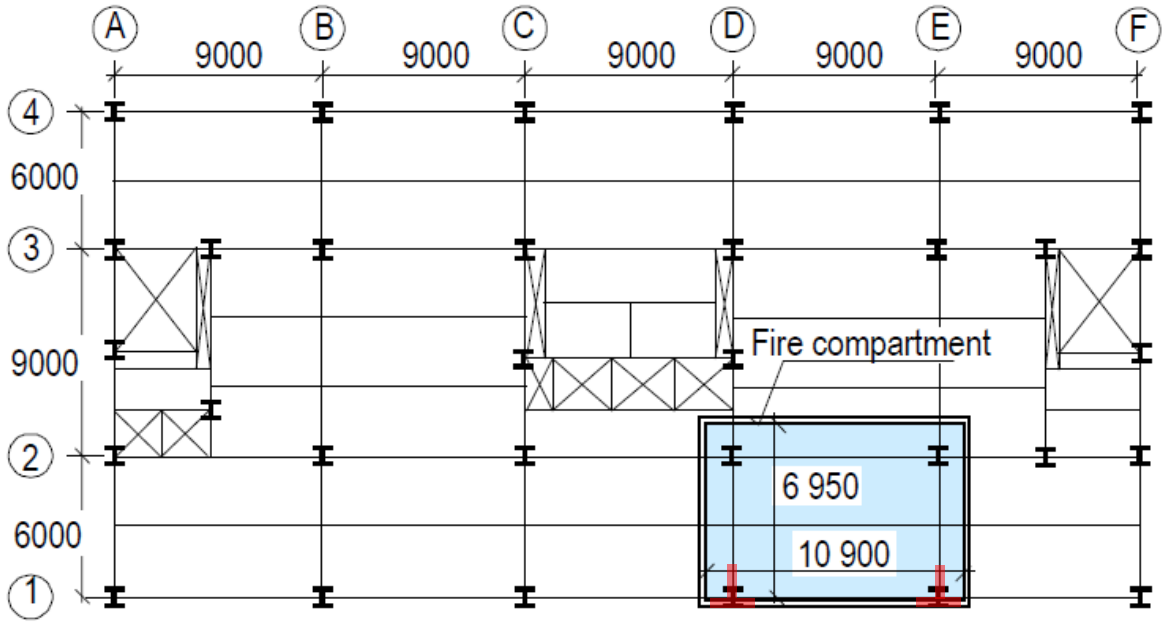

Figure 2-9 Cardington test floor plan and fire compartment for Test 7

In total, seven fire tests were conducted in different areas of the building with most floor beams unprotected, but columns protected to either their full height (including the connections) or up to the bottom flange of the connected beams against fire and various fuel loads in order to stimulate fires in different scenarios. Studies on the structural response to fire involved: restrained beams, plane frames, corners, a large compartment, as well as a demonstration test as shown in Figure 2-10 (Al-Jabri et al., 2007). A detailed description of each test is available in previous publications (Wald et al., 2005).

In particular, the seventh Cardington was undertaken on January 16, 2003 with a primary focus on studying the behaviours of tensile membrane action and simple steel connections as a part of a real building frame when exposed to a natural fire (Wald et al., 2005). The experimental test was conducted in a purpose built compartment on the 4th floor of the 8 storey building as in Figure 2-9. The structural components exposed to fire in this test were constructed using primary and

secondary composite beams of grade S350 336 x 171 x 51 UB and grade S275 305 x 165 x 40 UB respectively – both supporting a floor slab with an overall depth of 130 mm and steel decking with a trough depth of 60 mm. Grade S350 305 x 305 x 198 UC and S350 305 x 305 x 171 UC sections were used for the internal and external columns respectively. In order to maintain global structural stability during the fire tests 18 – 22 mm of vermiculite-cement spray was applied to internal columns up to the bottom flange of connecting beams, and along the full height of perimeter columns including the connection and short lengths of the connected beams for "coatback" as approximately shown in Figure 2-9 (Wald et al., 2005). Beyond these, structure was left unprotected.

To induce a natural fire, the floor area of the fire compartment was covered with 40 kg/m^2 of wooden cribs which was burned until completion to produce a fire representing one which may occur in an office building. Temperatures were measured using thermocouples which were placed at 300 mm below ceiling level throughout the compartment, and at points of interest on structural components, particularly at the mid-span of beams and on the plates of the connections adjacent to the bolts.

The observed behaviour of the connections in this experiment is discussed in detail in Chapter 4. It is important to note that this test showed the following damage mechanism, thereby allowing close study of the: significant vertical deflections of beams and floor slabs (shown in Figure 2-10), localised buckling of lower beam flanges, buckling of beam webs, end plate fracture, and the elongation of bolt holes in the fin plate connections (shown in Figure 2-11). As a result, these observations of structural response of the connections and adjoining members from the Cardington tests highlighted the unknown behaviour of connections under elevated temperatures and their potential vulnerability in severe fire, prompting further investigations.

Figure 2-10 Deformation of structural elements (Al-Jabri et al., 2007)

Figure 2-11 Fin plate connection after test (Al-Jabri et al., 2007)

More recently, a series of experimental tests have been conducted at the University and Sheffield and University of Manchester in order to study the behaviour of steel connections under elevated temperatures in detail (Hu, 2009; Yu et al., 2009a, Yu et. Al. 2009b; Yu et al., 2008) . These tests were conducted on a range of isolated bolted connections which included fin plates, web cleats,

and end plates in order to better understand the behaviour of individual components when subjected to high temperatures.

In the tests, isolated beam-to-column connections with UC254x89 and UB305x165x40 sections were placed in an electrically heated oven which slowly heated the specimens to one of four constant temperatures: 20°C, 450°C, 550°C or 650°C. Once the test specimens had been slowly heated to the desired temperatures, a load was then applied at an angle of 35° or 55° until failure was observed through the fracturing of components. An illustration of a flexible endplate test specimen and the test set up is shown in Figure 2-12.

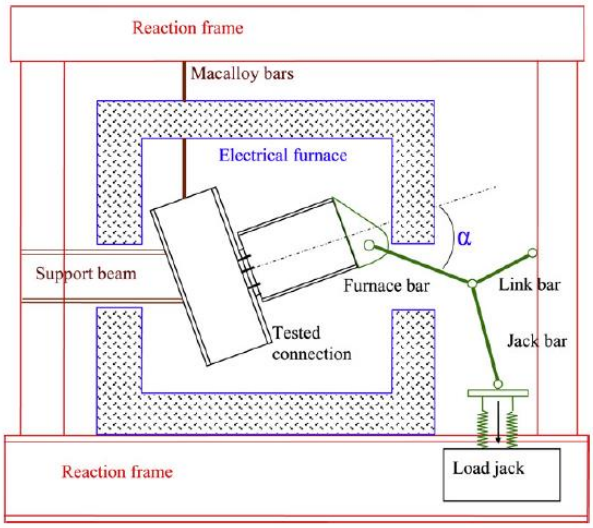

Figure 2-12 Isolated connection test set up (Yu et al., 2009a)

Based on the reported observations, the tests were able to highlight the failure modes experienced by different types of connections at a range of temperatures. In particular, it was reported that all connections experienced significant losses of strength due to elevated temperatures, as well as various failure modes which occurred in different types of connections. It was observed that fin plate connections failed due to bolt shear over the full range of tested temperatures, whereas on

the other hand, the endplate tests showed that the connections failed as a result of endplate fracture at temperatures below 450^{o}C, and bolt fracture at temperatures above 550^{o}C. However as the test specimens were held at a steady state temperature before a load was applied and that the experimental set up of the unrestrained beam did not allow for the influence of axial forces caused by thermal expansion/contraction which arose in the Cardington frame tests, the results from this test do not fully represent the behaviour of connections in a fire with increasing temperatures. Nonetheless, the overall results from these experiments highlighted the vulnerability of the steel connections under elevated temperatures due to the decrease in strength.

In order to more accurately represent the axial forces acting on various beam-to-column connections as a result of catenary action and thermal expansion of connecting beams, experiments at the University of Manchester have been undertaken on the behaviour of steel connections in fire based on frames in the Cardington tests (Liu et al., 2002; Y. C. Wang et al., 2011). As shown in Figure 2-13, the experiments consisted of H-shaped frames; each with two columns (UC254x254x73 or UC152x152x23) and a connecting UB178x102x19 beam connected with different types of joints including fin plate, web cleat, flush endplate, flexible endplate and extended endplate. To simulate the effect of a concrete slab on the beam in real construction, the top flange was covered with a ceramic fiber blanket and supported laterally by a specially designed steel truss. All other parts of the frame were left unprotected.

In the experiment, the frames were placed inside a gas furnace where two point loads of 40kN magnitude were applied by jacks as shown in Figure 2-13. The gas furnace then applied heat to elevate the internal temperature to follow the standard fire curve. However due to the small furnace and relatively large sample, it was reported that the temperature inside the furnace varied up to 200^{o}C in different areas.

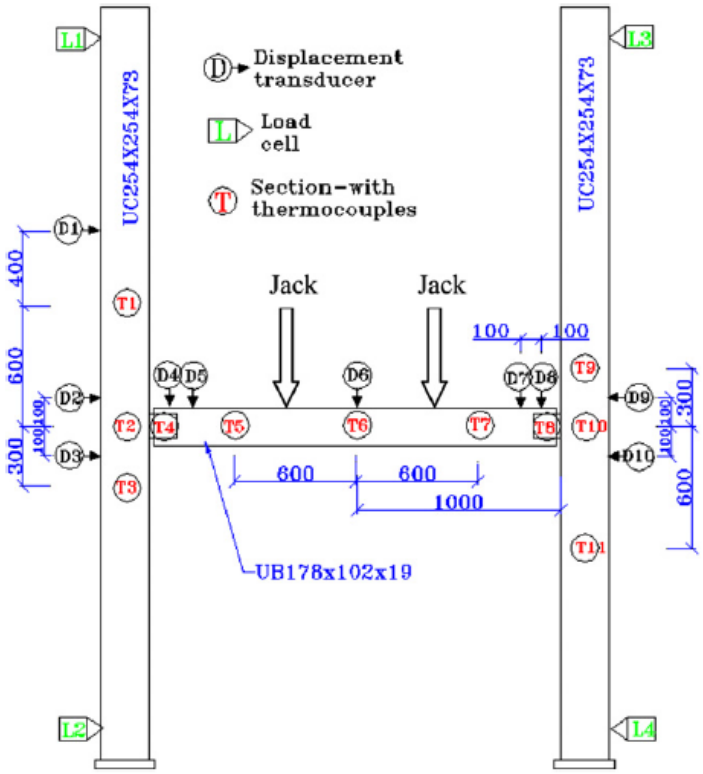

Figure 2-13 Test set up (Wang, Dai, and Bailey, 2011)

Nonetheless, results from the experiment indicate that although failure in the connection was experienced by all five types of connections, no failure occurred as a result of large beam deflections. While multiple joint failures were reported, it was proven that different joint designs allowed for differing levels of rotation, where the fin plate and web cleat connections possessed high rotational capacity, whereas the endplate connections were also able to rotate to a lesser extent due to the bending of the endplate. From this set of experiments, it was determined that the lateral restraint of the top flange of the connecting beam is largely influential on the overall behaviour of the subassembly in fire.

2.5.2 Analytical Investigations

Liu (1996) was amongst the first who attempted to model the behaviour of steel connections using finite element software (Al-Jabri et al., 2007). Using eight-noded isoparametric elements, Liu was able to model the behaviour of different types of joints using a model developed using the finite element software FEAST which considered the non-linear thermal expansion and behaviour of steel. Analysis of the data from the models created in this study displayed a close agreement with experimental data for different types of joints and hence was able to demonstrate the capability of using finite element analysis to model steel connections (Al-Jabri et al., 2007).

Al-Jabri (1999) conducted three-dimensional finite element models of flush endplate steel connections under elevated temperatures both with and without the contribution of a composite slab. In these models, the connections were created using the finite element software ABAQUS, where each component in the model was represented by a three-dimensional brick element. These models also took into account the non-linear strength properties of steel, as well as the interaction between the components as the connection deformed at higher temperatures by using Coulomb friction. In comparison with the experimental data, the finite element models exhibited relatively close results regarding the moment-rotation temperature characteristics and the failure modes in both elastic and plastic regions.

In the work by Sarraj (2007), the author studied the behaviour of steel fin plate connections under elevated temperatures, also using the finite element program ABAQUS. Sarraj (2007) was able to introduce and successfully achieve the effect of the interaction between the bolts and the fin plate caused by the rotation of the connection. As a result, the finite element models of steel fin plate connections provided a good understanding of the behaviour of shear connections under elevated temperatures, where load and displacement data was created for the beam web bolt holes in bearing

and the bolts in shear. The reported data was validated against tests on lap joints at ambient temperatures, and also an experimental test conducted at the Czech Technical University by (Wald et al., 2005) and also provided a benchmark for future researchers studying similar connections. Overall, this research was paramount in modeling the shear interactions at ambient and elevated temperatures, capturing failure mechanisms of bolt shearing and plate bearing.

Following the tests on isolated steel beam-to-column connections at the Universities of Sheffield and Manchester, the authors were then able to recreate the web-cleat and endplate connections over a range of steady state temperatures using ABAQUS (Hu, 2009; Hu et al., 2008; Yu et al., 2009b). In the models, it was demonstrated that ABAQUS was able to accurately determine and predict the behaviour and failure modes of steel connections at both ambient and elevated temperatures, with the numerical solutions in good agreement with experimental results. However, it was reported that the models are unable to accurately predict the failure of components, which may lead to an increased ultimate load carrying capacity in the finite element analysis.

More recently, research on steel beam-to-column connections under elevated temperatures using the finite element analysis software ABAQUS has placed focus on the influence of frame assemblies with realistic structural behaviour which accounts for forces gained as a result of restrained connections, where beams undergo thermal expansion and catenary action with temperatures increasing and decreasing in accordance with a realistic fire scenario. Selamet and Garlock (2014), were able to use the finite element software to model fin plate connections between the secondary and primary beams in Cardington Test 7. In their model, the authors were able to develop deflections in their beam during both the heating and cooling phases which were comparable to those recorded in the experimental test. Although their models were able to recreate the buckling behaviour in the bottom flange of the beam as observed in the experiment, it was

reported that the connection in the numerical analysis had shown extensive distortion in the beam web due to bolt bearing without failure, whereas it was reported that the fin plate connections in the Cardington test failed due to bolt shear as shown in Figure 2-11. This may be a result of the model not including a physical component for the concrete slab due to simplicity - instead, the effect of the slab was taken into account through the use of vertical spring elements along the top flange of the beam. Despite the spring elements being able to feature a varying stiffness with temperature similar to that of a concrete slab, the springs do not provide the same horizontal stiffness of a floor slab which is likely to influence the behaviour and ultimately the failure mode of the connection.

In the research conducted by Selamet and Bolukbas (2016) the authors modelled a subassembly of a floor from an existing tall steel building exposed to fire in Istanbul, Turkey. In this study, the authors examined the fin plate connection of a particular bay which was geometrically comparable to that of the Cardington test, with a trapezoidal floor slab supported by secondary and primary beams of 9 m and 6 m lengths respectively. In their model, the authors incorporated the floor slab by assuming a rectangular profile which was permanently fixed to the top flange of the beam using the "Tie" function in ABAQUS. Although the modelled subassembly also incorporated temperatures similar to those recorded in the Cardington test in both the heating and cooling phases, it was reported that this model ultimately showed the bolts in the fin plate to fail as a result of the axial forces developed in the beam as it contracted when cooled. Compared to the study conducted by Selamet and Garlock (2014), it is evident that the influence associated with incorporating the concrete slab in the model will alter the behaviour of the connection, and should be included when modelling experiments with composite floors to ensure accuracy.

These connection studies have all been undertaken overseas, on simple connections not designed and detailed for dependable ductility. This project is based on determining the performance under elevated temperatures of simple connections designed and detailed such that their load carrying capacity is maintained during the levels of rotation expected in severe earthquakes.

2.6 Research Approach

Undertaking experimental testing on structural components at elevated temperature is expensive and time consuming, and not currently possible in New Zealand. Hence the use of accurate modelling techniques is necessary has been looked upon as the desirable method for understanding the behaviour of steel structures in fire. This has led the increasing use of finite element modeling in commercial software such as ABAQUS being used structural fire engineering applications (Wang, 2002).

As highlighted in Section 2.5 the finite element analysis software ABAQUS has been well established to be able to predict and model the behaviour of steel and concrete composite structures in fire, exemplified through its ability to recreate test results gained from the Cardington fire tests, where structural phenomenon such as member buckling and tensile membrane action were able to be numerically analysed and verified with experimental results (M.; Gillie et al., 2001; Moss and Clifton, 2004). Utilising the numerous modelling elements with various advantages provided by ABAQUS, the software has indicated its capability in accurately modelling details of structural components and behaviour such as buckling, torsion as a result of elevated temperatures (Hu, 2009).

More recently, researchers have been able to successfully and accurately model the behaviour of detailed connections in fire, where the connections were both isolated and as a part of a larger

structure, having been validated against experimental test data (Dai et al., 2010; Sarraj et al., 2007; Selamet and Garlock, 2014; Yu et al., 2009b). The models used three-dimensional brick elements in order to replicate the behaviour of components such as bolts and plates which naturally behave in three dimensions and are not able to be accurately simulated using two dimensional models. As a result, finite element modelling using ABAQUS has been established as a relatively efficient method of studying the behaviour of steel connections in fire and hence will be used as an as analytical tool for this investigation.

In order to understand the functions and capabilities of the software, ABAQUS, steel connection assemblies have first been modelled based on the physical and numerical experiments undertaken by previous researchers which are of similar geometries to the web side plates and flexible end plate connections used in New Zealand. This was completed in order to validate the understanding and proficiency of using ABAQUS by comparing the model with experimental speculations such as the displacement-temperature curves, failure modes and general observations. Due to the current lack of experimental data regarding the behaviour of New Zealand steel connections in fires and lack of experimental testing capability in New Zealand, this approach will serves as a tool for determining the accuracy of the finite element models developed in the later stages of this study.

In particular, the experimental tests conducted by the University of Manchester and University of Sheffield on simple connections have firstly been modelled based on the tests being undertaken on isolated joints, where modelling particular scenarios from this set of experiments allows for a comparatively simpler modelling approach due to the relatively small number of components compared to tests involving a structural frame. Based on the tests on endplate and angle cleat connections having been previously modelled using ABAQUS (Yu et al., 2009a; H. Yu et al., 2011), this study has utilised the previously documented techniques to model the fin plate

connection tests in order to provide a basis for accurately understanding the modelling packages offered by the software.

Upon successfully modelling the experimental investigations on isolated connections, a beam-to-column flexible endplate connection which experienced fracture during Cardington Test 7 was then modelled to allow for better understanding of the behaviour of the connection in a real fire, given the focus of this study on beam-to-column connections and that the beam-to-beam fin plate connections of the Cardington test having been previously studied (Selamet and Garlock, 2014). It is recognised that the documented results from the experiment will yield greater difficulty to replicate due to the connection being attached to a large structural frame with steel and concrete composite floors being exposed to a fire with transient temperatures. However, the benefit encompasses its higher accuracy in representing the behaviour of an authentic steel connection under elevated temperatures by taking the influence of the structural frame and varying temperatures due to the heating and cooling of a natural fire into consideration.

Following the validation of the finite element models with experimental results, the steel connections specified within the models were then redesigned in accordance with the relevant New Zealand standard which include the design against seismic loading. These connections were then analysed to determine their behaviour in the Cardington fire, ultimately providing a basis of understanding and comparing between the performance differences as a result of differing design philosophies between New Zealand and the U.K.

3 Development of Finite Element Models

As a result of the significant experimental and numerical research that has been undertaken on structural fire performance in Europe since the 1990's, the development of numerical software

based on the use of finite elements to analyse the complex behaviour of structures in fire have been established to provide engineers and researchers with tools for understanding the physics behind these behaviours (M. Gillie et al., 2001; Huang et al., 1999).

For the purpose of structural fire engineering, the available numerical software consists of general purpose finite element programs such as ABAQUS, ANSYS or LS Dyna, and specific structural fire engineering software packages such as Vulcan (Huang et al., 2004) or SAFIR (Franssen, 2005). The software listed herein are able to predict the behaviour of structures in fire by considering non-linear behaviour resulting from actions such as thermal elongation, large displacements, and non-linear temperature dependent material properties (Lim and Feeney, 2015).

The listed programs exhibit specific advantages and disadvantages, and have previously shown to be capable of modelling the behaviour of various structural components in fire. However, when specifically modelling the detailed behaviour of steel connections, it was found that three-dimensional models available in general purpose software such as ABAQUS, ANSYS, or LS Dyna were able to produce results with increased displacements and stresses , and hence more accurate results than two-dimensional models such as those generally offered by specific structural engineering software (Krishnamurthy and Graddy, 1976; Kukreti et al., 1987a). Furthermore, given that the behaviour of bolted steel connections is three-dimensional, they cannot be satisfactorily represented by two-dimensional models (Vegte, 2004).

As such, study utilises the general purpose finite element software – ABAQUS due to its availability within the University of Canterbury and its advantages in its versatility in modelling different materials and rich element library which allows for various types of analysis including heat transfer and mechanical, which can then be combined in a coupled thermal and mechanical analysis (Buchanan and Abu, 2017). Subsequently, these advantages have allowed previous

researchers to accurately model and validated the behaviour of steel connections in fire (Hu, 2009; Selamet and Garlock, 2014; Yu et al., 2009b). However, given that ABAQUS is a general-purpose finite element software, its range of modelling packages must first be understood in order to produce valid results.

3.1 Recreation of Isolated Fin-Plate Connections

For the purpose of understanding the modelling packages and techniques associated with ABAQUS including the types of available analysis, selection of finite elements and boundary conditions, contact interactions and input of material properties through, this section of the study investigates and recreates the isolated fin plate connection experiments undertaken by Yu et al. (2009a) through the use of the finite element software.

As discussed in Chapter 2, the Universities of Manchester and Sheffield undertook projects investigating the behaviour of isolated steel connections under constant elevated temperatures. Grade 8.8 M20 bolts were used in all tests, in addition to the columns and beams constructed of Grade S355 UC254×89 and Grade S275 UB305×165×40 sections respectively, and a custom-made connector for the application of loads bolted to the end face of the beam as shown in Figure 3-1(Yu et al., 2009a, 2009b; H. Yu et al., 2011). These tests were performed on a range of isolated connections in an electric furnace which slowly heated the samples to a constant temperature, with increasing loads applied at 35^{o} or 55^{o} angles until failure was reached. Specifically, this study focuses on the recreation of the tested fin plate connection as it has not been modelled by previous researchers.

3.1.1 Model Assembly

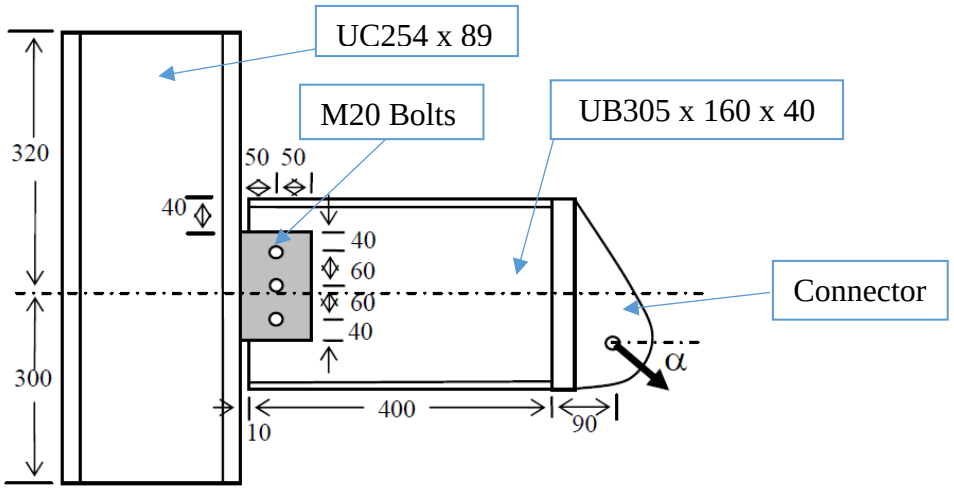

Figure 3-1 Fin plate connection design (Yu et al., 2009a)

A model using 3-D finite element bricks was created to scale based on the fin plate connection details used in the experiment as shown in Figure 3-1 above, where each individual structural component including the column, beam, bolts and the fin plate were created separately and assembled into one model as shown in Figure 3-2. To represent the connector used in the experiment, rigid body elements were created and attached to the end of the beam to capture the effects of eccentric loading, a method used and validated by the angle cleat connection model created by Yu et al. (2009b).

In order to accurately recreate the results generated by the experimental testing, the details within the model were recreated as accurately as possible based on the reported information (Yu et al., 2009a). As per the connections used in the experiment, the bolt holes were modelled to be 22 mm in diameter – 2 mm wider in diameter compared to the bolts. In regards to the welds between the fin plate and the column, limited data on the use of finite elements to represent the fracture of welds at elevated temperatures currently exists (Selamet and Garlock, 2014), and was therefore modelled using a "Tie" constraint which assumes a perfect bond between the two surfaces.

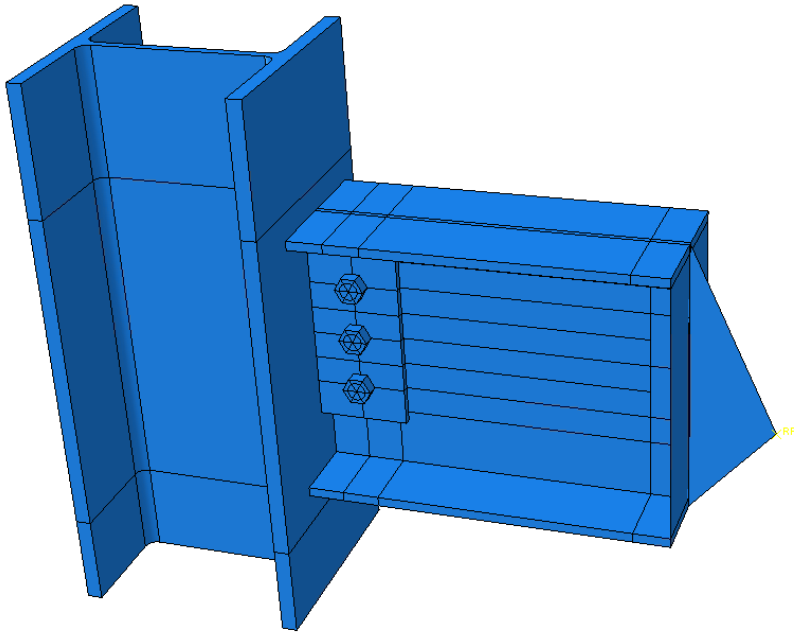

Figure 3-2 Modelled fin plate connection assembly

3.1.2 Modelling Packages

ABAQUS offers two packages: Standard Analysis and Explicit Solution to solve nonlinear problems associated with the numerical modelling in structural mechanics (ABAQUS, 2014b). These can be summarised and exemplified as:

- Material nonlinearity - Materials undergoing yielding to the point of which it is irreversible
- Boundary nonlinearity – Change of boundary conditions within the model during an analysis. For example when the bottom flange of the beam comes into contact with the column face under high rotations, creating a lever action so that the initial response of the connection is no longer linear.
- Geometric nonlinearity – Dramatic change in stiffness caused by actions such as large deflections

ABAQUS/Standard uses an implicit numerical solution based on linear and nonlinear equations which rely on static equilibrium throughout the structure (Vegte, 2004).This requires the solution to converge at each given time step, using the Newton-Raphson method and adjusting the time increments by default in order to provide nonlinear solutions. According to Hu (2009), although this approach is suitable for a wide range of nonlinear problems, instabilities may arise from nonlinear structural phenomena such as buckling/distortions or changes in stiffness due to fire. To overcome these instabilities, ABAQUS/Standard offers two solutions by adding – volume proportional damping, and utilizing the Arc-Length algorithm (Riks Method). Nonetheless, it has been reported that models with numerous complicated interactions such as those present in steel connections are likely to face difficulties in providing a smooth solution (Hu, 2009).

ABAQUS/Explicit offers a numerical package where the forces and displacement of each node is calculated to progress through time increments using a dynamic approach. Instead of requiring convergence at each time step, the explicit solver determines the forces in the body by first assuming that there is no contact between subsequent time steps. In an occurrence of overclosure (overlapping of contacting surfaces), the model then calculates and adopts the forces and displacements required to maintain contact between bodies (Vegte, 2004). This approach allows for certain advantages over the Standard solver including cases where instances are not initially in contact, such as bolts in clearance holes, which are designed to be 2 mm larger in diameter. Using the Standard solver, this results in a numerical singularity error unless the bolts are initially and carefully aligned with the components in contact under load which is difficult and inefficient for structural components with complicated load paths (Yu et. al, 2008) . Additionally, this issue is likely to cause convergence issues within the Standard solver when modeling components with large numbers of contact pairs such as bolted connections, as it is very difficult for the solver to

achieve convergence of all contact pairs at each time step (Yu et al., 2008). Hence based on the validation and recommendation of using the explicit solver to model steel connections in fire by previous researchers (Hu, 2009; Yu et al., 2008), ABAQUS/Explicit is adopted in this study.

3.1.3 Finite Element Library

Within ABAQUS, the software includes a large range of pre-programmed hexahedron (brick), shell, contact and beam elements which have different properties and functions based on the application for which they are applied. Specifically for modeling the deformation behaviour of bolted steel connections, the finite element models created for this research will use three-dimensional brick elements, as they produce results with significantly more accurate deformations when compared to the same models created with two-dimensional shell elements (Kukreti et al., 1987b).

To best represent the plasticity-type problems such as those involving the behaviour of steel connections, first order elements will be used to in order to accurately model the yield lines and strain fields experienced by the connection under load. There are three types of first order brick elements integrated into ABAQUS: C3D8, C3D8R and C3D8I, which differ based on their integration due to varying numbers of Gauss points (ABAQUS, 2014b). Where the C3D8 element with full integration and 8 Gauss points produces a shear locking phenomenon when simulating structures in bending which may overestimate failure loads (Bursi and Jaspart, 1998), the C3D8R elements with reduced integration and hourglass control underestimate the strength value and plastic failure load due to its theoretical formulation, and C3D8I elements with full integration and incompatible modes perform comparatively well for simulating elastic, plastic and bending behaviour. Hence, based on the research conducted and models created by previous researchers,

C3D8R elements will be used for this study due to its suitability in controlling hourglass modes, allowing for a conservative prediction of behaviours (Hu et al., 2008).

3.1.4 Contact Modeling

In order to model the contact between elements in ABAQUS, the standard analysis provides two formulations for the calculation being "small sliding" and "finite sliding" (ABAQUS, 2014c), where the "small sliding" formulation is computationally less expensive as it only accounts for contact surfaces which undergo relatively limited movements and permits arbitrary rotation of the elements. On the other hand, the "finite sliding" formulation accounts for instances where the elements may slide, separate and rotate in finite amplitudes. The explicit analysis used in ABAQUS incorporates varied contact equations where the friction conditions between surfaces is represented by the Coulomb friction model which has been proven to be suitable for analyzing steel (Charlier and Habraken, 1990). In this, the model considers the effects of surface weighting and tracking, as well as the sliding formulation, ultimately allowing for greater efficiency when modeling elements that engage in contact or separate during an analysis. In the present model, the "finite sliding" formulation was used with a friction co-efficient of 0.3 for all contact surfaces based on previous studies on modelling the behavior of steel connections (Dai et al., 2010).

As there is currently limited experimental or numerical data on the behaviour of welds under elevated temperatures, the welded section between the fin plate and the column has been modeled using the TIE command in ABAQUS, which represents a perfect bond by not allowing for any relative motion between them (ABAQUS, 2014b).

3.1.5 Material Properties

The material properties adopted in the finite element model were in conjunction with those from from the experimental tests, with the basic ambient temperature parameters of each steel section being shown in Table 3-1.

Table 3-1 Ambient Temperature Material Properties

Material Type	**Yield Stress (N/mm^2)**	**Ultimate Stress (N/mm^2)**	**Density (kg/m^3)**	**Young's modulus (kN/mm^2)**	**Poisson's ratio**
Beam and Plate	356	502	7850	176.35	0.3
Column	355	550	7850	205	0.3
Bolt	640	800	7850	205	0.3

In order to correctly interpret material behaviour, ABAQUS requires the material properties to be input as functions of true stress and true strain (ABAQUS, 2014a). Since most material data is provided in nominal stresses and nominal strains, a conversion is required using the following relationships provided in Equations (3-1) and (3-2):

$$\sigma_{\text{true}} = \sigma_{nom}(1 + \varepsilon_{\text{nom}}) \tag{3-1}$$

$$\varepsilon_{\text{true}} = \ln(1 + \varepsilon_{\text{nom}}) \tag{3-2}$$

where:

σ_{true} is the true stress

ε_{true} is the true strain

σ_{nom} is the nominal stress

ε_{nom} is the nominal strain

When inputting the parameters into ABAQUS, strain is required to be entered separately as true elastic strain ($\varepsilon_{el,true}$) and plastic strain ($\varepsilon_{pl,true}$) defined by equations provided by ABAQUS (2014b), and commonly found literature on structural analysis.

Upon determining the material properties at ambient temperature, the material properties of stress, strain and Young's Modulus at varying temperatures of the steel components can then be related based on the equations provided by EC 3 Part 1.2 as described in Chapter 2 of this report.

3.1.6 Boundary Conditions and Loading

In order to accurately replicate an experimental test, it is vital that the boundary conditions applied to the numerical model closely match those used in experimental set up. In the case of the isolated connection tests, the boundary conditions used in the numerical simulation were as follows:

- Encastre (fully fixed) top and bottom column surfaces
- The end of the rigid plate at which the load was applied is not permitted to move or rotate in lateral directions

The load applied to the end of the rigid plate was divided into vector forces in directions according to the 35 and 55 degree load angles to apply different combinations of shear and tying forces to the connections (Yu et. al, 2007). This load is applied using a smooth step amplitude curve which promotes a quasi-static solution by applying the load in a gradual approach. By default, ABAQUS/Explicit applies loads instantaneously which may produce undesirable results by inducing the propagation of stress waves throughout the model. The use of the smooth step amplitude curve addresses this by gradually ramping up and ramping down the loading from zero to the maximum specified magnitude respectively (ABAQUS, 2014b).

3.1.7 Modelling Results of Ambient Temperature Tests

To validate the finite element model, the results and observations are compared with those from the experiment conducted at the University of Sheffield (Yu et al., 2009a), where the main basis of comparison arose from the documented Force-Rotation graphs and the observed yielding and failure of structural components as illustrated by the solid line in Figure 3-3 for a fin plate connection test with loading at 35^{o} at ambient temperature conditions.

As shown in the Force-Rotation graph in Figure 3-3 corresponding to the ambient temperature test with a load angle of 35^{o}, the results gained from the finite element analysis show close agreement with those gained from the experimental study. It can be observed that although the modelled relationship between force and rotation follow an agreeable relationship with the experimental result up to the point of failure, some discrepancies between the two graphs do exist.

Firstly, it can be observed in Figure 3-3 that a difference between the initial rotations of the connection exists between the finite element model (F.E.M.) and experimental test. It can be observed that while the experimental test requires a force of approximately 10 kN to actualise rotation in the connection, the numerical analysis requires zero force up to a rotation of 1.7 degrees. This discrepancy in the initial stages of the finite element analysis is considered to result from the contribution of rotational stiffness from the pretension force applied to the bolts in the experimental tests, which was not considered in the finite element model due to the lack of data available.

.

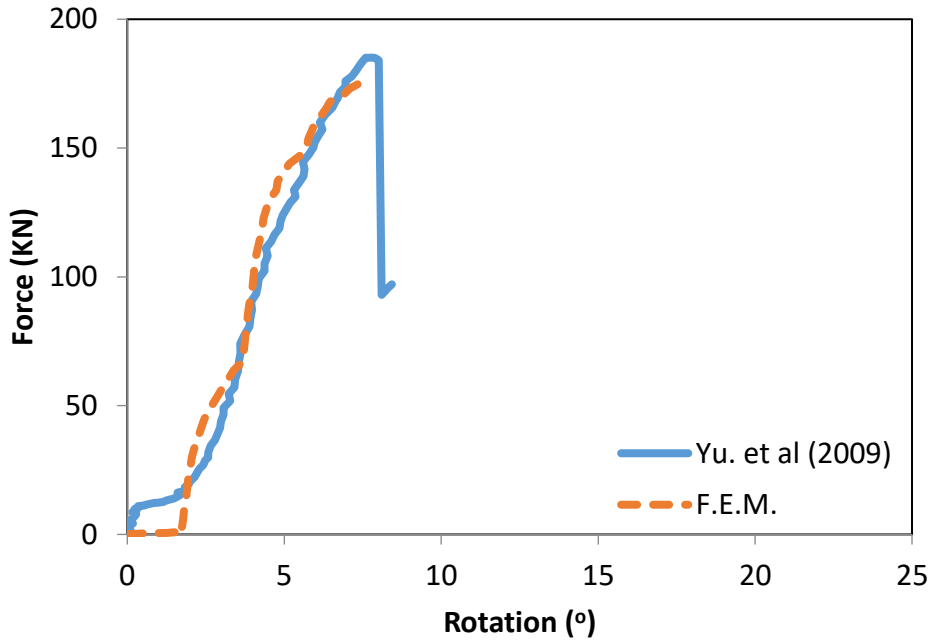

Figure 3-3 Fin Plate results at 35° loading and at ambient temperature

It can be seen that the relationship presented in the numerical analysis follows a staggered approach compared to the relatively linear behaviour recorded in the experimental test. The Force-Rotation relationship of the numerical analysis is presented in three subtle phases separated at approximately 60 kN, 145 kN and the point of failure, with each phase following a trend in which the connection possesses a high rotational stiffness at the beginning of the phase, which then decreases in stiffness towards the end. Upon inspection of the model along the simulation timeline, it is observed that the rotation experienced during the first phase largely arises from yielding of bolt holes. This occurs until the rotation reaches a point where the bottom flange of the beam comes into contact with the column face as shown in Figure 3-4, thereby creating a lever arm and increasing the stiffness of the connection as a result.

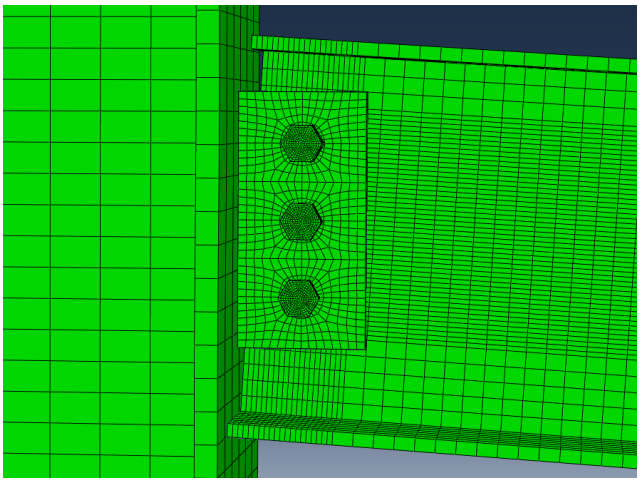

Figure 3-4 Contact between beam and column

Due to the newly formed lever arm, a chronologically increasing concentration of forces at the bolts arise when the connection is subject to higher rotations, with the relatively largest force being experienced in the region surrounding the top bolt. Therefore as the load increases during the second phase, the bearing of the bolts against the fin plate and beam web causes the bolt hole of the beam web to further deform, and the two components to yield and separate laterally in order to accommodate the increased rotations. This occurs until a point where the deformation is constrained by the bolts which experience large shear and tensile forces. Hence upon further loading and rotation, the top bolt in particular experiences significant yielding, and ultimately, failure as highlighted by the grey coloured areas in Figure 3-7. These behaviours are shown in Figure 3-5 to Figure 3-7, which illustrate comparisons between the behaviours of various structural components observed in the experimental test and the finite element models when loaded at an angle of 35^{o} under ambient temperatures using M8.8 bolts.

Although the behaviours described herein also occur in the experimental study, they are notably less obvious when considering the results reported in Figure 3-3. This may be a result of the experimental test set up shown in Figure 2-12, where the link arms attached to the loading plate

did not sustain a constant angle of applied load throughout the tests. Considering the ambient temperature tests, it was reported by Yu et al. (2009a) that initial loading angles of 53.85 and 33.80 degrees had rotated to 32.41 and 34.06 degrees at the conclusion of their respective tests, whereas the loads applied in the models were held constant throughout their analysis for simplicity. Hence, by allowing the loading angles to change reactively in each test, the Force-Rotation relationships recorded in the experimental studies follow comparatively stable trends.

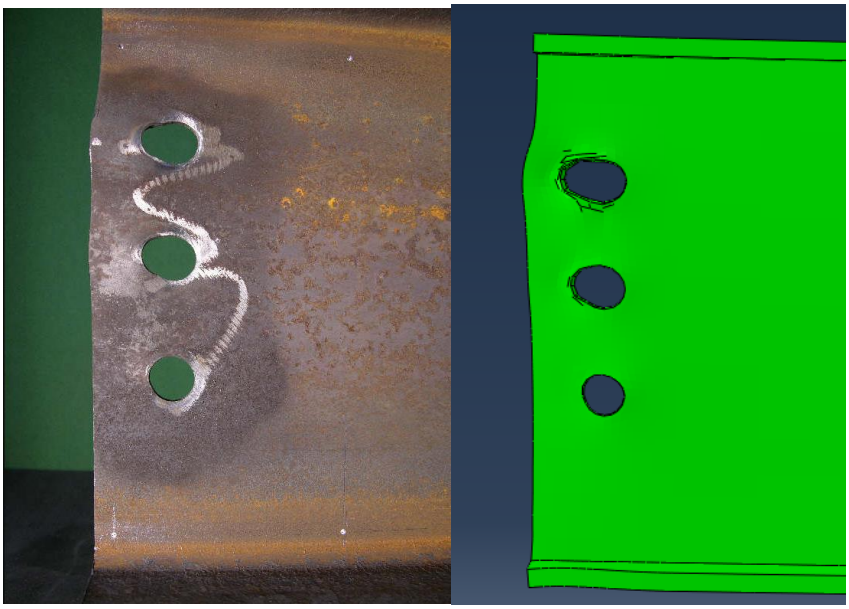

Figure 3-5 Deformation of bolt holes in beam web

Left – Experimental test observation of the deformed bolt holes at ambient temperature
Right – Finite element model of the deformed bolt holes at ambient temperature

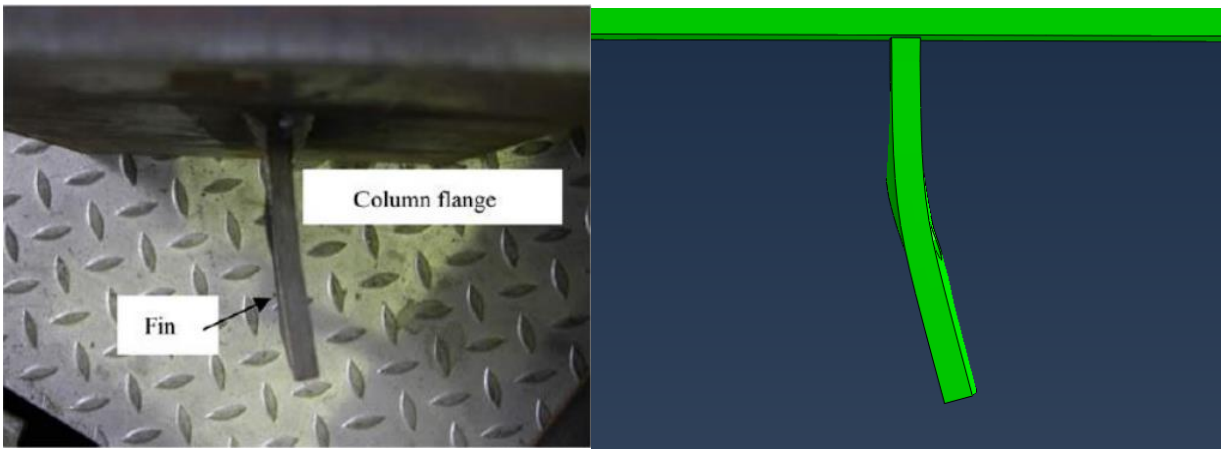

Figure 3-6 Lateral deformation of fin plates to allow for increased rotation

Left: Experimental test observation at ambient temperature
Right: Finite element model of the laterally displaced fin plate

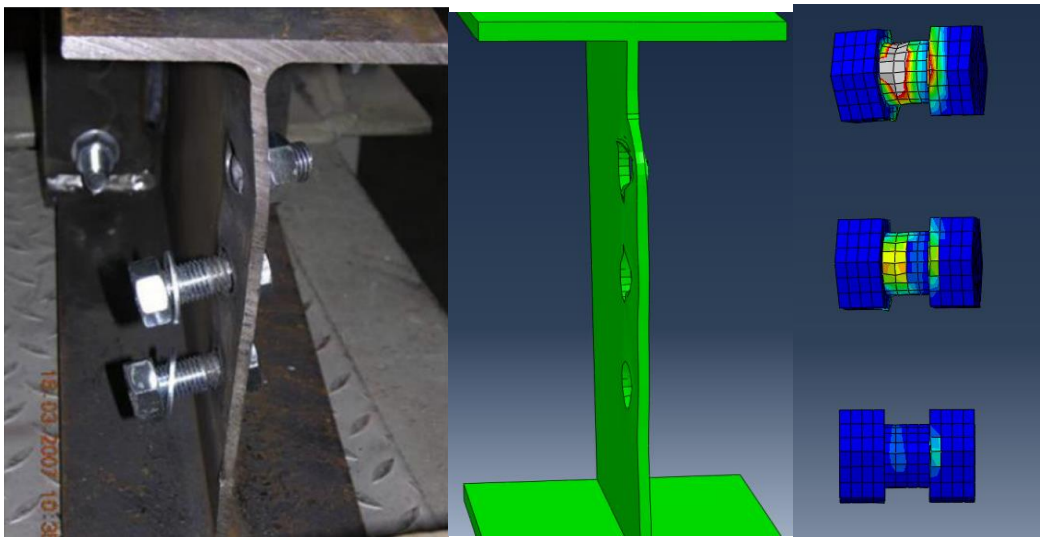

Figure 3-7 Lateral deformation of beam web and failure of bolts

Left: Experimental test observation of the deformed beam web and failure of top bolt
Center: Finite element model replicating the deformed beam web
Right: Strain contours of the bolts used in the connection in the finite element model

Similarly, the numerical model for the fin plate connection loaded at 55 degrees was able to show close agreement with the experimental results when considering the maximum sustained load and rotation as well as the relationship between force and rotation as shown in Figure 3-8. As illustrated in the figure, the documented result from the experimental test exhibits a sustained period of increasing rotation with a relatively constant load up to approximately 5 degrees. This is attributed to the way in which this particular experiment was carried out, where according to Yu et al. (2009), the specimen was loaded until approximately half its load carrying capacity before being unloaded and retested until failure. Upon being retested, the specimen had already experienced plastic deformation up to 1 mm at the bolt holes of the beam web. In order to account for the prior yielding of the experimental test, the results of the finite element analysis have been accordingly offset by approximately 5 degrees to achieve an accurate representation of the subsequent behaviours caused by additional loading.

It can be observed in Figure 3-8 that the numerical simulation of this experiment was able to capture its relatively more ductile response and lower corresponding maximum force. As per the numerical simulation with a load angle of 35 degrees which was able capture the deformations in the beam web and failure through bolt shear, the simulation used to model this experimental test was also able to reproduce its behaviour and failure mode through bolt shear. For illustrative purposes, the model under maximum rotation is shown in Figure 3-9.

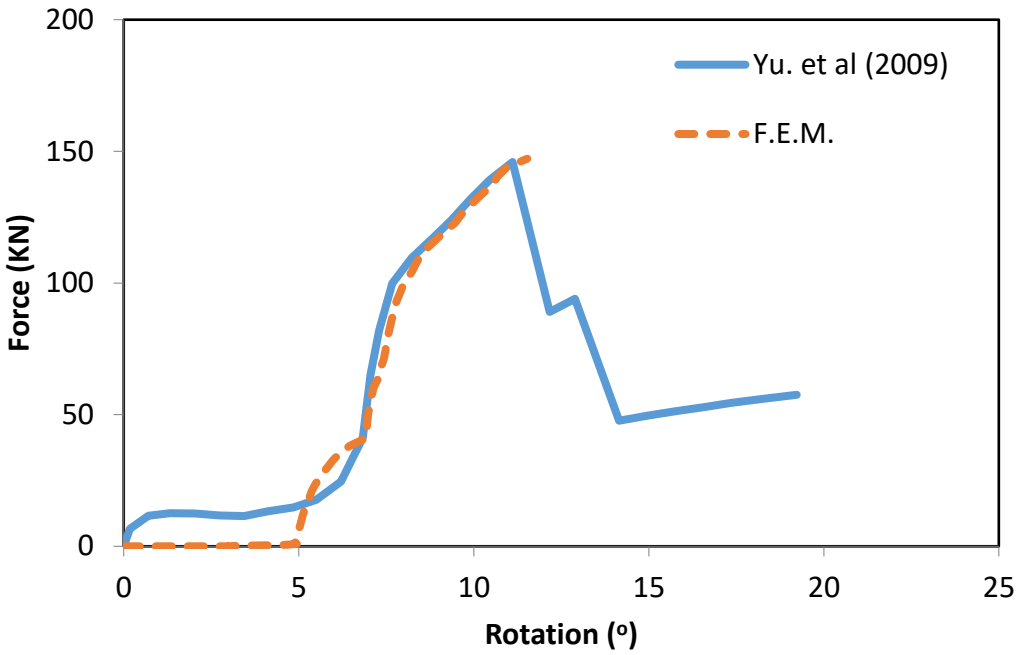

Figure 3-8 Fin Plate results at 55° loading

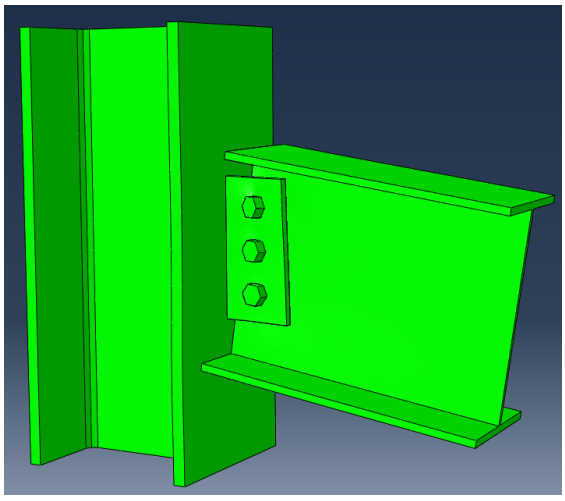

Figure 3-9 Numerical analysis with loading at 55 degrees

3.1.8 Tests at Steady State Temperatures

Yu et al. (2009) then repeated the experimental tests on the isolated connections under constant elevated temperatures, specifically at 450°C, 550°C and 650°C. Limited by the performance of the

furnace, the tested specimens were heated at a slow rate - taking approximately two hours to reach 700^{o}C. Once the specimen reaches and is maintained at the desired steady-state temperature, a load is then slowly applied at either 35^{o} or 55^{o} until the specimen undergoes failure. Although this test set up allows for a simplistic study of the performance of the various components within the fin plate connection when held at constant temperatures, it does not provide an accurate representation of the behaviour of steel connections as a part of a structural frame being exposed to the transient temperatures of real fire as discussed in Section 2.5.

The methodology of applying an increasing load to a specimen at steady state temperatures results in different behaviours of the materials. Considering the temperature dependent properties of steel provided by EC3 (shown in Figure 2-3) are based on experimental results developed by tests undertaken at transient temperatures for structural fire engineering purposes (Wang et. al, 2013), they are inapplicable in the context of steady-state studies such as that described herein (Yu et al., 2009b). Instead, the material properties of steel determined under slow loading at steady-state temperatures which are considerably different to those provided by EC3 as illustrated in Figure 3-10, have been shown to provide good correlations for modelling the behaviour of isolated flexible endplate and angle cleat connections at constant temperatures (Hu, 2009; Yu et al., 2009b). However, previously undertaken studies have shown that loading in steady state conditions, particularly in consideration of the applied strain rates have a profound effect on the overall ductility and must be considered when determining the strength of the material (Renner, 2005).

Given that the scope of this study encompasses the behaviour of steel connections exposed to fires with transient temperatures with limited considerations given to applied strain rates, and their contrasting differences with the experimental test described herein, the numerical simulation of

the fin plate experiments at elevated temperatures has not been further pursued or discussed in this study.

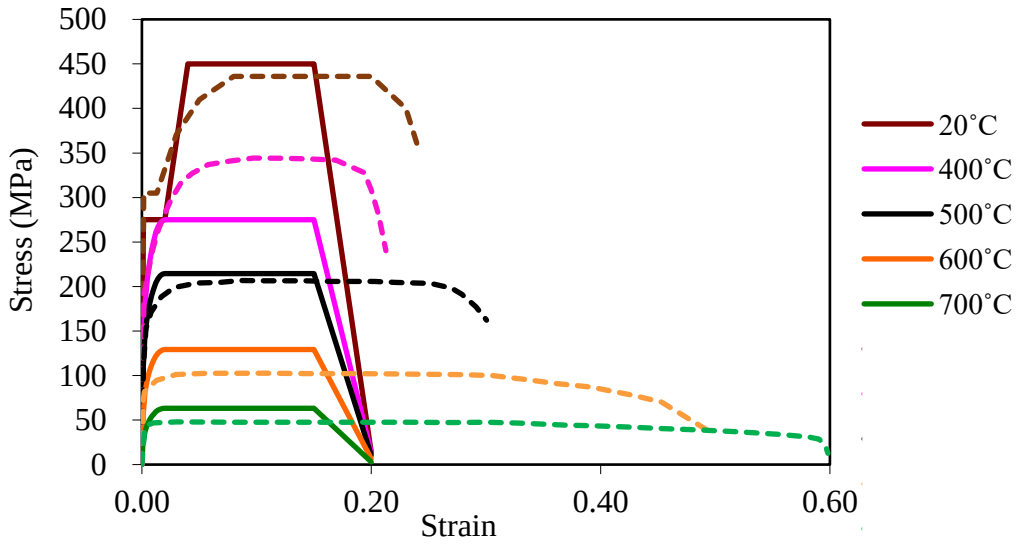

Figure 3-10 Strength of steel when subject to loading at steady state and transient temperatures (European Committee for Standardization, 2005a; Renner, 2005)

4 Development of Finite Element Models for Cardington Test 7

Once the finite element modelling of isolated steel connection was completed, it is important to model the behaviour of the connection as a component of a frame undergoing temperature changes in fire to study the influence of the external forces which form as a result of axial loads from the thermal expansion and contraction. Hence modelling a portion of a previously tested connection in the structural frame of Cardington Test 7 will provide a more realistic representation of the behaviour of connections in fire.

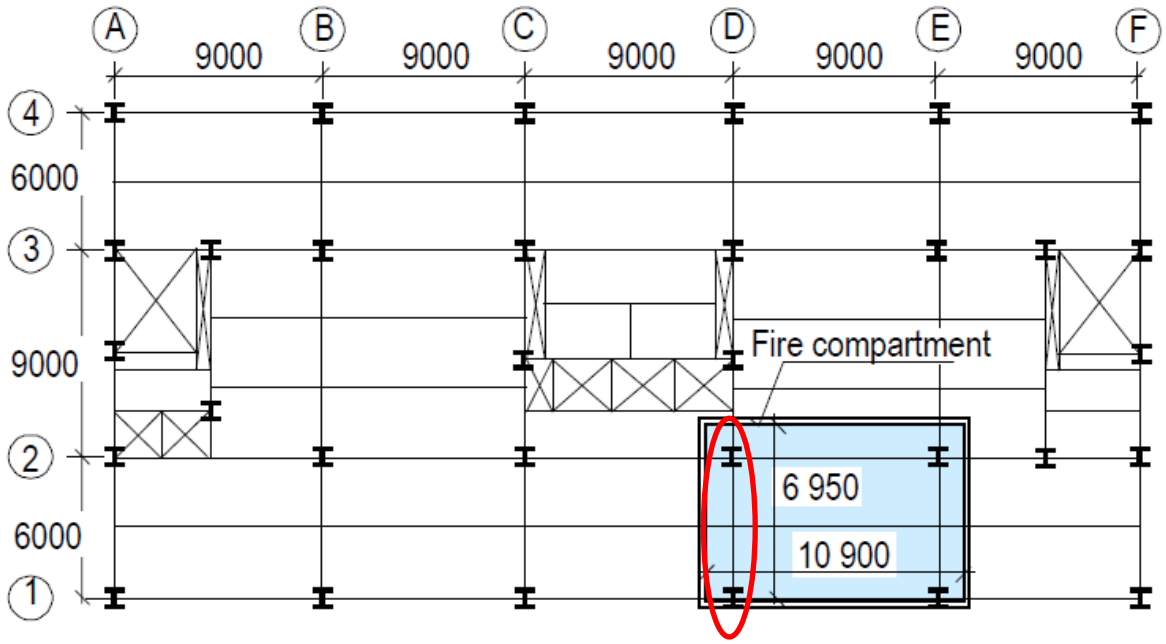

Figure 4-1 Cardington fire test layout (Wald et al., 2005)

In accordance with the scope of this study, focus is placed on studying the subassembly of the primary beam spanning between columns D2-D1 as circled in Figure 4-1 due to the reported fracture of a flexible endplate connection between the beam and column. The connection was constructed as a flexible end plate of 8 mm thickness and connected to the column using a total of 8 M20 bolts.

The recorded temperatures of the overall compartment, top and bottom flanges of the D2-D1 primary beam and bolt rows of the flexible endplate connection reported from the experiment are illustrated in Figure 4-2, with the location of the corresponding thermocouples subsequently shown in Figure 4-3 (BRE, 2004).

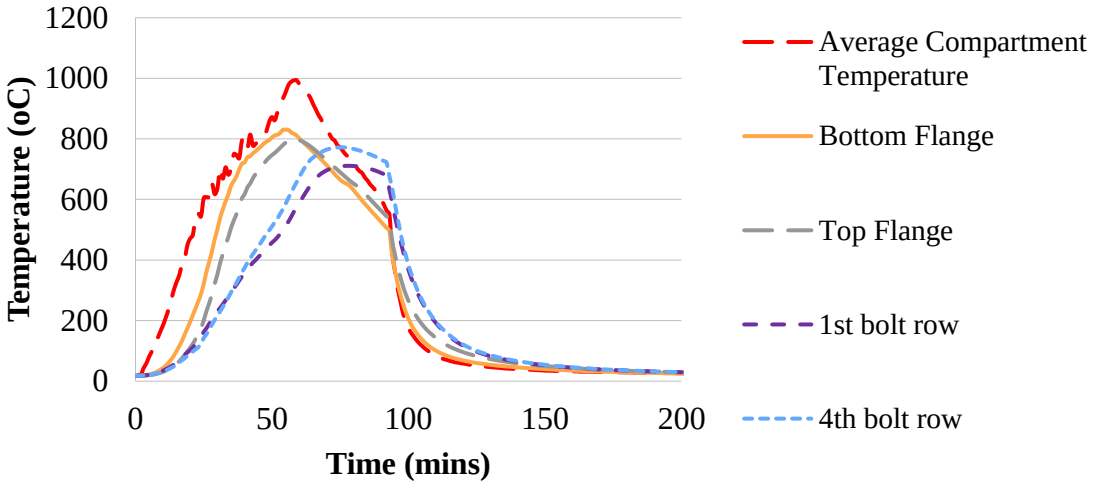

Figure 4-2 Average compartment temperature (BRE, 2004)

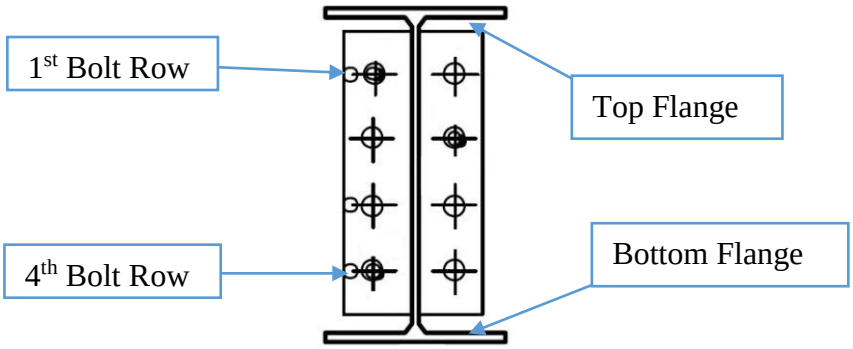

Figure 4-3 Placement of thermocouples

Regarding the behaviour of the connections in the experiment, it was observed that the buckling of the lower flange of the beam was one of the main mechanisms which occurred during the heating phase (Wald et al., 2005). Through the use of a thermal imaging camera, it was determined that as the beam underwent thermal expansion and increased deflections during heating, the beam ends

were restrained by the cooler adjacent structure while the top flange was restrained by the concrete slab. Hence, once the bottom flange of the beam came into contact with the column under continuous heating at approximately 23 minutes, the lower flange was unable to transmit forces through the column due to its higher temperatures and buckled as a result.

Upon cooling, the steel beam began to contract, leading to tensile forces on the connection which ultimately caused fracture along one side of the endplate along the weld as shown in Figure 4-4. Consequently, this allowed for the connection to behave in a more ductile manner by allowing larger deformations without failure.

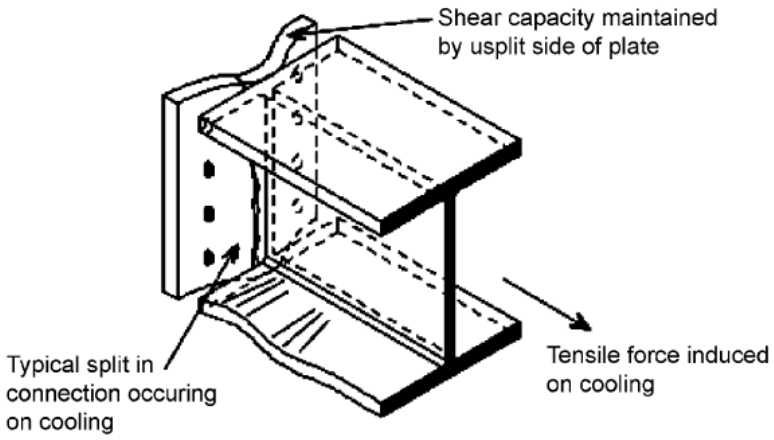

Figure 4-4 Fracture of endplate during cooling phase of the fire (Al-Jabri et al., 2007)

Hence, based on the reported data and observations from the experimental test of the flexible endplate connection, this section of the study is dedicated to recreating the behaviour of this particular connection through the use of finite element modelling.

4.1.1 Finite element model description

In order to incorporate the transient temperatures of the test, a sequentially uncoupled thermo-mechanical analysis was required to be undertaken to accurately represent the material and

geometric variations with elevating and decreasing temperatures as a result of the fire. This firstly required a thermal heat transfer analysis to be undertaken to calculate the temperature distributions throughout the cross section at each time step without considering the effects caused by loading. The temperatures calculated from the heat transfer analysis are then directly integrated into the mechanical model once loads have been applied to determine the deformed shape with respect to time and temperature.

4.1.2 Heat Transfer Model

The heat transfer model was conducted by using the "Heat transfer (transient)" capability of Abaqus/Standard, which utilises sets of standardised equations to calculate heat conduction through solid materials. These equations are explained in detail by (ABAQUS, 2014b), and are widely available in literature.

For the purpose of determining the heat transfer through a structural frame, the main methods of heat transfer considered in this study are the radiative and convective heat transfer from the compartment/fire, and the conduction of heat through the specimen.

4.1.2.1 Assembly

To achieve coherence between the experimental test and the finite element model, the steel components created in the model such as the beam, column, and flexible endplate connection were of the same scale and featured the same detailing as the components used in the experimental test, with the connection highlighted in Figure 4-5.

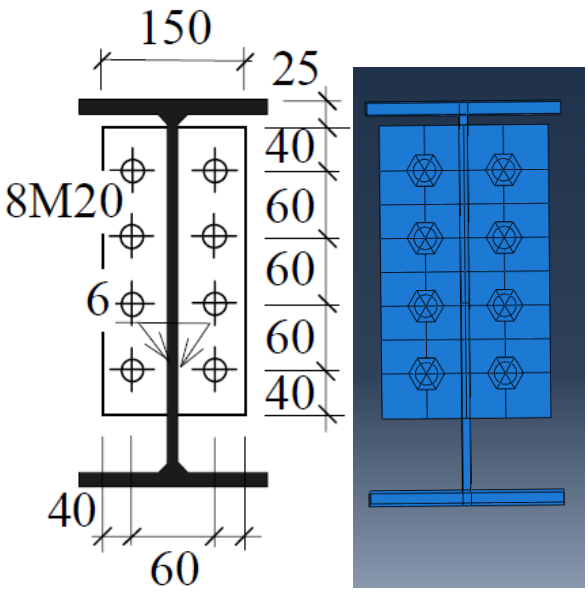

Figure 4-5 Flexible endplate detail (left) and finite element assembly (right)

For the purpose of achieving simplicity in the finite element model, the width and depth of the composite concrete slab were determined in accordance with Eurocode 4, with the effective width being taken as L/4, and the 100 mm effective thickness of the trapezoidal slab being calculated as per Equation (4-1) below (European Committee for Standardization, 2005b):

$$h_{eff} = h_1 + 0.5h_2(l_1 + l_2)/(l_1 + l_3) \quad (4\text{-}1)$$

The full assembly used in this finite element model is shown in Figure 4-6. In order to achieve increased computational efficiency, only half of the beam of interest is modelled, with the remaining half being simulated by the "Symmetry" boundary condition to reduce the time taken to undertake simulations. As shown in Figure 4-6, only a 700 mm length of the connecting 305 x 305 x 198 UC column was modelled in this analysis. This was to represent the internal column in the experimental study, where protection was applied up to the underside of the connecting beam in order to place emphasis on the behaviour of the connection (BRE, 2004).

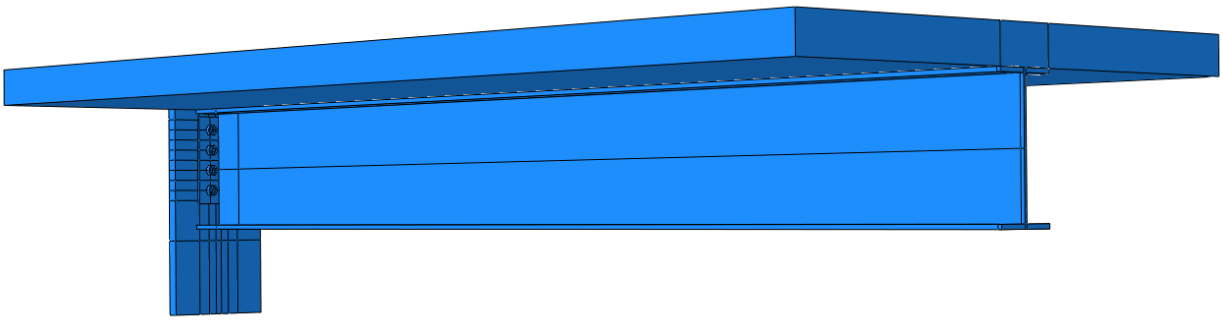

Figure 4-6 Model of Cardington sub assembly

4.1.2.2 Element Type

The element type used for the three-dimensional analysis was the DCC3D8D 8-node linear convection/diffusion heat transfer brick. Each node of this element possesses temperature degrees of freedom and are best suited for heat transfer analysis (ABAQUS, 2014b).

4.1.2.3 Material Properties

To accurately model heat transfer, the finite element model requires an accurate representation of the properties of the material. In particular, the properties: specific heat, density, conductivity, and thermal expansion are paramount in accurately calculating the temperature distribution throughout the subassembly.

In regards to the thermal properties of steel, the density is taken as 7850kg/m^3 over the range of exposed temperatures, with values for specific heat and thermal conductivity being taken based on the equations provided by Eurocode 4 as illustrated in Figure 4-7 below.

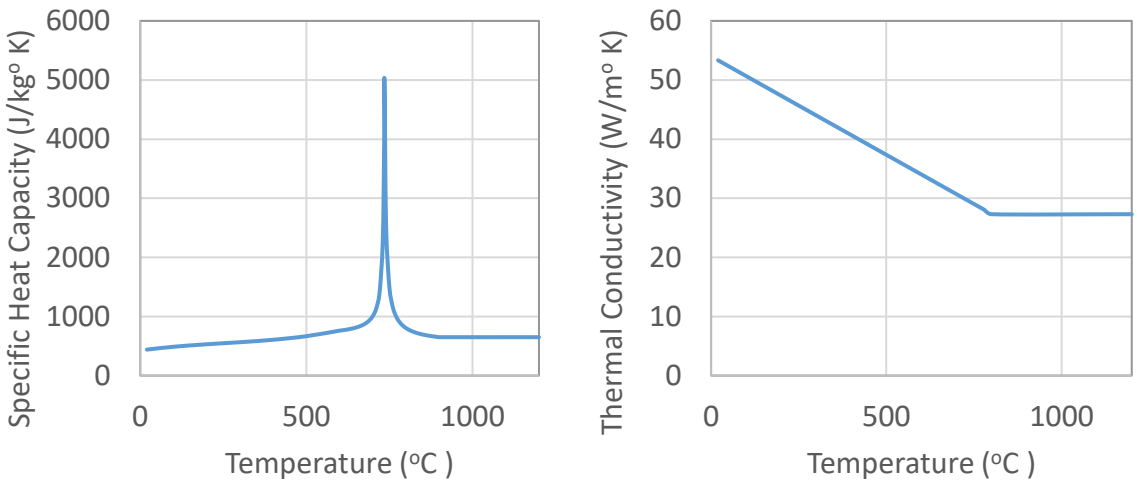

Figure 4-7 Specific heat (left) and thermal conductivity (right) of carbon steels with respect to temperature (European Committee for Standardization, 2005a)

On the other hand, the density of concrete was modelled to vary with temperature as per the suggestion of Eurocode 2 (European Committee for Standardization, 2004a), while the specific heat, thermal conductivity and thermal expansion for concrete used in the model was based on the equations provided by Eurocode 2 for siliceous concrete. The material property inputs for concrete are shown in Figure 4-8 below.

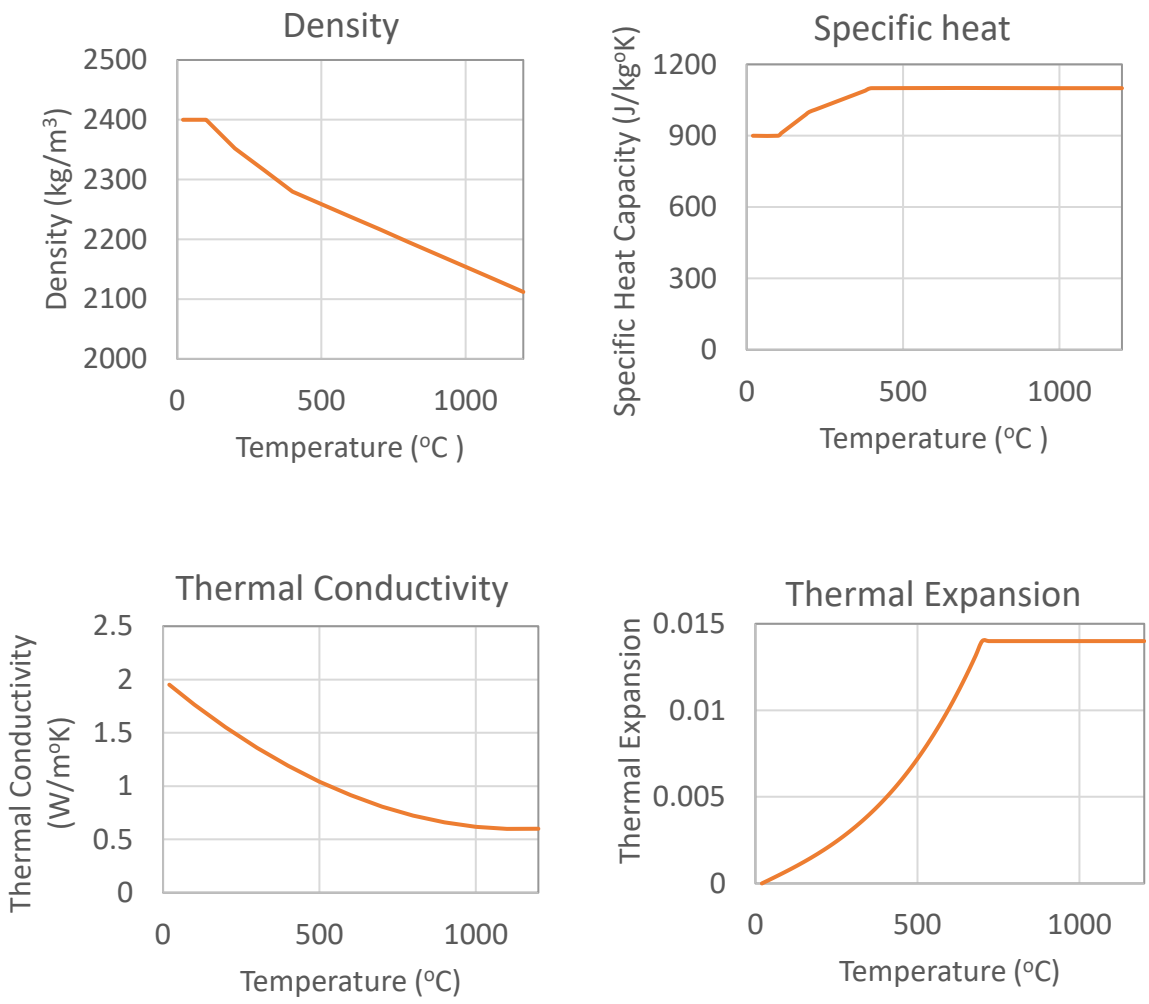

Figure 4-8 Material property input for concrete (European Committee for Standardization, 2005b)

4.1.2.4 Model Interactions

To replicate the temperatures experienced by the different structural components during the experiment, the recorded temperatures at various locations of the subassembly were tailored using an iterative approach and applied to the corresponding surfaces of the subassembly through radiation and conduction. The coefficient of heat transfer by convection was specified in accordance with the values recommended by Eurocode 1 for a parametric fire with the

consideration of convective and radiative losses, where surfaces exposed and unexposed to the fire use the values of 35W/m^{2}K and 4W/m^{2}K respectively (European Committee for Standardization, 2002). Similarly, the emissivity coefficient for heat transfer by radiation was 0.8 (European Committee for Standardization, 2005a). While the temperature of the compartment above was not measured in the experiment, the top surface of the concrete floor slab was modelled to be exposed to a constant temperature of 20^{o}C to conservatively represent ambient temperatures in the floor above.

With this model being used for heat transfer analysis, it was not necessary to consider the contact interactions between various surfaces or structural boundary conditions, and hence were not specified in this model.

4.1.2.5 Heat Transfer Model Results

Generally, the resulting temperatures gained from the heat transfer model (HTM) produced agreeable results in comparison to the temperatures experienced by the steel components of the experiment (EXP), where the temperatures for various parts of the subassembly are illustrated in Figure 4-9 and Figure 4-10. Figure 4-11 shows an illustration of the model where the steel beam reaches the maximum temperature of 830^{o}C at 56 minutes.

In comparison to the average compartment temperatures shown in Figure 4-9, the maximum temperature of the steel beam in both the experiment and heat transfer model is approximately 170 degrees lower than the maximum average compartment temperature. Although it is observed that the heating of the steel beam in the heat transfer model closely follows those recorded in the experiment, the top flange of the steel beam cools at a relatively slower rate. This discrepancy is considered to arise from the simplification in the modelling of the concrete floor slab which is in

direct contact with the top flange, without considering the influence of the steel decking. Given that concrete has a considerably lower thermal conductivity and ability to dissipate heat, it would have caused the top flange to cool at a slower rate.

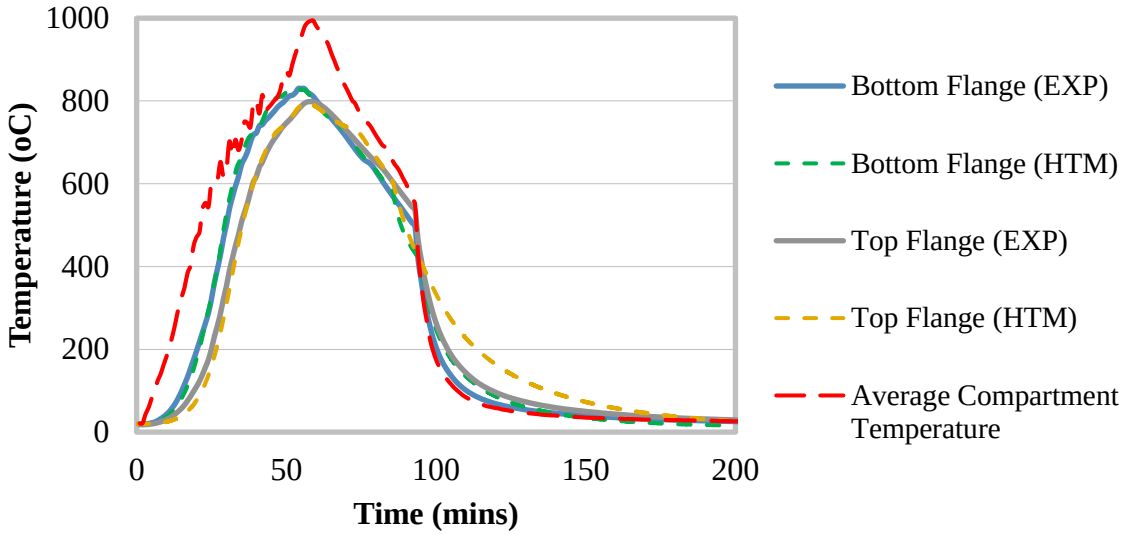

Figure 4-9 Temperatures in steel beam

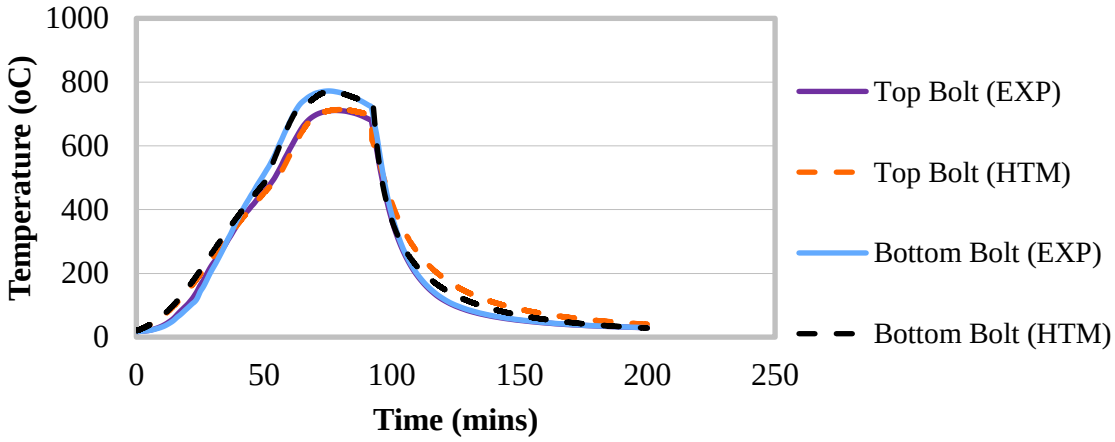

Figure 4-10 Temperatures at the connection

The temperature in the flexible endplate connection at the end of the beam are shown in Figure 4-10, where the values are taken adjacent to the top and bottom bolts as per the experimental test.

It is illustrated in this figure that the temperature rise at the connection is slower than that of the beam, while reaching a notably lower maximum temperature by approximately 100°C compared to the bottom flange of the connecting beam. It is also recognised that a temperature gradient exists along the depth of the connection, with the top bolt row being cooler than the bottom bolt row due to shielding by the column and adjacent slab (Wald et al., 2005).

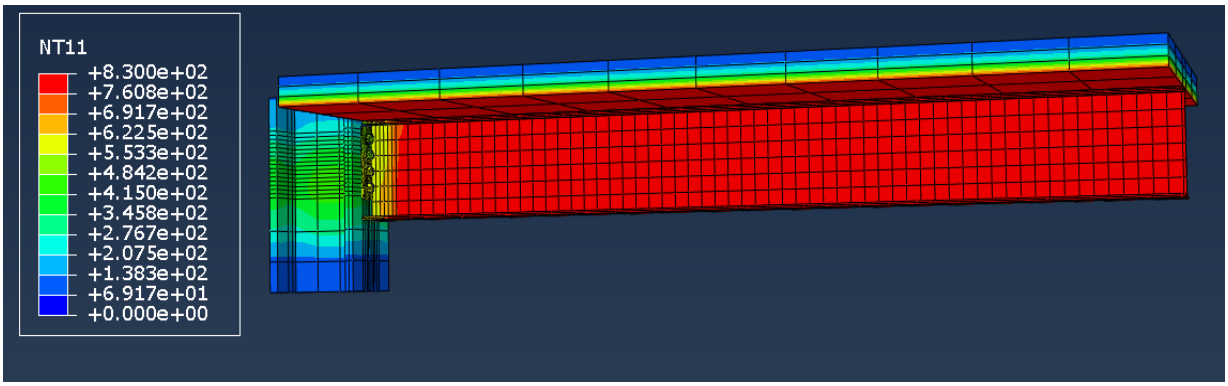

Figure 4-11 Heat transfer model at 56 minutes

4.1.3 Mechanical Model

4.1.3.1 Assembly

The assembly of the model for the mechanical analysis was identical to that of the heat transfer analysis in order to ensure that variations in temperature throughout the subassembly are able to be transferred into the mechanical model. Described as a sequentially coupled thermal-stress analysis (Mago et al., 2014), the methodology used in this study incorporates the thermal stresses into the analysis through a two-step approach. In Step 1, gravity/imposed loads are applied and held constant until the completion of the simulation In Step 2, the results of the thermal analysis are embedded into the model, which takes the variation of material properties with temperature into account. The application of this methodology considers that the existence of gravity/imposed

loading has a negligible effect on the thermal resistance and hence the temperature distribution throughout the subassembly.

The model created to represent the Cardington test followed the same approach to the isolated connections as described in Section 3.1 in regards to the selection of the finite element modelling package ABAQUS/Explicit, and the element type C3D8R for the mechanical analysis. Similar to the earlier models created in this study, the mechanical model for the Cardington subassembly was created using ABAQUS/Explicit due to its advantage in overcoming the convergence issues experienced by ABAQUS/Standard as a result of the large number of surfaces repeatedly coming in and out of contact during the analysis. As per the previous models, the three dimensional brick model with 8 gauss points and reduced integration (C3D8R) was used for this mechanical analysis based on its ability to control hourglass modes.

4.1.3.2 Material Properties

The material properties used in the finite element model were taken from the ambient temperature tests at the Cardington experiment and shown in Table 4-1(Lennon and Moore, 2004). Young's modulus was taken as 207 GPa for all steel members, with the properties for hot rolled steels at elevated temperatures being calculated from EC3 and the properties of bolts from Kirby (1995). Accordingly, the strength properties of concrete were determined using as per Eurocode 4 and are subsequently shown in Table 4-1.

Table 4-1 Material properties

E (GPA)		F_y (MPa)			F_u (MPa)			F (MPa)
Steel	**Concrete**	**S355**	**Plate**	**Bolt**	**S355**	**Plate**	**Bolt**	**Concrete**
207	32.04	396	275	695	544	430	869	644

4.1.3.3 Contact modelling

In accordance with Section 3.1.4, the "finite sliding" formulation was used with a friction co-efficient of 0.3 for all tangential contact surfaces, while the "hard" contact formulation was used for all normal contact surfaces. The "TIE" command, which assumes a perfect bond, was used to represent the welded section between the beam and the endplate due to current limitations of modelling welds at elevated temperatures (Selamet and Garlock, 2014).

Additionally, as the study of the behaviour of shear connectors is beyond the scope of this study, this model assumes full composite behaviour between the top flange of the steel beam and underside of the concrete slab by using the "TIE" command between the two surfaces as illustrated in Figure 4-12 below.

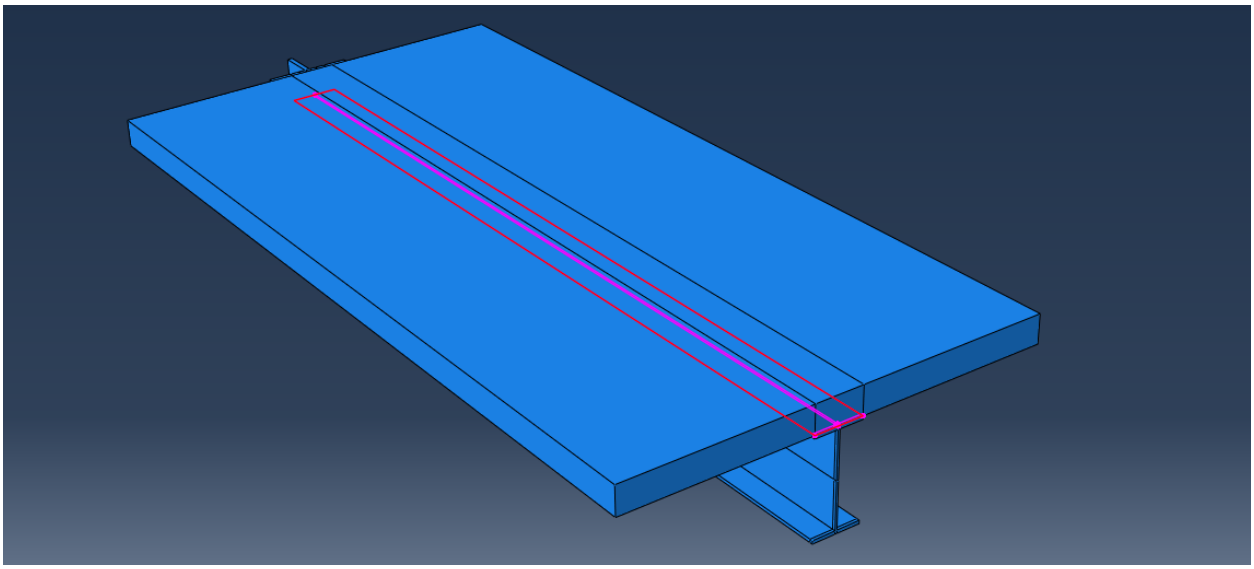

Figure 4-12 Interaction between steel beam and concrete slab

4.1.3.4 Boundary Conditions and Loading

As only part of the subassembly was modelled to maximise computational efficiency, the boundary conditions assumed in the analysis is critical for accurately reproducing the results gained from the experimental study. The boundary conditions used in the model were set in order to most accurately represent the conditions experienced by the structural members throughout the experiment, and are summarised in Table 4-2 below, where the term “encastre” refers to a fixed condition.

Table 4-2 Boundary Conditions

Component	Set	Boundary Condition	Assembly
Column	Top and bottom faces	Encastre	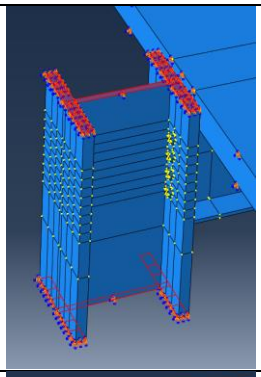
Concrete Slab	Face adjacent to column	Encastre	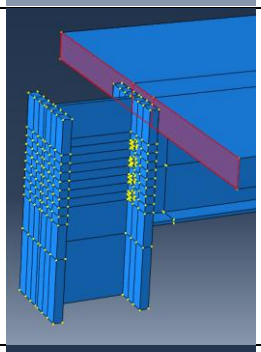
Beam	Lateral restraint of top face	UR2=0	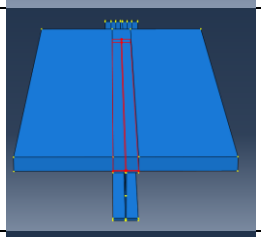
Beam and Concrete slab	End face	Symmetry (YSYMM)	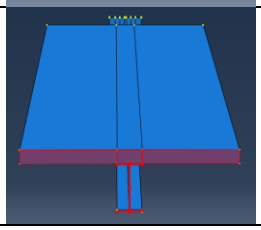

Considering the combined dead and live load of 7.15kN/m^2 on the fire floor as discussed in Section 4 and the layout of the frame system, it was determined that the primary beam considered in this analysis was to sustain a point load at mid-span of 193.05kN from the connecting secondary beams. In the finite element model, this load was applied to the beam web at the end face to simulate the shear forces caused by connection between the beams.

4.1.3.5 Results

To validate the results obtained by the model, the mid-span deflection of the subassembly determined by the finite element analysis is compared to that measured in the experimental test. Generally, finite element model was able to replicate reasonably well the deflection of the measured experimental results during the heating and cooling phases, with comparative results being shown in Figure 4-13.

As per Figure 4-13, the deflection results gained from the finite element model begins to deviate slightly from the experimental results at approximately t=40 minutes, with the deviation increasing for the remainder of the heating phase. This deviation may be explained by the method used in modelling the temperature distribution throughout the beam, as given that the experimental data for the temperature of the steel beam was only recorded at two locations (mid-span and near the connection), an assumption was made in the heat transfer model where the beam experiences a uniform temperature throughout its length. Comparatively, the temperatures within fire compartments are likely to be non-uniform (Welch et al., 2007) and therefore cause variations in the temperature of the beam and ultimately lead to differences between the deflections shown in Figure 4-13.

Additionally, the beam in the experiment featured 1 m of coated length measured from column D1 which provided a 90 minute fire resistance rating through the use of CAFCO C300 (BRE, 2004). This was not taken into account in the numerical analysis due to the lack of measured temperatures at the protected section of the beam. As a result, the vertical displacement of the beam of the finite element analysis increases at a higher rate while reaching an increased maximum deflection compared to that of the experimental study.

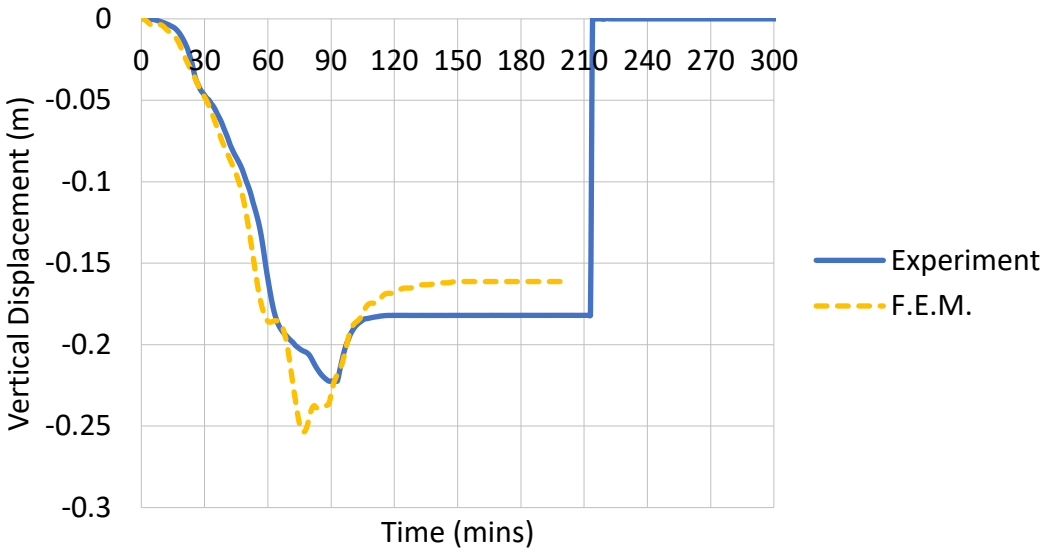

Figure 4-13 Experimental and modelled vertical deflection of the D2-D1 beam

In the plot of vertical deflection of the numerical analysis in Figure 4-13**,** it can be seen that steep downward deflection gradient momentarily stalls at approximately 60 minutes. Upon inspection of the temperatures throughout the beam at this time step as per Figure 4-9, it can be determined that this is the period of which the beam experiences peak temperatures upwards of 750^{o}C - and subsequently lowest strength. Giving consideration to the relationship between temperature and thermal expansion of steel as prescribed by EC3, is at temperatures between 750^{o}C and 860^{o}C where the expansion of the material stalls as it undergoes a phase change. As a result, the lack of continuous thermal expansion during the said temperatures along with the uniform temperatures throughout the beam in the numerical analysis leads to the momentarily stalled displacement, especially considering the entire length of the beam was exposed to uniform temperatures throughout the analysis. The experimental data also reflects this effect as the recorded deflection can be seen to decelerate at a similar time, although to a lesser extent, which can be attributed to the beam in the physical test experiencing a distribution of temperatures throughout its length due

to the non-uniformity of the temperatures in a compartment fire. Furthermore this may also be attributed to the top of the concrete slab being modelled to be exposed to a constant temperature of 20ºC due to the lack of experimental data in the compartment above as discussed Chapter 4.1.2.4, which may induce additional forces in the beam due to potential temperature differences.

An additional discrepancy between the finite element model and the experiment is the recovery of vertical displacement during the cooling phase of the fire as a result of steel regaining stiffness. Comparatively, the finite element model recovers 36% of the maximum vertical deflection at mid-span, whereas the experiment recovers 18%. This can be rationalised by observations of the experiment, where it was reported that the concrete slab experienced cracking as shown in Figure 4-14, in turn leading to irreversible deflections which was not considered within the scope of this study. Hence, the recovery of vertical deflection in the experiment is reduced compared to that of the numerical study where cracking was not modelled.

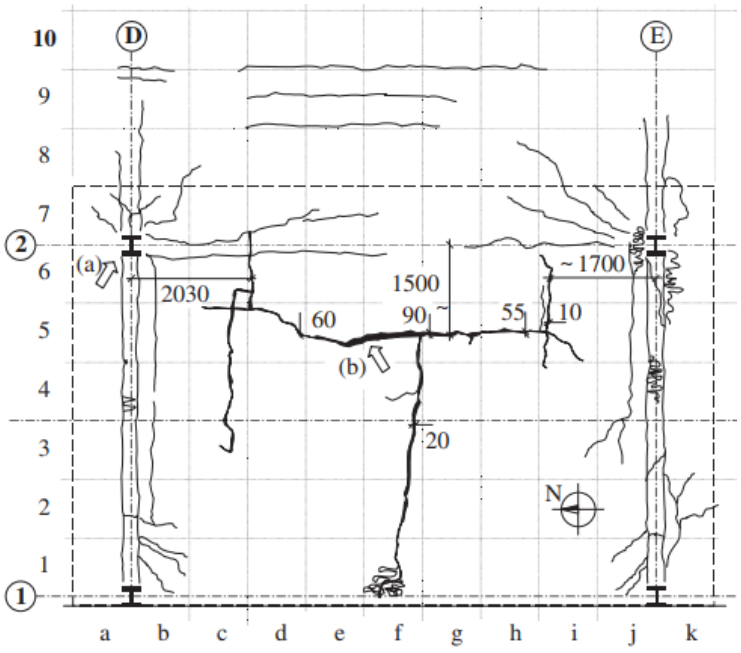

Figure 4-14 Cracks in the concrete slab at the Cardington experiment (Wald et. al, 2005)

Upon observation of the structural components in the subassembly, it was exemplified that the finite element model was able to largely reproduce the behaviours experienced by the flexible end plate components of the connection in the Cardington experiment, where it had been reported that the flexible endplate connection in the experimental study experienced tensile fracture as a result of the contraction of the connecting beam during cooling.

This behaviour is able to be apprehended and analysed through the finite element analysis output as shown in Figure 4-15, which demonstrates the effect of heating and cooling the steel beam. As the temperature of the steel beam begins to increase as a result of rising compartment temperatures caused by the fire, it can be observed that the axial force within the beam changes from its initial tensile condition to acting in compression as signified by the positive and negative x-axis in Figure 4-15. The axial compression force in the beam can be observed to then increase at a consistent but rapid rate between the time periods of 10 to 25 minutes in comparison to the earlier stages, which is a direct reflection of the temperature increase in the beam as shown in Figure 4-9. During this period, the steel retains majority of its strength and mid-span deflections remain relatively low, hence thermal expansion is prevented at this stage and in turn creating an axial force against the connection.

At the time of 25 minutes, the thermal expansion caused by increased temperatures in the beam lead to the exertion of a maximum axial compression force of 603kN against the endplate, where the axial forces then rapidly decrease. Although the beam was undergoing a further increase of temperature and thermal expansion during this period, it was observed that this was the time which the bottom flange of the beam came into contact with the column as shown in Figure 4-16. It is also the time at which the temperature of the steel beam reaches upwards of 400^{o}C, where the strength of the material beings to decrease rapidly. Therefore, as the beam continues to rise in

temperature, the material undergoes further expansion, causing the bottom flange to yield against the column as shown in Figure 4-19 and causing the axial compression to decrease as a result. Eventually as the steel beam loses majority of its load carrying capacity due to the high temperatures, the deflection of the beam increases rapidly – generating tensile forces in the member as it undergoes catenary action (Wang et al., 2013). This observation is consistent with those reported by Wald et al. (2005), where it was reported that the bottom flange of the beam came into contact at approximately 23 minutes, and had experienced buckling upon further heating.

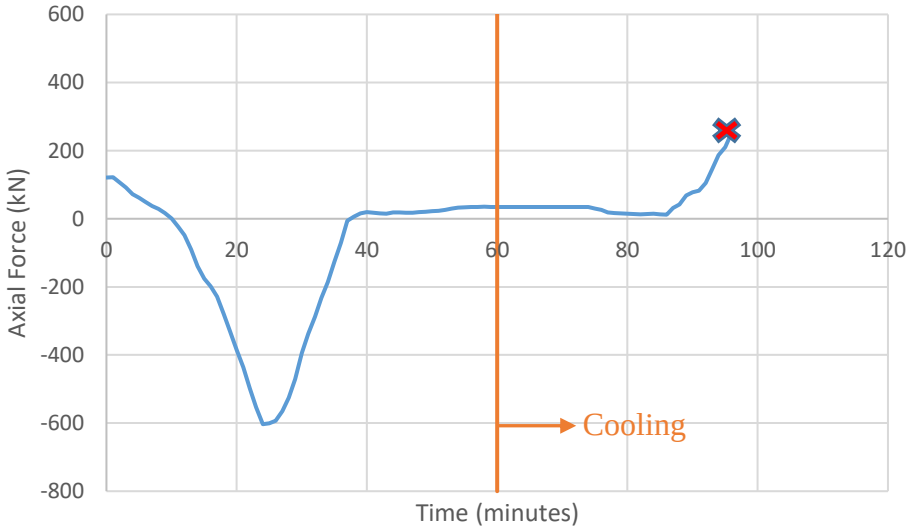

Figure 4-15 Axial force in the beam due to thermal effects

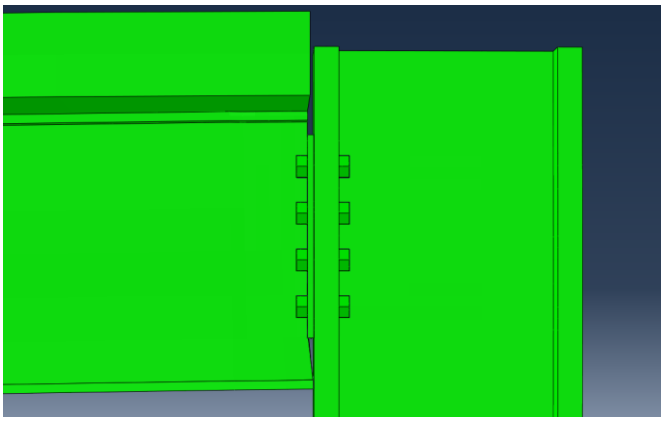

Figure 4-16 Contact between the beam and column at 23 minutes

Upon cooling, the steel beam forces reverse as it contracts, in turn exerting an increasing tension force of up to 278 kN on the connection. As the beam cools over time, it causes an out-of-plane yielding of the flexible endplate, and ultimately leading to fracture of the plate at the time of approximately 94 minutes as shown by plastic yielding throughout the length of the endplate. The significant yielding of the endplate was able to be modelled as shown in the figures below, where Figure 4-17 and illustrates the contracting beam causing the endplate to yield and fail as indicated by the areas shaded in grey which highlights areas which have experienced strains above 0.2, while Figure 4-19 shows the failure along the length of the endplate section.

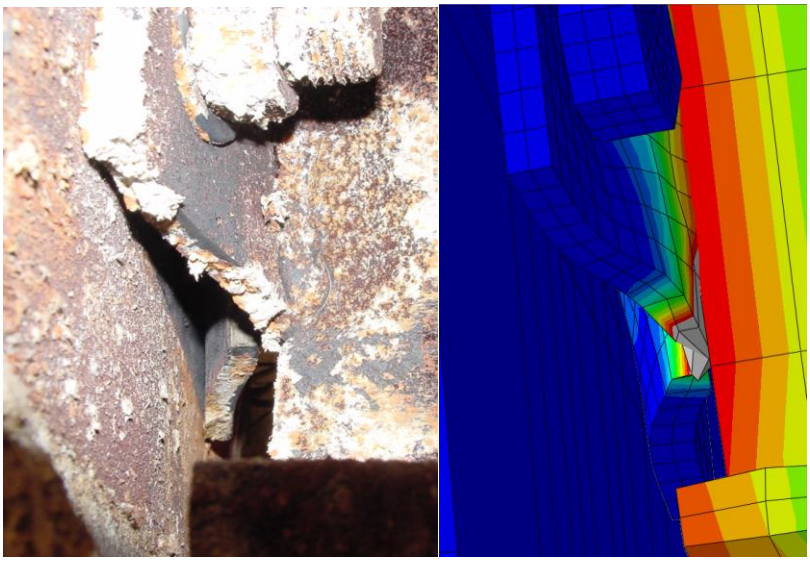

Figure 4-17 Yielding of flexible end plate. Left: Cardington experiment (Borges, 2003). Right: Finite element analysis

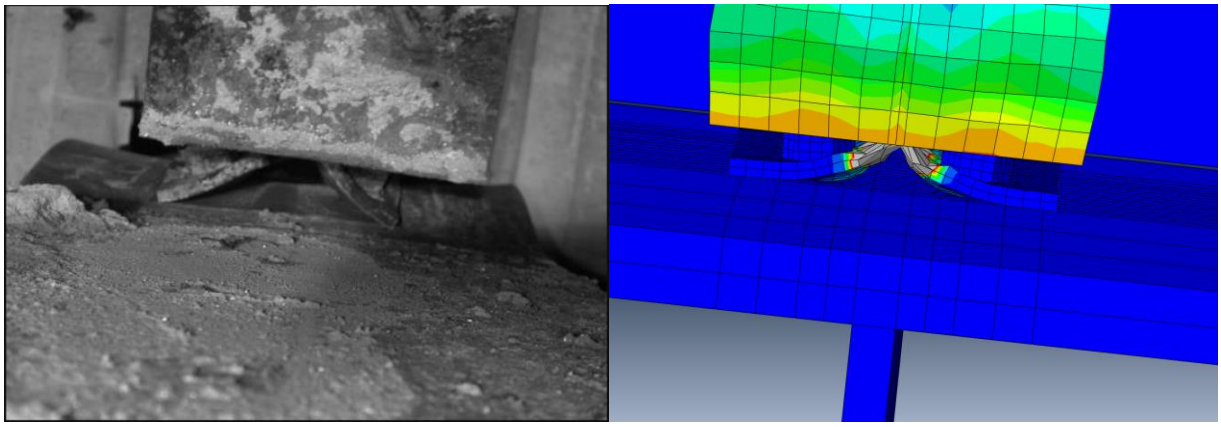

Figure 4-18 View of connection from below.

Left: Cardington experiment (Borges, 2003). Right: Finite element analysis

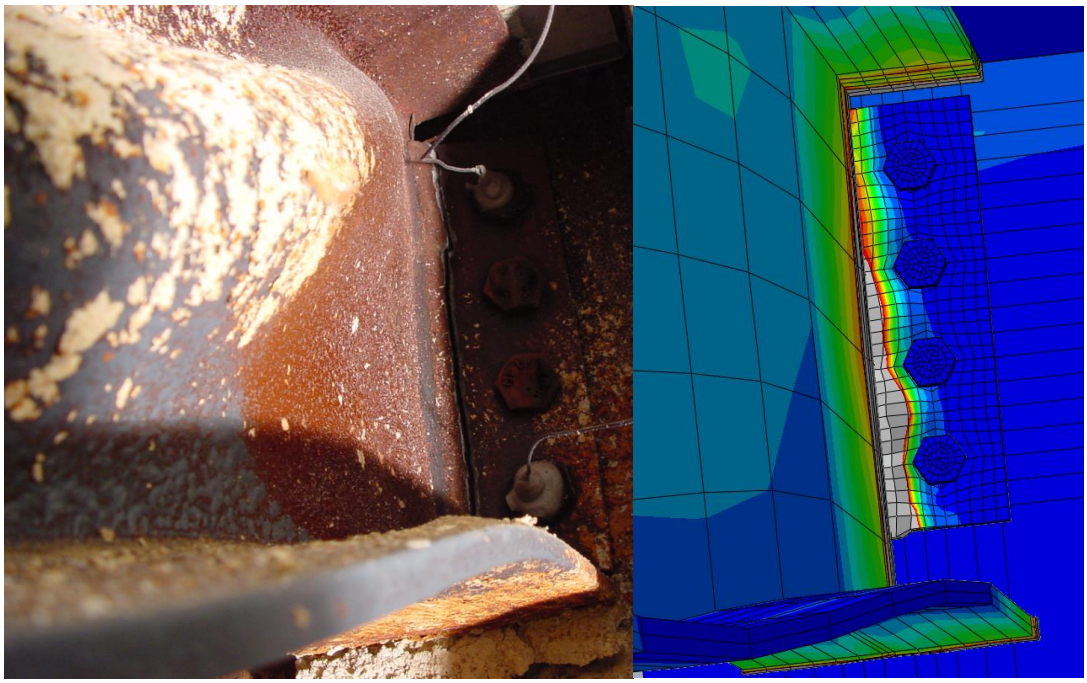

Figure 4-19 Fracture of flexible endplate and yielding of bottom flange.
Left: Cardington experiment (Borges, 2003). Right: Finite element analysis

As shown in Figure 4-19, a discrepancy exists in regards to the behaviour of the web of the connecting beam when comparing the observations in the numerical and experimental studies. While the beam in the experimental test experienced buckling in the web, this action was not presented in the finite element analysis since the deformation may have been a consequence of column shortening – a phenomenon generated by the thermal elongation of a column during the heating phase, where it compresses against fixed restraints (Shepherd and Burgess, 2011). Although this was not taken into consideration in the finite element model which featured a 700 mm section of the connected column, the subassembly modelled herein provides a comparison of the connection, whereas the difference in the observed behaviours may be due to the effect of the column which may warrant further study for confirmation.

The lack of buckling in beam web of the numerical simulation can also be attributed to various factors resulting from the method in which the model was assembled. Given that the model was

limited to the subassembly between columns D1 and D2 with the slab taken as an effective thickness for simplification, the influence of the neighbouring structural systems, particularly the floor slab, was not considered in this analysis. As per (Wald et al., 2005), the floor slab in the experimental test underwent a maximum deflection of 925 mm whilst maintaining structural integrity as shown in Figure 4-20 - significantly higher than the 222 mm maximum deflection of the D2-D1 primary beam. This phenomenon is due to the occurrence of tensile membrane action (Bednář et al., 2012), based on the principle that the slab is able to resist the loads through stretching of the reinforcement mesh and placing the reinforcement at the centre of the slab through tension (Wang, 2002) . Subsequently, the load from this action is then transferred to the supporting beams, where combined with the differentially stresses arising from the differential temperatures throughout the section, leads to rotation and contribution towards the buckling of the beam webs.

Figure 4-20 Deflection of floor slab (Wald et al., 2005)

Additionally, the welded area between the endplate and the connecting beam web was simulated using the "Tie" command in ABAQUS which assumes a perfect bond between the two surfaces in order to substitute for the current lack of data for modelling the behaviour of welds using finite elements. Because the "Tie" constraint ties two surfaces together so that there is no relative motion

between them (ABAQUS, 2014b), it also provides some restraint for the beam web against buckling, however the weld also provides this as long as its integrity is maintained. However it does mean that the bearing area of the beam web onto the endplate in the model is much less than it was in practice, being through the double sided fillet weld, allowing the compression stresses in the model to cause compression bearing failure in the model as shown in Figure 4-21 which is not observed in practice during the heating phase. . In order to appropriately account for this discrepancy between the modelling results and the experimental test, strains occurring at the endplate as a result of compressive yielding were not considered in the post-processing of results.

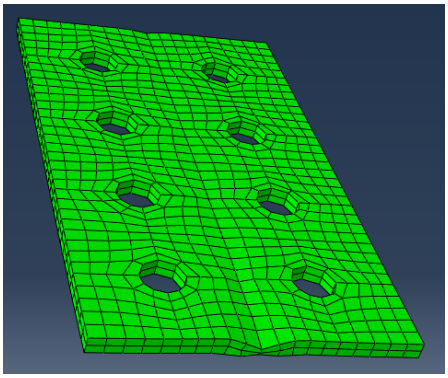

Figure 4-21 Bearing into endplate during heating

The structural behaviour of the endplate component in the connection is highlighted in Figure 4-22 which illustrates the strain experienced along the depth of the endplate at various temperatures during cooling where the strain was measured along the centreline of the plate.

As indicated in the figure below, the top and bottom of the endplate begins to experience strains when the bottom flange of the beam is at 800^{o}C, shortly after the cooling phase begins. Referring to the results from the heat transfer model illustrated in Figure 4-9 Figure 4-10, it can be seen that as the bottom flange of the beam starts to cool and regain strength, the top flange simultaneously

reaches its maximum temperature of approximately 800°C while the connection is still experiencing heating. As a result of the effects caused by the differential stresses caused by temperature differences in addition to the hogging of the steel beam, strains can be seen to develop particularly at the ends of the endplate during this time.

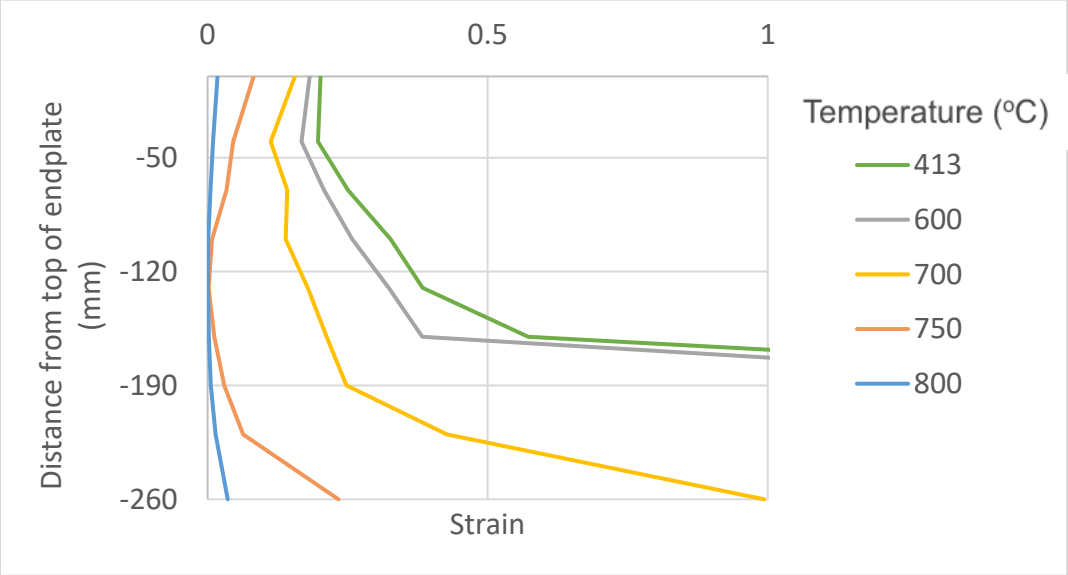

Figure 4-22 Strain along depth of endplate during cooling

\

In accordance of the heat transfer results indicating that the top and bottom flanges of the connected beam cool at a simultaneous rate between 800°C and 700°C, the contraction of the beam throughout its depth is expected to be relatively uniform during this period. Referring to the strains induced in the endplate, it is exemplified at the temperature of 750°C that the top and bottom ends of the plate are first to undergo yielding, of which they are most susceptible, due to being restrained by bolts from only one end. At this point, it can be observed that the base of the endplate exceeds the failure strain of 0.2. With the base of the endplate losing its load carrying capacity due to surpassing the failure strain, the yielding at the base of the plate is then propagated upwards at a rapid rate in

comparison to the upper parts of the endplate as the connected subassembly experiences further cooling and contraction.

Moreover, it can be observed in Figure 4-22 that the upper sections of the endplate appears to undergo significantly less strain compared to that of lower sections throughout the cooling process. With the bottom flange of the beam reaching higher temperatures than the top flange, it is expected that the temperature gradient causes lower parts of the beam to experience relatively higher amounts of contraction – hence leading to lower levels of strain. Additionally, considering that the top flange of the steel beam is attached to the base of the supported concrete slab, and the differences in the thermal expansion and contraction between the two materials, the slab can be accredited to restraining the top section of the beam against excessive horizontal displacements. Nonetheless, the failure strain of 0.2 is eventually met throughout the depth of the endplate at approximately 94 minutes into the analysis when the steel beam cools to approximately 413^{o}C. With reference to the observations of the experimental test, the numerical analysis is able to show the behavior of the endplate in the Cardington Test which was reported to fracture along the depth of the plate. In the tests, the fracture occurs on one side which allows the other side to deform as a one sided connected plate thus maintaining the vertical load path through the beam into the plate and row of bolts attached to the column.

Table 4-3 Strain contour of the endplate at different temperatures during cooling

800ºC	700ºC	600ºC	413ºC	Key
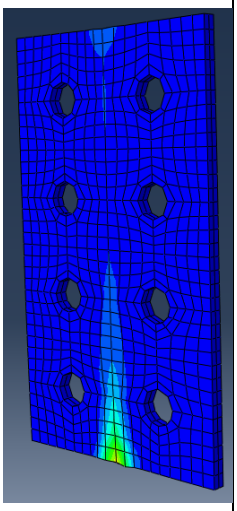	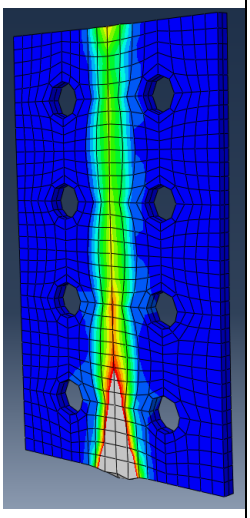	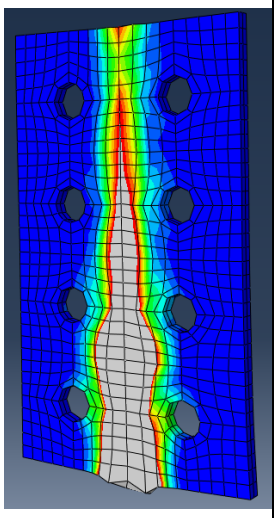	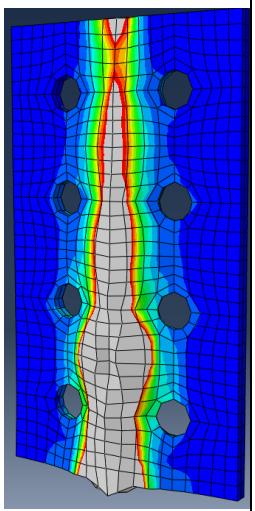	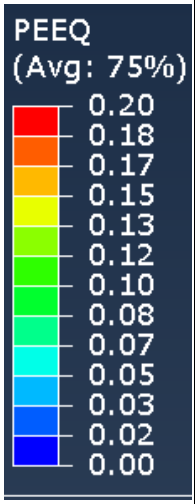

Subsequently, Table 4-3 provides a visualization of the strains along the endplate through contour plots, where the color differential between blue and red indicate the increasing level of strain at each particular part of the plate and the areas shaded in grey showing areas which have surpassed the failure strain of 0.2.Although the areas shaded in grey of the numerical analysis illustrated in Table 4-3 has lost its load carrying capacity, the modelled subassembly does not undergo collapse or excessive deformation as a result of the failed endplate. This is primarily due to the assumptions made for the analysis, particularly with the boundary conditions where the end face of the connected floor slab was taken as “fixed”, and therefore able to support the steel beam despite the failure of the connection. In comparison to the observations after the experiment, the boundary condition described herein is able to be verified as it was reported that the supporting floor slab was able to maintain structural stability before and after the fire despite experiencing cracking and the failure of the endplate connection below (Wald et al., 2005).

To understand the behaviour of the endplate along its width, Figure 4-23 examines the strain experienced along the base of the endplate at various temperatures during cooling, where the X-axis represents the distance from the center of the 150 mm wide endplate, with bolts being located at ±30 mm. As a reflection of the strains experienced along the depth of the endplate shown previously in Figure 4-22, the figure below reinstates that the strain experienced at its base increases significantly as the temperature of the overall subassembly cools as a result of both the differential temperatures within the plate, and the tensile forces exerted by the beam. From this figure, it can be observed that the center of the endplate experiences the largest relative strain due to its direct connection to the beam web which contracts upon cooling. The strain then rapidly decreases along the width of the plate where it can be observed that no strain is experienced past the location of the bolts as shown by the contour plot in Figure 4-24.

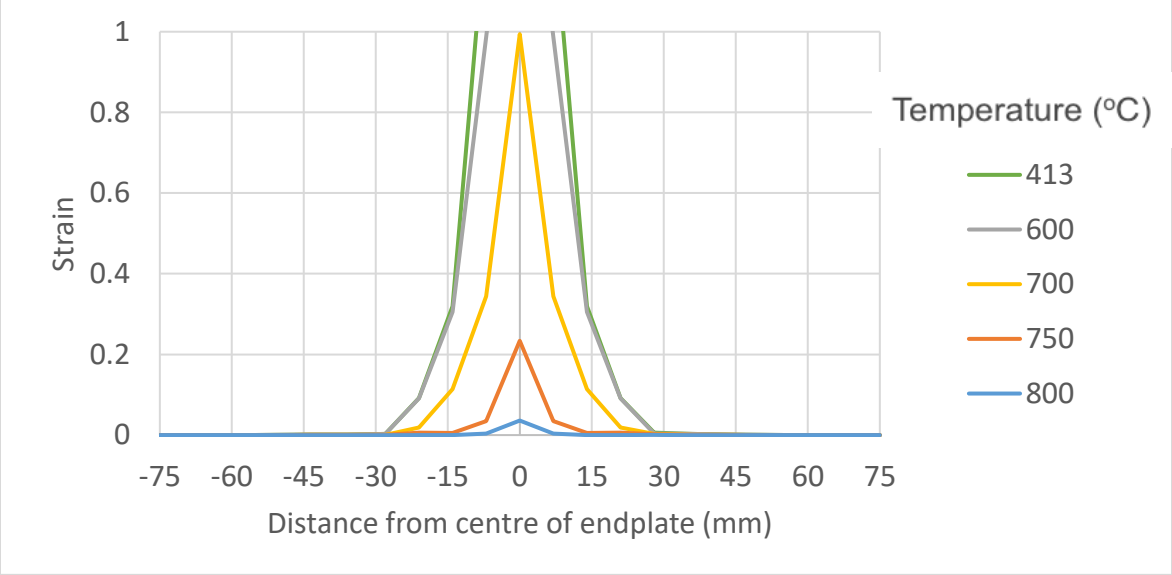

Figure 4-23 Strain along base of the endplate during cooling

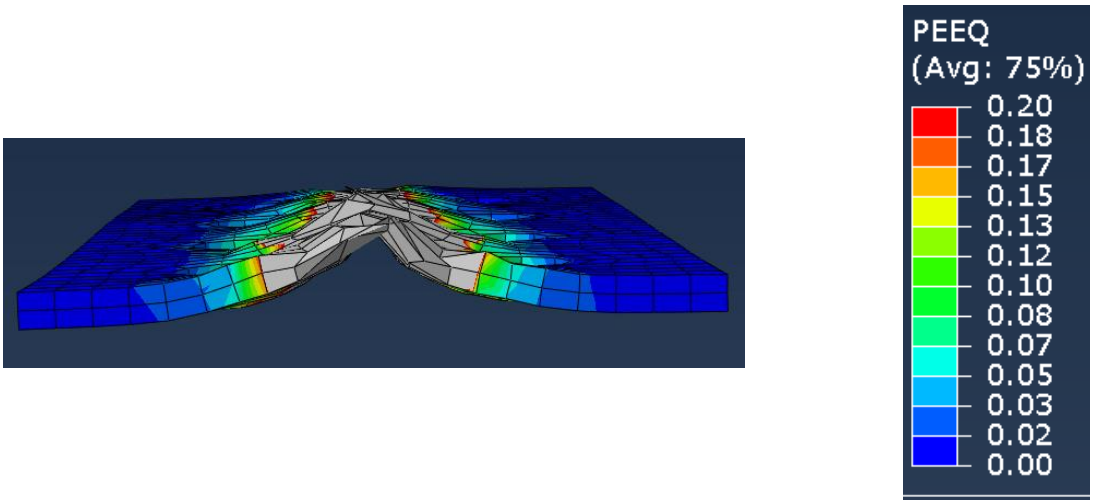

Figure 4-24 Strain contour along the base of the endplate at failure

In regards to the behaviour of the structural bolts, all 8 bolts used in the connection were shown in the finite element model to have performed adequately throughout the respective studies by maintaining structural integrity, and had not undergone significant damage. This is agreeable with the experimental results where damage to the bolts of the flexible endplate connections was unreported.

To conclude, the modelling packages offered by the finite element software, ABAQUS, have been explored and discussed in this chapter of the study. Using the modelling packages and approaches reported herein, the behaviours of the fin plate connection and flexible endplate connection in the experiments conducted by (Yu et al., 2009a) and (Wald et al., 2005) have been able to be recreated and analysed. Subsequently, the behaviour of contemporary simple connections will be studied in the following chapter.

5 Modelling the Behaviour of New Zealand Flexible Endplate Connections

Upon successfully validating the use of the software package ABAQUS to model the behaviour of connections as per Sections 3 and 4, the Cardington connection was redesigned to suit current connection design guides from New Zealand (SCNZ, 2008a), and then its behaviour was modelled in comparison to the U.K. connections (SCI, 2014). Particularly, the connections were designed to the loads sustained by the subassembly of the Cardington test in order to create accurate representations of the observed behaviour of the connections in fire. This was achieved by the inclusion of the connecting beam and the concrete slab in the connection model in ABAQUS. As per the Cardington subassembly, the connection designs account for a 193 kN point load at the centre of a 6 m length of beam.

The design of the connections incorporate the difference in detailing requirements between New Zealand and the U.K. as per Section 2.4, which highlights the variability in factors such as edge and bolt separation distances, as well as material properties which New Zealand and U.K. design guides recommend the use of G300 and S275 type steel respectively.

In regards to the finite element analysis of the New Zealand and U.K. connections, the simulations covered variations in structural detailing of the connections, such as: material properties and plate thicknesses from the UK design and NZ design, respectively, in order to determine the influence caused by the alterations in design.

5.1 Design of Flexible Endplate Connections

Upon successfully validating the use of the software package ABAQUS to model the behaviour of connections as per Chapters 3 and 4, the Cardington Test 7 connection was redesigned to suit

current connection design guides from New Zealand (SCNZ, 2008a), and then its behaviour was modelled in comparison to equivalent U.K. connections (SCI, 2014). Particularly, the connections were designed to the loads sustained by the subassembly of the Cardington test in order to create accurate representations of the observed behaviour of the connections in fire. This was achieved by the inclusion of the connecting beam and the concrete slab in the connection model in ABAQUS. As per the Cardington Test 7 subassembly, the connection designs account for a 193 kN point load at the centre of a 6 m length of beam.

The design of the connections incorporate the difference in detailing requirements between New Zealand and the U.K. as per Section 2.4, which highlights the variability in factors such as edge and bolt separation distances, as well as material properties which New Zealand and U.K. design guides recommend the use of G300 and S275 type steel respectively.

In regards to finite element analysis of New Zealand and U.K. connections, the simulations covered variations in structural detailing of the connections such as: material properties and plate thicknesses from the UK design and NZ design, respectively, in order to determine the influence caused by the alterations in design.

5.2 Design of Flexible Endplate Connections

In accordance with the structural frame used in Cardington Test 7, the primary beam to column flexible endplate connection of the subassembly studied in Chapter 4 has been redesigned using current design guides from New Zealand and the U.K.. In particular, these rules are Section VIII of the New Zealand Structural Steelwork Connections Guide (SCNZ, 2008a) and Chapter 4 of Joints in Steel Construction: Simple Joints to Eurocode 3(SCI, 2014) respectively. As previously discussed in Chapter 2 of this study, the designs were then modelled in the Cardington

subassembly as a means for assessing the performance of the connections in fire. For the purpose of consistency, the nomenclature for detailing of the connection reported in this study follows those used in the New Zealand Connection Design Guide as shown in Figure 5-1, where:

- s_g is horizontal bolt spacing
- s_p is the vertical bolt spacing
- a_{e1} is the vertical distance between the centre of a bolt hole to the edge of the endplate
- a_{e3} is the horizontal distance between the centre of a bolt hole to the edge of the endplate
- t_i is the thickness of the endplate
- d_i is the depth of the endplate

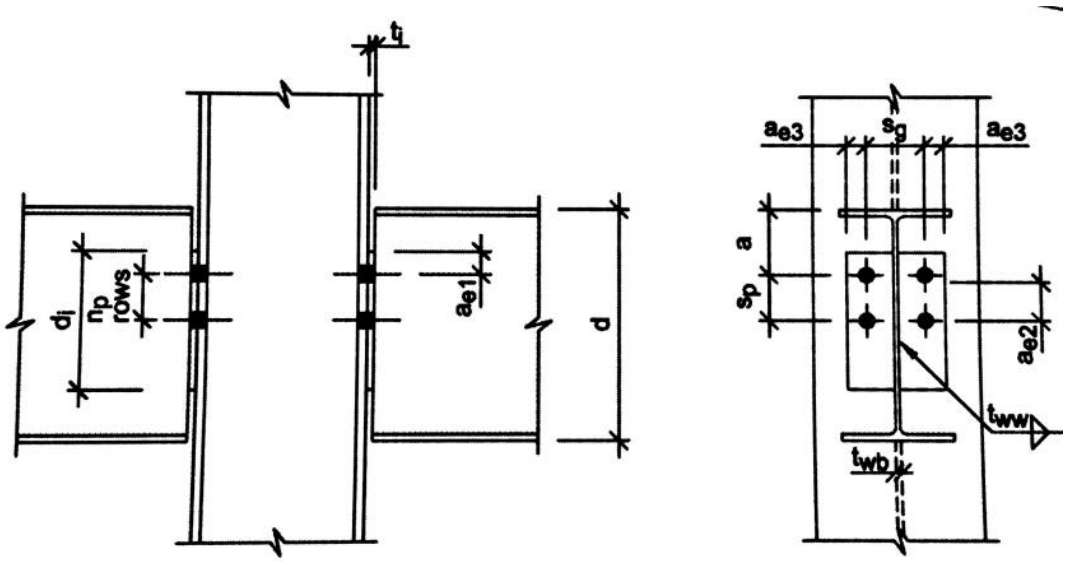

Figure 5-1 Flexible endplate connection (SCNZ, 2008a)

The design of the flexible endplate connections in accordance to the respective design guides is shown in Table 5-1. The table includes the specifications of the connection used in the Cardington test as a comparison. In the connections designed to the NZ and U.K. specifications, minimum detailing criteria such as plate length and end distances of the respective design guides was utilised

where possible. As a result, this allows for an accurate representation of the minimum code requirements, in turn capturing the essence of the various design philosophies between New Zealand and U.K. connections.

Table 5-1 Flexible endplate designs

	SCNZ (NZ)	SCI (U.K.)	Cardington Experiment
Grade (MPa)	300	275	275
Width (mm)	160	150	150
Length (mm)	250	290	260
Thickness (mm)	8	10	8
Number of Bolts	8	8	8
Grade	8.8	8.8	8.8
Bolt Diameter	M20	M20	M20
Bolt Hole Diameter (mm)	22	22	22
s_g (mm)	100	90	60
s_p (mm)	60	70	60
a_{e1} (mm)	40	40	40
a_{e3} (mm)	40	30	45
Ambient Temperature Design Factor: ϕR/R*			
Bolt Shear/Bearing	5.0	4.1	3.7
Gross Shear	4.1	5.0	3.6
Block Tearing	5.0	4.7	3.7
Tying	2.9	2.6	2.6

Noting the differences in the geometry of the connections within Table 5-1 and comprehensive design calculations in accordance with various failure modes at ambient temperature shown in Appendix A, it is apparent that substantial differences exist between New Zealand and U.K connections. For the flexible endplate connection, the U.K. design incorporates an endplate with increased robustness and rigidity compared to its New Zealand counterpart through a 16% and 25% increase in length and thickness respectively, and a 10% decrease in horizontal bolt spacing. The differences in the designs are a product of varying design philosophies highlighted in Chapter

2.1, where the New Zealand design places a larger emphasis on the ductility of the connection. In this scenario for the design of flexible endplate connections, the main differences are as follows:

- SCNZ (2008a) specifies Grade 300 steel to be used in New Zealand connections compared to S275 grade steel specified by SCI (2014) in U.K. connections.
- SCI (2014) recommends the use of 10 mm thick endplates, whereas 8 mm thick endplates are commonly used in New Zealand for similar applications.
- Following the respective design criteria and recommendations, the horizontal bolt spacing for the New Zealand and U.K designs at 100 mm and 90 mm are substantially higher than 60 mm spacing used in Cardington Test 7.
- Small discrepancies exist between the vertical bolt spacing and edge distances in the specified connections as discussed in Chapter 2.

Due to the differences in geometry between the connections and variations in design philosophies in the two countries, variations arise in the designed strength capacity of the connections as shown at the bottom of Table 5-1, the table highlights the ambient temperature design factors for the various failure modes of the connections. In regards to the design of bolts, the New Zealand connection considers their strength limit to be based purely on their transverse shear capacity, whereas Section 4 of the U.K. design guide (SCI, 2014) also considers the bearing resistance of the supporting members under the same criteria . In turn, this extra consideration results in the lower limiting factor for both the U.K. and Cardington bolt strength designs despite all three connections specifying eight M20 Grade 8.8 bolts.

Regarding the gross shear strength of the connections, the U.K. connection utilises slightly a larger endplate which provides a greater capacity for shear resistance due to its increased area as reflected

in Table 5-1, where the design factors for gross shear for the New Zealand and U.K. endplate are 4.1 and 5.0 respectively. However when considering the calculation of the block tearing capacities of the connections, the New Zealand design guide (SCNZ, 2008a) offers a comparatively more conservative approach by providing two equations for determining the area for block shear of which the largest calculated area is taken as the limiting criteria. In turn, this consideration leads to the placement of greater emphasis on the tying resistance of connection - a preferred failure mode due to its ductile mechanism.

Considering the ambient temperature design factors for tying resistance between the three connections, the calculated values indicated by Table 5-1 show that the Cardington and U.K. possess effectively the same design factor at 2.6, while the New Zealand connection offers higher resistance with a design factor of 2.9. In this scenario, the similarity between the Cardington and U.K design factors is a product of the considerations within the equations provided by SCI (2014), where the detailing of edge distances are of high influence compared to other geometric factors. Therefore, as the connection used in the Cardington test used an edge distance of 40 mm compared to the minimum 30 mm distance specified by SCI (2014), the two connections are shown to provide an effectively equal design resistance for tying capacity despite the Cardington connection being thinner and less robust. On the other hand, the formulas presented by SCNZ (2008a) follows a different approach by placing greater influence on other geometric factors such as the length of the plate and the bolt gauge, resulting in a higher design factor.

Therefore, the comparison between the connection geometries and ambient temperature design factors for the flexible endplate connections designed in accordance with their respective design guides can be observed to highlight the differences in philosophy outlined in Chapter 2, where it

is emphasised that the New Zealand connection design places a heavier consideration on the ductility of the connection by allowing for an increased yield capacity of the endplate.

5.3 Flexible Endplate Modelling Scenarios

Following the modelling approach undertaken for the fin plate connection, the process of creating models with intermediate detailing requirements is repeated for that of the flexible end plate connection. Given the variations between the New Zealand and U.K. designs, two additional connections incorporating the varying features were modelled in pursuance of better understanding the performance of the connections in fire.

As shown in Table 5-2, the intermediate connection labelled FE2 utilises the connection detailing of the New Zealand design with a 10 mm thick endplate of grade S275, whereas FE3 on the other hand uses the detailing of the U.K. design whilst incorporating an 8 mm thick endplate graded to 300 MPa. In turn, the two intermediate connections will aid in illustrating the influence of varying details on the behaviour of steel connections in fire.

The modelled connection designs are highlighted in Table 5-2, where the four variations are modelled to replace that used in the Cardington Test 7 subassembly.

Table 5-2 Flexible endplate modelling scenarios

Model	FE1 NZ Design	FE2 Plate Properties	FE3 Plate Detailing	FE4 UK Design
Grade (MPa)	300	275	300	275
Width (mm)	160	160	150	150
Length (mm)	250	250	290	290
Thickness (mm)	8	10	8	10
Bolts	8	8	8	8
Grade	8.8	8.8	8.8	8.8
Bolt Diameter	M20	M20	M20	M20
Bolt Hole Diameter (mm)	22	22	22	22
S_g (mm)	100	100	90	90
S_p (mm)	60	60	70	70
a_{e1} (mm)	40	40	40	40
a_{e3} (mm)	30	30	30	30

5.4 Finite Element Models

Similarly, the modelling approach undertaken for the flexible endplate connections followed that of the Cardington Test 7 model outlined in Section 4, where a sequentially coupled thermal and mechanical analysis was used. All input parameters used in these series of models were taken from the previously validated models, with the singular difference being purely based on the design of the flexible endplate connections as shown in Figure 5-2 and Table 5-3. As illustrated in Table 5-3, the differences are apparent when considering the lengths, thicknesses and bolt gauges between FE1 to FE4. Hence, applied temperatures, loading, boundary conditions and general modelling inputs were left unchanged from those described in Section 4.

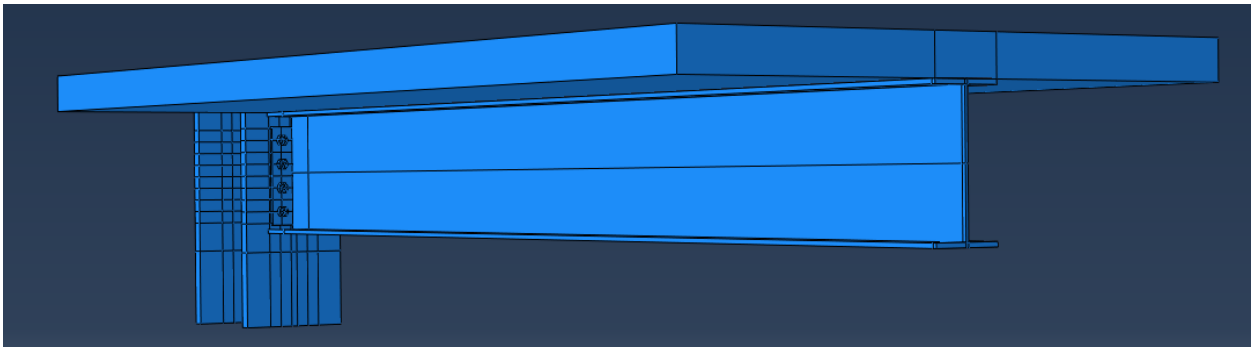

Figure 5-2 Model with flexible endplate connection

Table 5-3 Endplate models

FE1	FE2	FE3	FE4
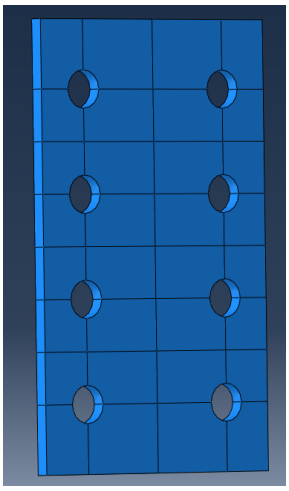	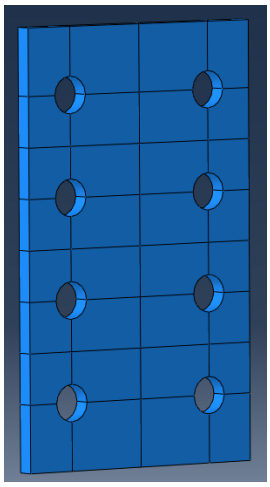	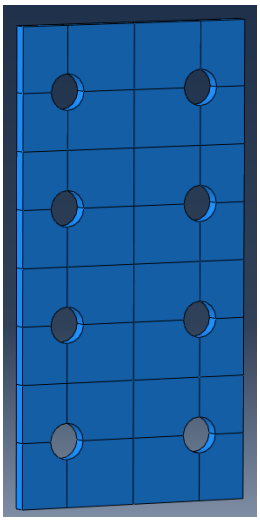	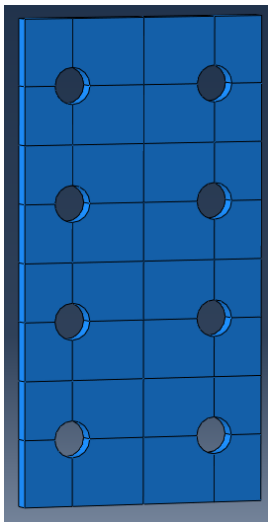

5.5 Results and Discussion

5.5.1 Heat Transfer

Following the temperature and heat transfer inputs described in Chapter 4, the temperatures throughout the subassembly determined by the heat transfer analysis for models FE1 to FE4 are largely similar to those determined previously in Chapter 4.1. For illustrative purposes, the temperature distribution through the subassembly in FE1 is shown in Figure 5-3 below. Similar to

heat transfer analysis of the Cardington test, it can be seen that the temperature distribution in FE1 follows a similar trend with the bottom flange of the steel beam reaching the relatively highest temperatures, and the connection being heated at a slower rate to reach a comparatively lower maximum temperature as a result of the increased thermal mass. While the size of the endplates between the models FE1-FE4 varied in size and detailing, the geometrical differences were not considered to be large enough to result in any surmountable influence on the resulting temperatures and therefore behaviour of the components. As such, the temperatures shown in Figure 5-3 were applied to all numerical models to form a comparative basis.

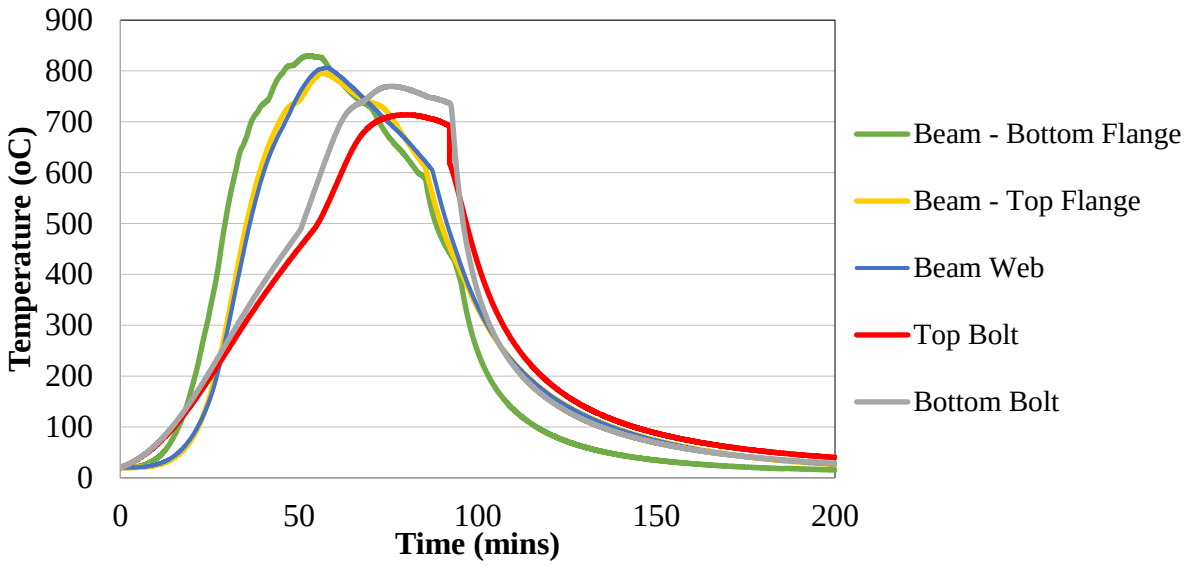

Figure 5-3 Temperatures of subassembly components

5.5.2 Subassembly Behaviour

Given that the four modelling scenarios shown in in Table 5-2 (FE1-FE4) incorporate an identical subassembly to that of the Cardington test, it is based on observations of the modelling output that the connection designs modelled in FE1-FE4 offer significant differences in performance under equal conditions. From the four modelled scenarios, it was determined that the mid-span deflection of the composite beam throughout each model are equal to those presented by the Cardington

model, as shown in Chapter 4. As a result, this provides an indication that the alteration of the flexible endplate design provides little influence on the overall behaviour of the subassembly under the modelling conditions previously discussed in this study.

Accordingly, models FE1 to FE4 all showed that the bottom flange of the connecting beam experienced some yielding against the column face at approximately 23 minutes as a result of thermal expansion and beam end rotation, which caused the two members to come into contact. As per the numerical analysis and experimental study reported in Section 4.3, neither the beam nor the supporting column experienced significant structural damage.

The axial forces developed in the beam in FE1 with respect to time is illustrated in Figure 5-4, and while they have not been explicitly determined for models FE2-4, it was considered that they would not vary significantly due to the ability of all four connections in sustaining the applied loading. It can be deduced that the axial forces generated within the steel beam during the heating and cooling phases are also largely coherent with those determined in Chapter 4 due to geometry of structural components and applied temperatures being consistent between the models. As a result of the added robustness of the flexible endplate connections designs modelled in FE1 to FE4, all four connections were able to sustain the tensile loads applied during cooling, allowing the computational models to reach completion at the simulation time of 200 minutes as shown in Figure 5-4, at which point the subassemblies did not undergo any further deformations as a result of changes in temperature.

Through Figure 5-4, it is highlighted that the continued cooling of the beam results in an axial tensile force which increases in accordance with its rate of cooling, as the axial force can be seen to ramp up at a rapid rate between 85 and 100 minutes. When the beam is cooled it contracts at a

relatively quickly. Then as the cooling and rate of contraction in the beam decelerates, the increase of axial force within the beam also slows proportionally.

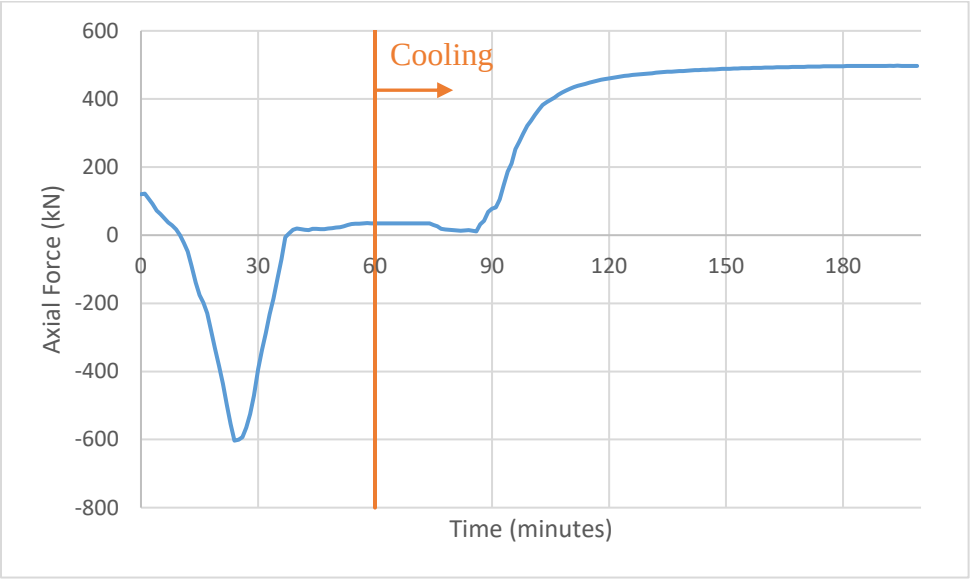

Figure 5-4 Axial forces in the beam modelled in FE1

While the flexible endplate connection of the Cardington experiment was calculated to fail at the time and axial tension force of approximately 94 minutes and 278 kN respectively, the axial forces recorded for models FE1 to FE4 continued to increase at an inverse proportional rate to the temperature of the beam which could be observed to slow down at 120 minutes, where the axial force in the beam then increased at a diminished rate up to a maximum of 497kN as the beam temperature approached room temperature. Although the connection designs used in all four models were adequate in providing structural stability, closer analysis of the endplate in each model indicated that the seemingly minor differences in detailing between the connections impose notable differences in performance in the case of fire.

5.5.3 Stiffness and Ductility of Endplates

Despite the temperatures and deflections of the connected beam being equal in modelling the four scenarios FE1-FE4, the numerical analyses was able to demonstrate that the effect of changing the detailing requirements of the flexible endplates in each scenario significantly alters the performance of the overall connection in fire conditions due to differences in strength and ductility. To highlight the performance of the connections, the strain contours for the endplate at the conclusion of the numerical analysss is presented in Table 5-4, with red and blue shaded areas showing the relatively higher and lower strain concentrations respectively, and the grey shaded area signifying areas which have reached limiting plastic strain of 0.2.

Table 5-4 Strain contours at the conclusion of each model

FE1 NZ Design	FE2 Plate properties	FE3 Plate Detailing	FE4 UK Design	Key
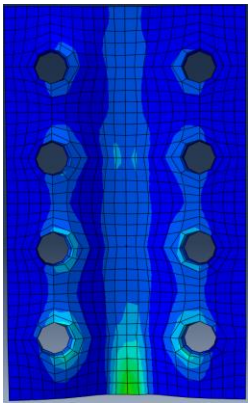	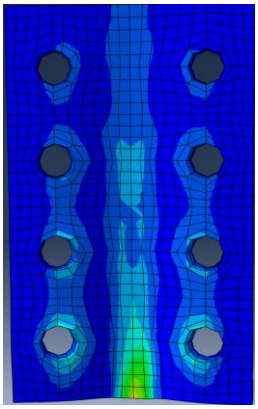	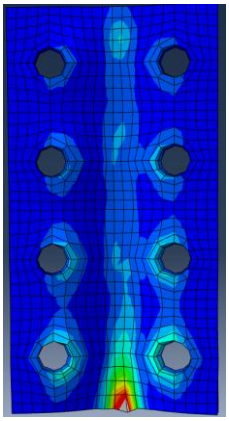	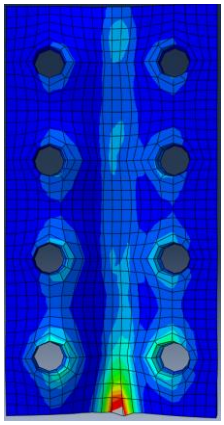	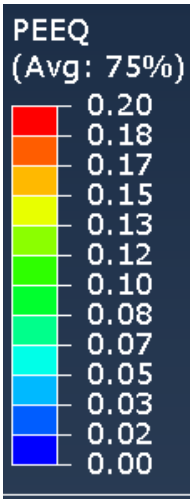

From the contour plots of the four connections, it can be observed that the differences in detailing leads to a noticeable difference in the performance of the connection, particularly between FE1/FE2 and FE3/FE4. The endplates in FE1 and FE2 designed using the detailing recommendations of the New Zealand guidelines (SCNZ, 2008a) shown in Table 5-4 were

expected to remain completely in the plastic range without exceeding the failure strain of 0.2 by the end of the analysis. On the other hand, the endplates in FE3 and FE4 designed using the detailing recommendations provided by the U.K. design guides were shown to experience failure through plastic yielding in a very limited area at the base of the plate as highlighted in grey in the strain contour plots above. Overall, it can be observed from the contour plots in Table 5-4 that the strain distribution throughout each analysis follows a general approach, where the largest strains concentrate at the base of the endplate, and relatively higher strains being seen in areas adjacent to the bolt holes.

The behavioural differences of the endplate in each model is better visualized and compared when plotting the relationship between the levels of strain experienced at the base of the endplates against time and temperature. As shown in Figure 5-5, the strains experienced in each model follow a typical pattern which corresponds to the temperature of the steel beam shown on the secondary axis. It is observed from the figure that the behaviour of the endplate is of particular interest during the cooling phase when an out-of-plane tension force is applied by the contracting beam, as opposed to the heating phase where it undergoes compression due to the thermal expansion of the connected beam. It can be observed that the beam reaches its maximum temperature of 830^{o}C at approximately 55 minutes, and then begins to cool. Within the cooling phase, it is at approximately 60 minutes into the simulation when the steel beam reaches 800^{o}C that the endplates begin to experience strain. As previously discussed in Chapter 4, this initial strain can be interpreted to be a result of the stress induced within the endplate which experiences stresses within the element as a result of the differential temperatures through its depth, combined with the action caused by the steel beam beginning to regain strength and as it cools.

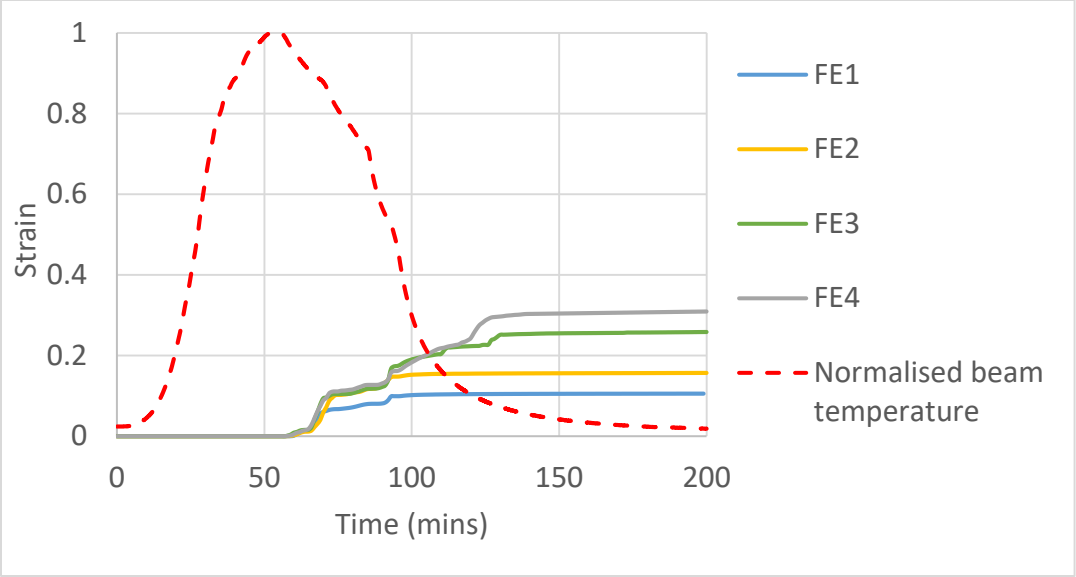

Figure 5-5 Strains experienced at the base of each endplate

Once the endplate begins to yield, it is shown to occur at a rapid rate due to the tensile forces of the contracting steel beam being met by minimal resistance from the connection due to the endplate being weakened by high temperatures. As time progresses and the beam undergoes further cooling, it can be observed that the rate of yielding in the endplate decreases due to the material regaining strength as it cools, subsequently offering more resistance against the tensile forces.

It is demonstrated in Figure 5-5 that the alteration of specific factors in the design of the flexible endplate connections highlighted in Table 5-2 lead to notable differences in the behaviour of the connection in fire. Particularly, although all models were shown to experience plastic yielding, FE1 and FE2 which incorporated endplates designed using New Zealand detailing requirements reached maximum strains of 0.11 and 0.16 respectively, and hence were able to remain below a limiting failure strain of 0.2. On the other hand, FE3 and FE4 designed using U.K. detailing requirements were shown to exceed 0.2 at the base of the endplate, as the maximum strains were recorded to be 0.26 and 0.33 respectively. From this, it can be determined that altering the detailing

aspects of the connection, particularly the bolt gauge distance and depth of the endplate affects the strain experienced by the endplate.

Considering the thickness and grade of steel used for the modelled endplates - with FE1 and FE3 having 8 mm of G300 steel compared to the 10 mm of S275 featured in FE2 and FE4, it is illustrated by Figure 5-5 that the models using the higher graded steel had higher stiffness. Noting that FE1/FE2 are both detailed in accordance with the New Zealand design guide, with the only differences being the thickness and grading of steel used for the endplate, they were shown to experience remarkably different strains at the base of the endplate, with FE1 and FE2 exhibiting strain levels of 0.11 and 0.16 respectively. Similarly, this was repeated by FE3 and FE4, both being designed with detailing in accordance with the Green Book exhibited strains of 0.26 and 0.31 respectively. Overall, this difference was expected given that the steel beams in each model underwent the same axial forces due to the consistent thermal expansion and contraction characteristics of the subassembly, and therefore endplates possessing higher yield and ultimate stresses were shown to experience relatively less plastic strain.

Although minimal, the differences in ductility resulting from the factors described above is also reflected by the out-of-plane displacements experienced at the base of the endplate by each scenario as shown in Figure 5-6. From the Figure Figure 5-6, the endplates incorporating the New Zealand detailing recommendations (FE1 and FE2) were able to displace approximately 0.6mm further while experiencing less strain than the U.K. designs (FE3 and FE4). On the other hand, endplates using steel with the higher 300 MPa grade (FE1 and FE3) displaced 0.2 mm less, and subsequently experienced less strain than their 275 MPa graded counterparts (FE2 and FE4).

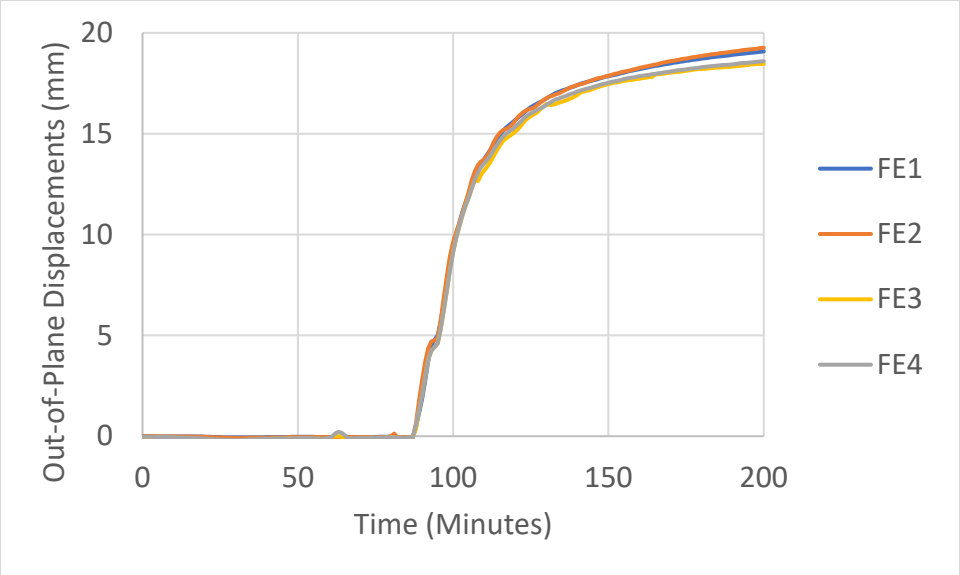

Figure 5-6 Out-of-plane displacement at the base of each endplate

Studying the behaviour of the two extremes - FE1 and FE4 in further detail (due to the similarities between connections using endplates of the same detailing), the relationship between strain and distance along the depth of the two endplate designs at various temperatures during the cooling phase have been illustrated in Figure 5-7, where the two models are represented by the solid and dotted lines, with the strain measurements being taken at centre width of the plates. Due to FE1 and FE4 featuring plates with the varying depths of 260 mm and 290 mm respectively, the distance from the top of the endplates have been normalised in the Y-axis of Figure 5-7 in order to provide a comparative basis between the two models. From the figure, it can be observed that the behaviour of both endplates follow a general pattern during the cooling phase when subject to equal conditions using the same subassembly.

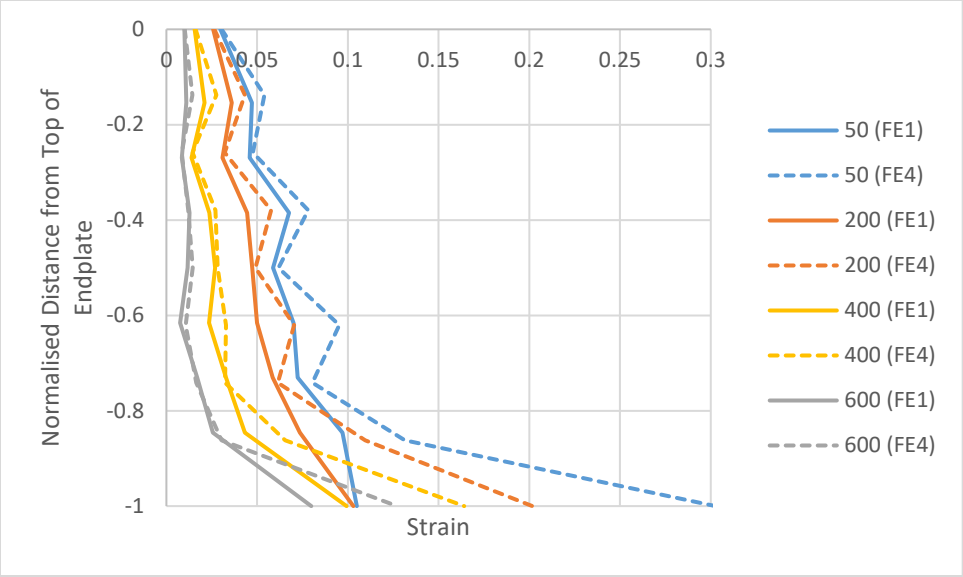

Figure 5-7 Strain along depth of endplates FE1 and FE4 during cooling

As the connecting beam and endplate undergoes cooling, it can be seen that the base of the endplates in both the FE1 and FE4 connections experience a relatively large strains throughout the analysis - particularly in the lower 15% of the plate when compared to the upper portions. This behaviour is similar to that reported previously in the Cardington model in Chapter 4, where the large strain at the base of the endplate can be attributed to a combination of actions caused by the differential temperatures along the depth of the plate and beam. Considering the strains at the bottom flange of the beam (which is at 600^{o}C and at 83 minutes into the simulation as shown in Figure 5-7, results from the heat transfer model shown previously in Figure 5-3 indicate that a variation in cooling exists within the beam, where the bottom flange cools and therefore contracts at a slightly faster rate than the top flange. Additionally, Figure 5-3 also shows a large temperature differential in the endplate during this time, where the areas adjacent to the top and bottom bolt rows are at 707^{o}C and 759^{o}C respectively. Hence as a result of the two actions occurring simultaneously, the base of both endplates can be observed to experience relatively higher strains at a temperature of 600^{o}C, which then subsequently increases upon further cooling.

Although the actions generated within the subassembly are equal in both models due to the similar set-ups, the strain experienced by FE4 can be seen to be comparatively higher than that of FE1 throughout its depth during the cooling phase as illustrated in Figure 5-7. Firstly considering the base of the endplate, it can be observed that the strains experienced in this area are significantly higher in FE4 compared to FE1 at the same temperatures, where the difference can be attributed to a combination of various factors. In addition to FE4 using a lower strength of steel, the depth of the endplate at 290 mm is also longer than that of the 260 mm plate in FE1 which is important when considering the strains caused by the differential temperatures in the plate and the connecting beam.

The increased length of the endplate in FE4 results in it being more susceptible to increased strains due to having a larger temperature differential along its length, as well as being attached to the lower portions of the beam web which cool and contract quicker compared to higher sections, hence further displacing the endplate. With the bolt gauge in FE4 being 10% shorter than that of FE1, it is of lower ductility when yielded in the out-of-plane direction between the centre of the bolts by providing closer restraints, in turn contributing to the increased strain of the endplate when compared to FE1. As a result of the combination of these factors, it can be seen in Figure 5-7 that the strain along the base of FE4 continues to increase as the subassembly cools, encountering the strain of 0.2 at approximately 200^{o}C where the material has been modelled to lose its load carrying capacity, and therefore increases significantly upon further cooling of the connected beam. Comparatively, although FE1 is subject to the same behaviour of the attached subassembly, the strain at the base of the endplate can be seen in Figure 5-7 to also increase as it cools but reaches a lower maximum strain of 0.11.

Table 5-5 Deformation of the FE4 endplate during cooling

600°C	400 °C	200 °C	50 °C	Key
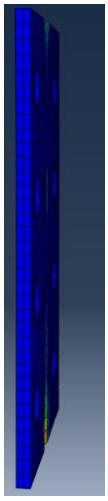	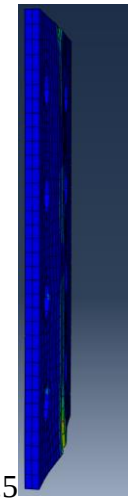 .5	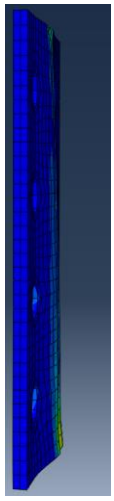	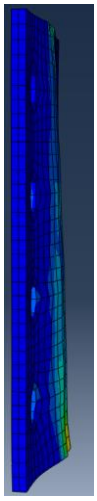	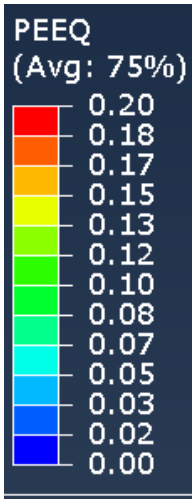

As the overall structure continues to cool, it can be observed that the strain experienced along the length of the endplate in both simulations increases with time as a result of being pulled in the out-of-plane direction by the contracting beam, where Table 5-5 illustrates the visual deformations and strain along the depth of the FE4 endplate at different temperatures during cooling. In both scenarios, the strain along the depth of the endplate follows a trend where it progressively increases with depth due to the actions caused by temperature differentials and contracting beam. Although the strains experienced by both FE1 and FE4 are seemingly similar along majority of the plates at 600°C as shown in Figure 5-7, the strain along FE4 becomes comparatively higher throughout the plate as the subassembly cools further. Supplementary to the effects of the connection being less ductile than FE1 due to its reduced bolt gauge and steel grade, the increased strain is also a result of the endplate losing its load carrying capacity at the base which is then sustained by the higher portions of the endplate for structural stability. This is highlighted in the peaks shown along the

depth of the plate in Figure 5-7 which represent the areas adjacent to the bolt rows where the larger forces are typically carried.

To understand the forces along the depth of the endplate, the stresses in the out-of-plane direction along the depth of the endplate have been plotted at various temperatures during cooling in Figure 5-8 to highlight the effects of the contracting beam. From this figure, it can be seen that the stresses along the depth of the endplates in both FE1 and FE4 follow a general trend, and are of relative magnitudes throughout the cooling stages of the analysis. Compared to the strains experienced in the endplate shown in Figure 5-7 which increase uniformly in accordance with decreasing temperatures, the intervals between the stresses plotted at the same temperatures can be seen in Figure 5-8 to increase as the subassembly cools due to the recovery of strength in the endplate. It can also be seen that the stresses along the depth of the endplate in both scenarios peak at particular points along the plate, which represent the locations of the bolt rows that are comparatively more rigid.

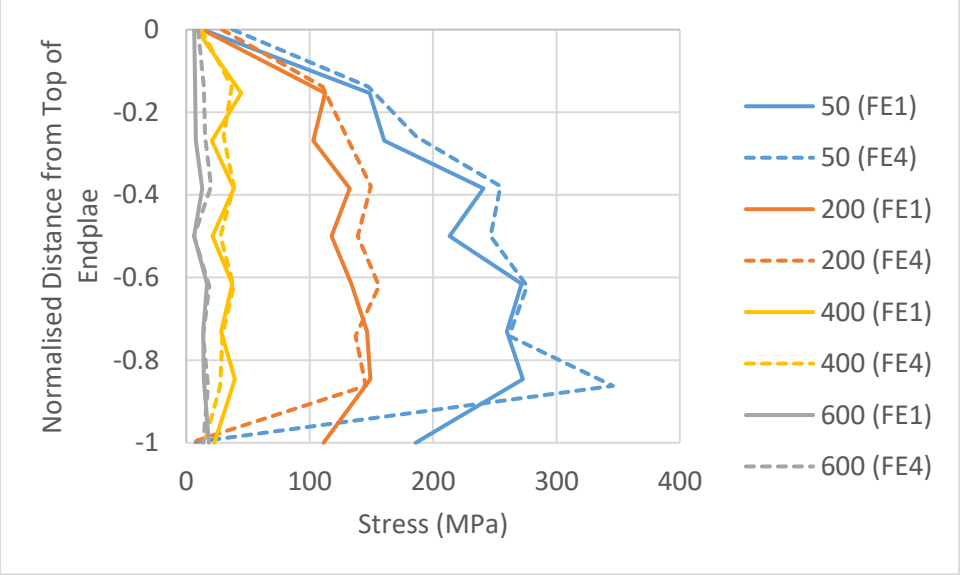

Figure 5-8 Out-of-plane stresses along depth of endplates FE1 and FE4 cooling

As shown in the figure, the stresses along the depth of the endplates in FE1 and FE4 are similar down to the temperature of 400^{o}C, where notable differences can be seen upon further cooling. Due to the bottom of the endplate in FE4 surpassing the limiting strain and losing its load carrying capacity at temperatures below 200^{o}C, the stresses at the upper portions of the endplate are increased in order to accommodate the contraction of the connected beam. It is also observed that while the stresses in line with the lowest row of bolts reaches approximately 340 MPa which exceeds its 275 MPa yield strength, it does not exceed its ultimate failure stress of 430 MPa and is therefore able to sustain the resulting loads. Despite the base of the FE1 endplate not exceeding the failure strain, it experiences relatively low stresses during cooling due to being restrained by bolts from only one direction.

Subsequently, in order to further determine the effects of the contracting beam on the connection during cooling, the magnitude of strain experienced at the base of the FE1 and FE4 endplates in relation to the distance along their width is then observed at various temperatures as per Figure 5-9 below. Given that the endplates in FE1 and FE4 are of 160 mm and 150 mm widths respectively, the widths have been normalised in the figure below for a comparative basis. Between the maximum strains experienced by the two endplates, FE4 experiences significantly higher yielding than FE1 at the same temperatures as a result of the differences in design as previously discussed.

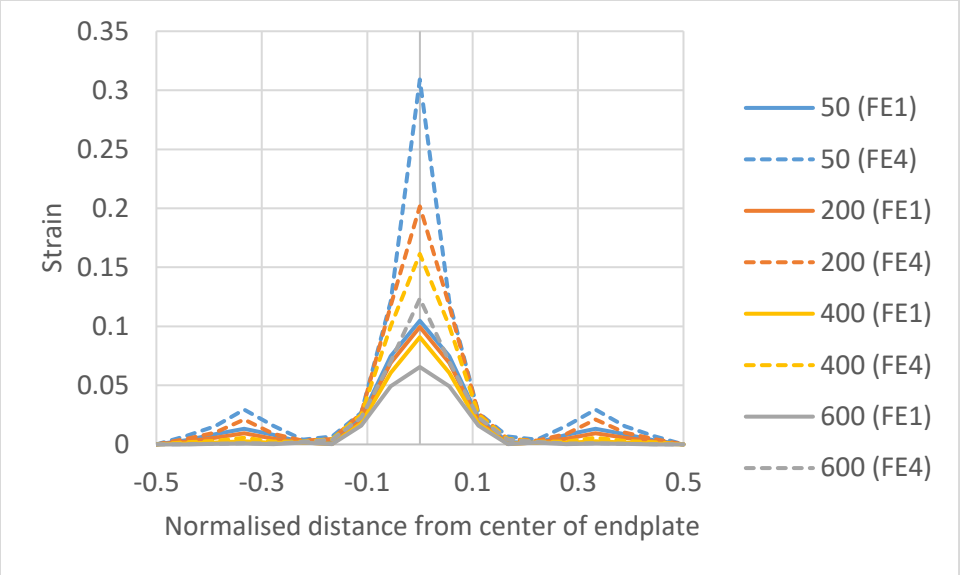

Figure 5-9 Strain along the base of endplates FE1 and FE4 during cooling

From Figure 5-9, it can be observed from the base of both endplates that they experience their largest respective strains at the centre of the plate as expected, being the point of contact between the endplate and the beam web. The strain experienced by the endplate then progressively decreases along the width of the plate, as it reaches 0 at the normalised distance of ±0.17 which signifies the midway points between the centre of the endplate and the bolts. Observing the strain at the distances of ±0.33 where the bolts are situated, it is not until temperatures below 400°C that strain begins to be experienced in both FE1 and FE4 simulations. Overall, this exemplifies the softening and decreased yield strength of the endplate under elevated temperatures, as the centre of the strip at the bottom of the endplate is able to sufficiently yield without meeting resistance from the bolted areas.

The differences in strain along the width of the endplate are able to be reflected by the resultant stresses at the same temperatures during cooling as shown in Figure 5-10. Similar to the stresses along the depth of the endplate previously shown in Figure 5-8, FE1 and FE4 also experience

similar magnitudes of stress along the width of the endplate during the earlier stages of cooling at temperatures of 600 ^{o}C and 400^{o}C, after which the differences in stresses diverge between the two simulations as a result of their disparity in the behaviour of the plates.

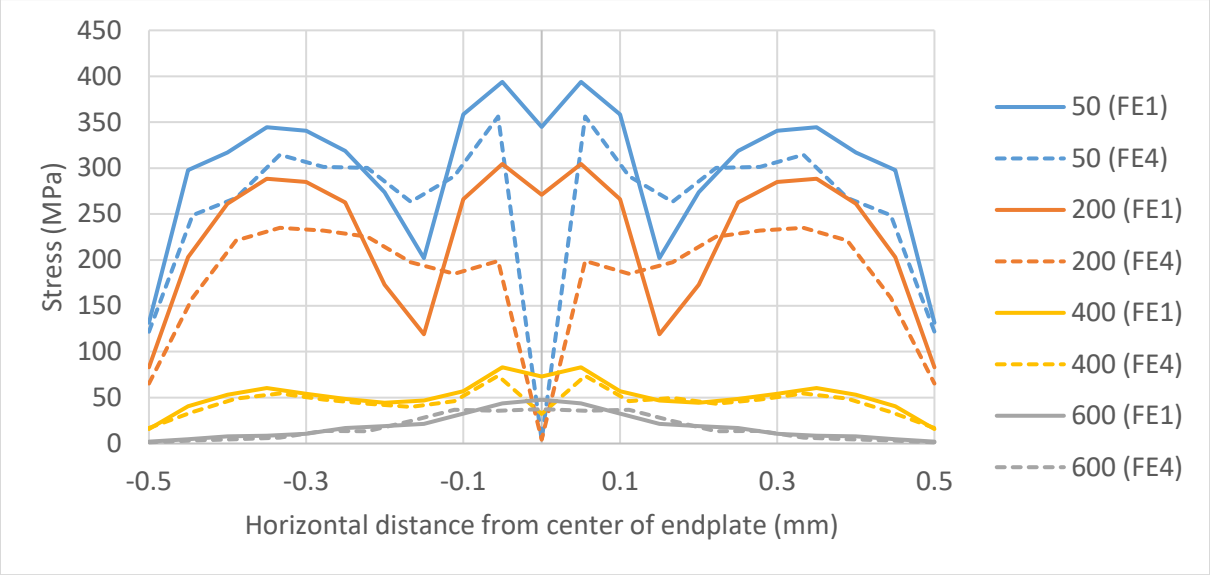

Figure 5-10 Stress along the base of endplates FE1 and FE4 during cooling

As per the stresses along the depth of the endplate shown previously, the stresses along the width of the strip at the bottom of the endplates in Figure 5-10 also indicate a large separation between the stresses at the temperatures of 400^{o}C and 200^{o}C as a result of the steel regaining its maximum failure strength in accordance with Eurocode 3 and therefore induced higher stresses as it offers increased resistance against further yielding, as reflected by the large increase in measured stresses at the location of the bolts.

Regarding the stress along the width of the FE1 endplate, the stress at the centre point shows a dip where it shows a slightly lower value in comparison to the peak stresses on either side as illustrated in Figure 5-10. This occurs as a result of the method of which the beam web was connected to the centre of the endplate using the “TIE” function in ABAQUS, causing the largest forces to occur

along the two sides of the beam web as opposed to directly in the centre as shown in the corresponding stress contour plots in Table 5-6 below, In reality, this effect can be considered to be similar to the behaviour of a welded connection where the tensile forces are largely sustained by welds on either sides of the web.

Table 5-6 Stress contour plots along the width of the FE1 endplate during cooling

Temperature during cooling	Stress Contour Plot	Key (Pa)
600°C	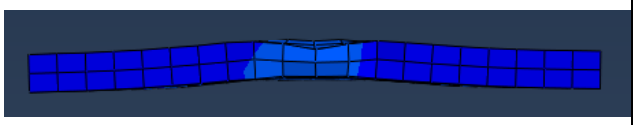	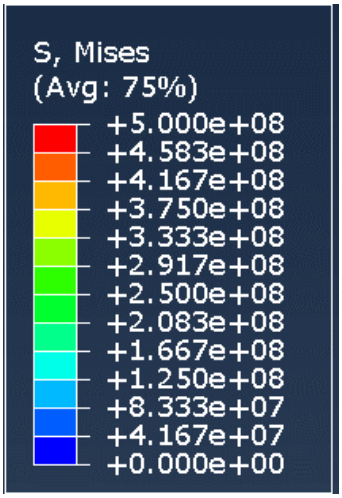
400°C		
200°C	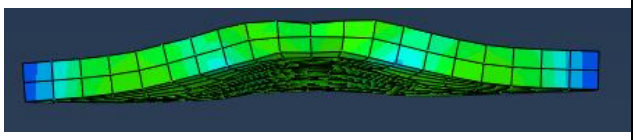	
50°C	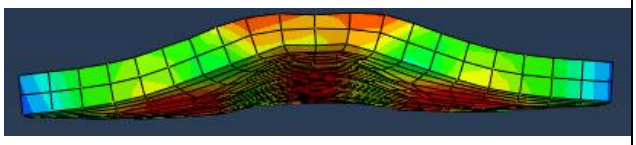	

From Figure 5-10 and the stress contour plot in Figure 5-11 below, it is determined that the FE4 endplate loses its load carrying capacity at 400°C at centre width as the recorded stress are shown to reduce significantly. As a result of this, the base of the endplate in FE4 is shown to carry comparatively lower maximum stress than the FE1 endplate, where the maximum stresses recorded at the temperature of 50°C are 356 MPa and 394 MPa respectively. In order for the base

of the plate to continue sustaining forces, the stresses along the FE4 endplate is distributed both upwards towards the centre of the endplate and also throughout its width, particularly in between its centre and the bolts on either side at distances of ±0.17.

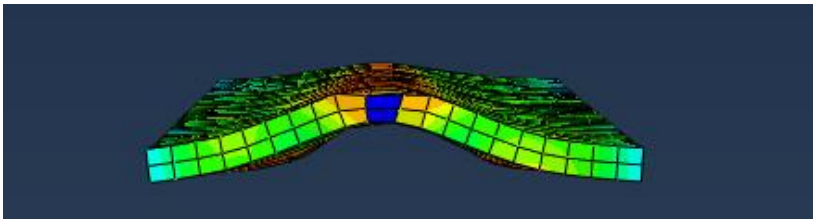

Figure 5-11 Stress contour plot at the base of the endplate in FE4

5.5.4 Bolt Behaviour

While the beam contracts as a result of cooling, the axial force generated in the beam is transferred into the connection. This axial force through the connection creates a prying force in the bolts connecting the flexible endplate to the column face. Figure 5-12 and Figure 5-13 below illustrate the development of tensile stresses in the bolts compared to the ultimate stress of the bolts in relation to temperature as per Eurocode 3, where it is clearly observed that the bolts in both simulations do not reach their full capacity during both the heating or cooling stages of the fire.

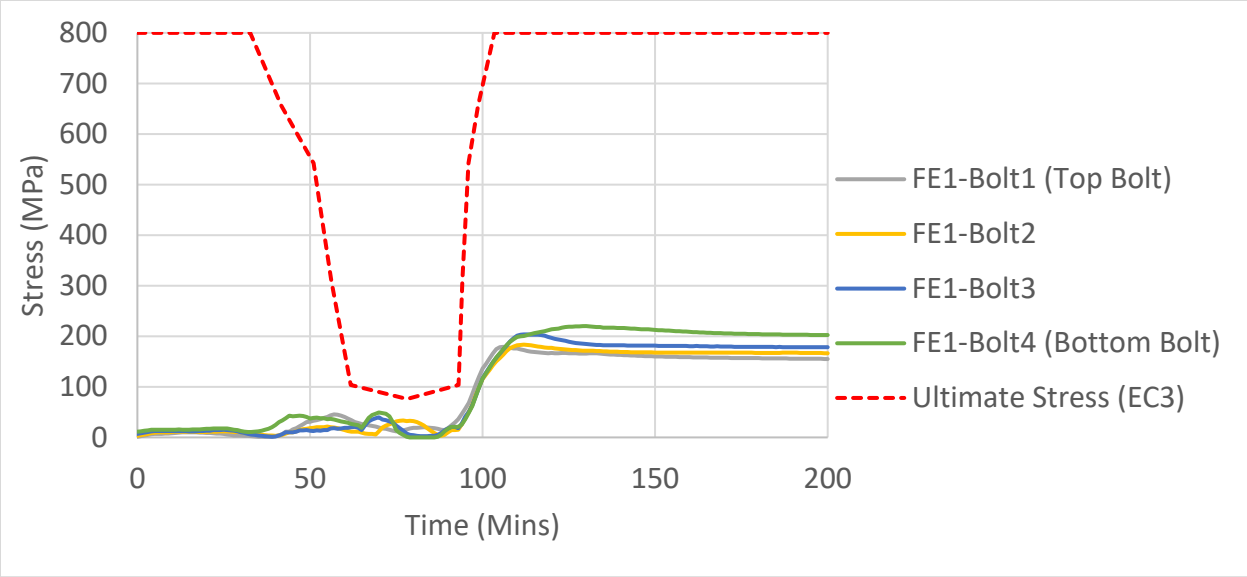

Figure 5-12 Tensile stress time history of bolts in FE1 due to prying action

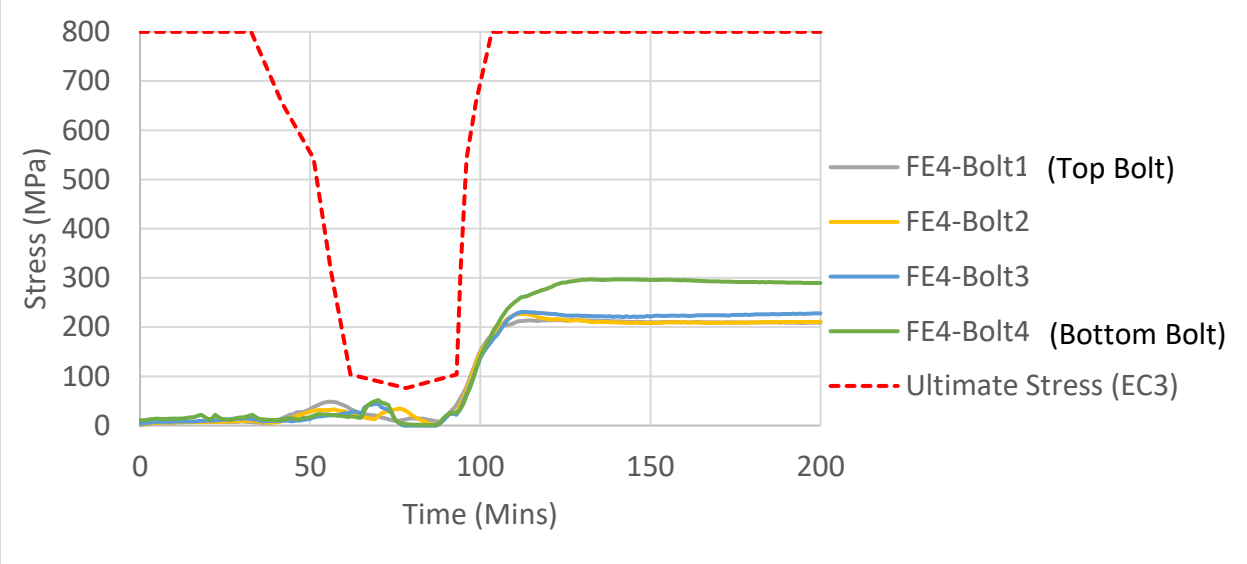

Figure 5-13 Tensile stress time history of bolts in FE4 due to prying action

Comparing the tensile stresses experienced by the bolts in the figures above, it is observed that the bolts in FE4 experience comparatively higher stresses than those in FE1 – particularly in regards to the bottom bolts. This is reflective on the stresses recorded along the depth of the endplate as

previously shown in Figure 5-8, where the lack of ductility in FE4 leads to failure at the base of the plate, consequently resulting in higher stresses throughout the depth of the endplate and at each bolt.

Thus, from the analysis undertaken through this section of the study, it can be concluded that although both flexible endplate connections designed as per the New Zealand and U.K. guidelines performed similarly during the heating phase of a fire, the additional ductility provided by the New Zealand design was advantageous as it allowed for comparatively less plastic yielding, particularly in the cooling phase.

6 Analysis of New Zealand Fin Plate Connection Designs

Following the analysis of the behaviour of flexible end plate connections in fire, this study then examines the difference in the design of fin plate connections between New Zealand and the U.K. As per Section 5, the primary beam to column connection of Cardington Test 7 has been redesigned using a fin (web side) plate connection in this chapter using Section VI of SCNZ (2008a) and Section 5 of SCI (2014) as a means for assessing the performance of the connections in fire. For the purpose of achieving clarity, the nomenclature for detailing follows those used in the New Zealand Connection Design Guide (SCNZ, 2008) as per Section 5 of this study, with the connection shown in Figure 2-5 reproduced below.

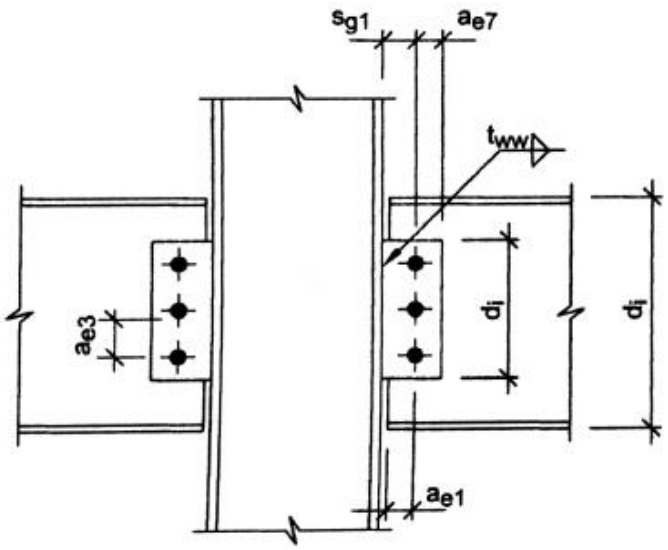

Figure 6-1 Fin plate connection (SCNZ, 2008a)

The design of the fin plate connections in accordance to the respectively design guides is shown in Table 6-1, where the designs utilise the minimum detailing criteria such as plate length and end distances of the respective design guides where possible. As a result, this allows for an accurate

representation of the minimum code requirements, in turn capturing the essence of the various design philosophies between the regions.

With the design of the fin plate connections highlighted in Table 6-1 and comprehensive design calculations shown in Appendix A, it is apparent that the differences in design between New Zealand and U.K. are seemingly minor considering the similarities in the geometries of the fin plate, size and number of bolts, and detailing requirements. Nonetheless considerable differences are present based on the varying design philosophies highlighted in Chapter 2, where the New Zealand design places a larger emphasis on the ductility of the connection. In this scenario for the design of web side plate connections, the main differences in addition to those discussed previously are as follows:

- SCI (2014) recommends the use of 10 mm thick fin plates for U.K. connections, whereas 8 mm thick fin plates are commonly used in New Zealand for similar applications.

- Following the respective design criteria and recommendations, the New Zealand connection utilises a bolt spacing of 65 mm and edge spacing of 35 mm. On the other hand, the U.K. design utilises a bolt spacing of 60 mm and edge spacing of 40 mm.

Table 6-1 Fin plate designs

Fin Plate Designs		
Design Guide	**NZ**	**Green Book (UK)**
Grade (MPa)	300	275
Plate Width (mm)	100	100
d_i (mm)	265	260
Plate Thickness (mm)	8	10
Number of Bolts	4	4
Grade	8.8	8.8
Bolt Diameter	M20	M20
Bolt Hole Diameter (mm)	22	22
a_{e1} (mm)	45	40
Bolt Spacing (mm)	65	60
a_{e7} (mm)	50	50
Ambient Temperature Design Factor: ϕR/R*		
Bolt Group Strength	1.3	1.5
Plate Strength	2.1	2.1
Section Web Strength	2.4	2.4
Bolt Bearing (Tear out)	1.1	2.0

Table 6-1 also shows the ambient temperature design factors for the various components of the connection using the two respective design guides. In regards to the design of bolts, the New Zealand connection considers a criteria for the flexural moment as a result of seismic forces (φM_b), calculated as a function of the shear capacity of the connection. As a result, this extra consideration incorporates an increased design requirement in the New Zealand design, hence resulting in a lower ambient temperature design factor of 1.2 compared the design factor of 1.5 of the U.K. connection. Therefore, as both designs utilise the same number and size of bolts with similar spacing, the discrepancy between the values highlights the differences in design philosophies, where the New Zealand design guide places greater priority on the strength of bolts.

With the connections being similar in geometry, the ambient temperature design factors for the web side plate connections using the New Zealand design proves to be analogous to their U.K. counterparts despite the differences in design philosophy highlighted in Chapter 2. With the corresponding calculations shown in Appendix A, it was determined that the limiting criteria for the web plate and beam web components of the connection for both the New Zealand and U.K. design are limited due to shear of the respective sections.

Considering the ambient design factors for bolt bearing in the web plate and beam web listed in Table 6-1, a significant difference exists between that determined by the respective New Zealand and U.K. design guides. This difference is a result of the contrasting approaches undertaken by the two design guides when determining the resistance provided by the components, where the U.K. design utilises a comprehensive equation which accounts for the bearing resistance of the bolts in both the horizontal and vertical directions based on the geometrical details of the connection as shown in Equation below, with detailed corresponding equations listed in SCI (2014):

$$V_{Rd} = \frac{n}{\sqrt{\left(\frac{1+\alpha n}{F_{b,ver,Rd}}\right)^2 + \left(\frac{1+\beta n}{F_{b,hor,Rd}}\right)^2}} \tag{6-1}$$

Where:

V_{Rd} = Bearing resistance of bolt group on web plate/beam web

n = Total number of bolts

α, β = Factors based on the detailing of the connection

$F_{b,ver,Rd}$ = Vertical bearing resistance of a single bolt

$F_{b,hor,Rd}$ = Horizontal bearing resistance of a single bolt

On the contrary, the New Zealand connection design guide offers a simplistic, generalised approach where the resistance of the web plate and beam web against bolt bearing is determined based on the lesser of the ultimate strength of the steel component through Equation (6-2) or the bearing capacity associated with plate tear out, given by NZS 3404 Equation 9.3.2.4(2) as reproduced in Equation (6-3) below, with further details listed in SCNZ (2008a):

$$\varphi V_b = \varphi_s 3.2\ t\ d_f\ f_u \tag{6-2}$$

Where:

V_b = Bearing resistance of bolt group on web plate/beam web

φ_s = Strength reduction factor for steel in bearing

t = Thickness of web plate/beam web

d_f = Bolt diameter

f_u = Ultimate strength of web plate/beam web

$$\varphi V_b = \varphi_s a_e t f_u \tag{6-3}$$

Where:

a_e = minimum distance from the edge of a hole to the edge of a ply, measured in the direction of the component of a force, plus half the bolt diameter (mm)

Typically for NZ connections, the bearing capacity associated with tear-out in Equation 6-2 governs.

Adopting the above equations for bearing resistance specified by the U.K. and New Zealand design guides respectively, it is calculated in Table 6-1 that the comprehensive equations set by the U.K.

design guide provides ambient temperature design factors which are significantly less conservative than those calculated using equations from the New Zealand design guide despite both connections incorporating similar beam and web plate dimensions. Subsequently, this further highlights the differences in connection design philosophies between the regions discussed in Chapter 2.4, as the relatively high design factors calculated using the New Zealand equations allow for the connection to experience higher stresses in bearing against the web plate and beam web – a desirable failure mode due to its ductile behaviour.

As a result, the comparison between the ambient temperature design factors for the connections designed in accordance with their respective design guides highlights the difference in philosophy outlined in Chapter 2, where it is demonstrated that the New Zealand connection design places a larger emphasis on the ductility of the connection by allowing for an increased capacity for bolt hole deformation through bearing and limiting brittle failure through bolts, opposed to the U.K. design which aims to allow deformation through the bolts as indicated by SCI (2014).

Notwithstanding the differences in design philosophies between the New Zealand and U.K. web plate connections, the connections detailed in accordance with their respective design guides in Table 6-1 indicate that the geometrical differences between the two connections are limited, with the largest notable difference being the variation in thickness and grade of the web plate. Based on the understanding of web plate connections as modelled in Chapter 3.1 and results previously determined in the flexible endplate simulations in Chapter 5, it is expected that the two web plate connections outlined in Table 6-1 would exhibit very similar behaviours when subject to the same loads in fire, with the New Zealand design likely to exhibit a marginal increase in ductility due to its use of a thinner web plate of higher grade. Therefore, due to the limited differences between the detailing of the New Zealand and U.K. web plate connections, this scenario has not been

examined in further detail in this study but is considered a high priority topic for further study, especially given the widespread use of this type of connection in New Zealand.

7 Conclusions and Recommendations

It has been established that maintaining the structural integrity of steel connections during and after fire scenarios is paramount for the overall survivability of a building as evidenced by past incidents. As a result, this study was undertaken with the main objective of examining the behaviour of New Zealand steel connections in fire. New Zealand steel connections were shown to differ from their European counterparts based on differences in design philosophies between the regions, leading to the local requirements including considerations for design against earthquake loads.

In particular, this study focused on the simple steel connections – flexible endplates and web side plates, in which the finite element modelling software, ABAQUS, was used to model their behaviour. This study first analysed and modelled the behaviour of connections undertaken in previous experimental studies, in particular, an isolated web side plate connection and subsequently a flexible endplate connection from a Cardington test. The connection in the Cardington test was then redesigned using current procedures from New Zealand and the U.K. and analysed in order to determine their relative behaviours in fire conditions.

7.1 Conclusions

From the set of analytical studies reported herein, the main findings can be summarised as follows:

- Experimental tests involving isolated connections at steady state temperatures do not provide a realistic representation of the behaviours of the same connections in real structures under fire scenarios, as isolated connections do not account for the large axial forces resulting from the thermal elongation and contraction of a full length beam with end restraints. Additionally, the material properties of steel at steady state temperatures vary

significantly to those at transient temperatures as a result of the large influence by the applied strain rate.

- The flexible endplate connection of Cardington Test 7 first experienced failure at the base of the endplate during the cooling phase, which then propagated upwards along its centre upon further cooling of the overall assembly. The endplate is expected to have failed along its depth at the time of approximately 94 minutes after the commencement of the experiment.
- The contrasting design philosophies and preferred failure mechanisms in connections between New Zealand and the U.K. leads to differences in calculated tolerances of various failure modes and subsequently, the detailing of the connections.
- Flexible endplate connections designed to the current New Zealand and U.K. recommendations were demonstrated to largely be able to maintain structural integrity when exposed to the Cardington Test conditions. However, increased ductility of the New Zealand design allowed it to perform better by remaining completely within its plastic limit throughout the analysis compared to the U.K. connection which surpassed its limiting plastic strain at the base of the endplate.
- The differences in ductility between the New Zealand and U.K. flexible endplate connections are based on a combination of factors including: grade of steel, thickness and length of the endplate, and bolt spacing.
- The geometrical differences between the web side plate connections designed in accordance with the New Zealand and U.K. design recommendations were determined to be relatively minimal, despite differences in allowable failure mechanisms, however the New Zealand connections are designed and detailed to allow dependable bolt hole

elongation under high rotational demands at ambient temperature which may improve their fire resistance. Detailed FEM of these connections has been beyond the scope of this study but is recommended as a future research priority. .

7.2 Recommendations for Further Research

The following areas are recommended for furthering research on the behavior of connections in fire conditions:

- Given that this work was limited to studying the behaviour of connections in the Cardington test conditions, further work should implement varying structural assemblies to determine their influence on the overall behaviour of connections.
- Model a wider library of connections to compare the advantages and disadvantages of various designs, with a priority focus on the WP connections.
- Larger portions of the structural frame should be studied in order to consider the effects of mechanisms such as tensile membrane action and column shortening
- The findings on the behaviour of New Zealand steel connections in fire should be validated by experimental testing in future studies
- To facilitate the use of this information in the industry, the development of component based models which represent the behaviour of New Zealand connections in fire should be investigated
- Undertake finite element modelling with increased details of the subassembly, including the influence of a full-length column and reinforcement within the concrete slab

8 References

ABAQUS. (2014a). Getting Started with ABAQUS, Hibbitt, Karlsson and Sorensen, Inc.

ABAQUS. (2014b). Standard user's manual. Hibbitt, Karlsson and Sorensen, Inc.

ABAQUS. (2014c). Theory Guide. Hibbitt, Karlsson and Sorensen, Inc.

Al-Jabri, K. S. (1999). The Behaviour of Steel and Composite Beam-To-Column Connections In Fire, PhD. Thesis, Department of Civil and Structural Engineering, University of Sheffield.

Al-Jabri, K. S., Davison, J. B., & Burgess, I. W. (2007). Performance of beam-to-column joints in fire—A review. Fire Safety Journal, 43(1), 50-62. doi: http://dx.doi.org/10.1016/j.firesaf.2007.01.002

Bednář, J., Wald, F., Vodička, J., & Kohoutková, A. (2012). Membrane Action of Composite Fibre Concrete Slab in Fire. Procedia Engineering, 40(Supplement C), 498-503. doi: https://doi.org/10.1016/j.proeng.2012.07.132

Block, F. M. (2006). Development of a Component-based Connection Element for Steel beam-to-Column Connections at Elevated Temperatures. PhD Thesis. University of Sheffield.

Booth, E., Lane, J., Ko, R., & MacKenzie, D. (1998). Overview of Earthquake Design and Development of UK NA for EN 1998-2 and PD 6698 Bridge Design to Eurocodes (pp. 183-191).

Borges, L. (2003). Structural Integrity Fire Test in Cardington - BRE Hanger II. Retrieved from http://www.dec.uc.pt/~lborges/cardington/

BRE. (2004). Client Report: Results and observations from full-scale fire test at BRE Cardington, 16 January 2003

British Standards Institution. (2003). Structural use of steelwork in building: code of practice for fire resistant design. London: British Standards Institution.

British Steel. (1982). The performance of beam/column/beam connections in the BS476: Art 8 fire test

Buchanan, A. H., & Abu, A. K. (2017). Structural Design for Fire Safety (2nd ed.): Wiley.

Bursi, O. S., & Jaspart, J. P. (1998). Basic issues in the finite element simulation of extended end plate connections. Computers & Structures, 69(3), 361-382. doi: http://dx.doi.org/10.1016/S0045-7949(98)00136-9

Butterworth, J. W. (1995). Inelastic Rotational Capacity of Grade 300 and Grade 350 Columns, School of Engineering Report Number 554. Department of Civil and Resource Engineering, University of Auckland, New Zealand.

Centre Technique Industriel de la Construction Métallique. (1982). Methode de Prevision par le Calcul du Comportement au Feu des Structures en Acier. Construction Metallique, 19(3), 39-79.

Charlier, R., & Habraken, A. M. (1990). Numerical metallisation of contact phenomena by finite element method. Comput. Geotech, 9, 59-72.

Clifton, G. C. (1994). New Zealand Structural Steelwork Limit State Design Guides

Clifton, G. C. (1995). Lessons to be Learned for New Zealand Structural Steel Design and Detailing Practice from the 1994 Northridge Earthquake; Proceedings of the NZNSEE Conference, Rotorua, New Zealand. New Zealand National Society for Earthquake Engineering.

Dai, X. H., Wang, Y. C., & Bailey, C. G. (2010). Numerical modelling of structural fire behaviour of restrained steel beam–column assemblies using typical joint types.

Engineering Structures, 32(8), 2337-2351. doi: http://dx.doi.org/10.1016/j.engstruct.2010.04.009

Dowling, J. (1997). Fire Protection Using Off-Site Applied Intumescent Coatings. Proc. Intn Civ. Engrs Structs & Bldgs, 112, 237 - 238.

El-Rimawi, J. A. (1989). The Behaviour of Flexural Members under Fire Conditions, PhD. Thesis, Department of Civil and Structural Engineering, University of Sheffield.

European Committee for Standardization. (2002). Eurocode 1: Actions on structures, Part 1.2: General actions - Actions on structures exposed to fire. U.K.: British Standards Institution.

European Committee for Standardization. (2004a). Eurocode 2: Design of concrete structures, Part 1.2:, General rules- structural fire design. U.K.: British Standards Institution.

European Committee for Standardization. (2004b). Eurocode 3: Design of steel structures, Part 1.8:, Design of Joints. U.K.: British Standards Institution.

European Committee for Standardization. (2005a). Eurocode 3: Design of steel structures, Part 1.2:, General rules- structural fire design. U.K.: British Standards Institution.

European Committee for Standardization. (2005b). Eurocode 4: Design of composite steel and concrete structures, Part 1.2:, General rules- structural fire design. U.K.: British Standards Institution.

European Committee for Standardization. (2006). Eurocode 1 - Actions of structures, Part 1.7:, General rules- Accidental actions. U.K.: British Standards Institution.

Feeney, M. J., & Clifton, G. C. (1995). Seismic Design Procedures for Steel Structures

FEMA. (2002). World Trade Center Building Performance Study: Data Collection, Prelimnary Observations, and REcommendations

Franssen, J. M. (2005). A Thermal/Structural Program Modelling Structures under Fire. Engineering Journal, A.I.S.C., 42(3), 143-158.

Gillie, M., Usmani, A., Rotter, M., & O'Connor, M. (2001). Modelling of heated composite floor slabs with reference to the Cardington experiments. Fire Safety Journal, 36(8), 745-767.

Gillie, M., Usmani, A. S., & Rotter, J. M. (2001). A structural analysis of the first Cardington test. Journal of Constructional Steel Research, 57(6), 581-601. doi: http://dx.doi.org/10.1016/S0143-974X(01)00004-9

Hu, Y. (2009). Robustness of flexible endplate connections under fire conditions. University of Sheffield, Sheffield, U.K.

Hu, Y., Burgess, I. W., Davison, B., & Plank, R. (2008). Modelling of flexible end plate connections in fire using cohesive elements. Fifth International Workshop, Structures in Fire.

Huang, Z., Burgess, I. W., & Plank, R. J. (1999). Nonlinear analysis of reinforced concrete slabs subjected to fire. ACI Structural journal, 96(1), 127-135.

Huang, Z., Burgess, I. W., & Plank, R. J. (2004). Fire Resistance of Composite Floors Subject to Compartment Fires. J. Construct. Steel Research, 60(2), 339-360.

Hyland, C. (2003). Flexible End Plate & Angle Cleat Connections. Steel Structures Seminar 2003.

Ingham, J. M., & Griffith, M. C. (2011). The Performance of Unreinforced Masonry Buildings in the 2010/201 Canterbury Earthquake Swarm

ISO. (1975). Fire Resistance Tests – Elements of Building Construction ISO 834: International Organisation for Standardisation.

IStructE. (2002). Safety in tall buildings and other buildings with large occupancy. The Institution of Structural Engineers, London, United Kingdom.

Kirby, B. R. (1995). The behaviour of high-strength grade 8.8 bolts in fire . J. Construct. Steel Research, 3(38).

Kirby, B. R., & Preston, R. R. (1988). High temperature properties of hot-rolled structural steels for use in fire engineering desgin studies. Fire Safety Hournal, 13, 27-37.

Krishnamurthy, N., & Graddy, D. E. (1976). Correlation between 2- and 3-Dimensional Finite Element Analysis of Steel Bolted End-Plate Connections. Computers and Structures, 6, 381-389.

Kruppa, J. (1976). Resistance en feu des assemblages par boulons haute resistance

Kukreti, A. R., Murray, T. M., & Abolmaali, A. (1987a). End plate connection moment-rotation relationship. Journal of Constructional Steel Research, 8, 137-157.

Kukreti, A. R., Murray, T. M., & Abolmaali, A. (1987b). End-plate connection moment-rotation relationship. Journal of Constructional Steel Research, 8, 137-157. doi: http://dx.doi.org/10.1016/0143-974X(87)90057-5

LaMalva, K. J. (2007). Failure Analysis of The World Trade Center 5 Building, Masters Thesis. Worcester Polytechnic Institute.

Lawson, R. M. (1990). Behaviour of steel-beam-to-column connections in fire. The Structural Engineer, 68(14), 263-271.

Lennon, T., & Moore, D. (2004). Client Report: Results and Observations from Full-Scale Fire Test at BRE Cardington, Client report number 215-741.

Lim, L., & Feeney, M. (2015). The application of advanced finite element analysis for structural fire design.

Lin, S. (2014). Development of Robust Connection Models For Steel and Composite Structures in Fire. PhD. Thesis, Department of Mechanical, Aerospace and Civil Engineering, Brunel University.

Liu, T. C. H. (1996). Finite element modelling of behaviours of steel beams and connections in fire. Journal of Constructional Steel Research, 36(3), 181-199. doi: http://dx.doi.org/10.1016/0143-974X(95)00016-O

Liu, T. C. H., Fahad, M. K., & Davies, J. M. (2002). Experimental investigation of behaviour of axially restrained steel beams in fire. Journal of Constructional Steel Research, 58(9), 1211-1230. doi: https://doi.org/10.1016/S0143-974X(01)00062-1

Mago, N., Hicks, S., & Simms, W. I. (2014). Sequentially coupled thermal-stress analysis of a new steelconcrete composite slab under fire. 2014 SIMULIA Customer Conference Proceedings.

MBIE. (2016). Acceptable Solutions and Verification Methods For New Zealand Building Code Cluase B1 Structure

Moss, P. J., & Charles Clifton, G. (2004). Modelling of the Cardington LBTF steel frame building fire tests. Fire and Materials, 28(2-4), 177-198. doi: 10.1002/fam.868

Murray, C. M., & Butterworth, J. W. (1990). Inelastic Rotational Capacity of Ductile Web Side Plate Connections, Hera Project 88/R6. University of Auckland, New Zealand.

New Zealand Standards Institute. (1935). NZS No. 95:1935, Model building By-Law, New Zealand Standards Institute, Wellington, New Zealand.

New Zealand Standards Institute. (1976). NZS 4203: Code of Practice for General Structural Design and Design loadings for buildings,, New Zealand Standards Institute, Wellington, New Zealand.

New Zealand Standards Institute. (1989). NZS 3404: Steel Structures Standard. New Zealand Standards Institute, Wellington, New Zealand.

New Zealand Standards Institute. (1997). NZS 3404: Steel Structures Standard. New Zealand Standards Institute, Wellington, New Zealand.

New Zealand Standards Institute. (2017). AS/NZS 2327:2016. Composite Structures - Composite steel-concrete construction in buildings. New Zealand Standards Institute, Wellington, New Zealand.

NIST. (2008). Final Report on the Collapse of World Trade Center Building 7

Priestley, M. J. N. (1993). Myths and Fallacies in Earthquake Engineering - Conflicts between Design and Reality. Bulletin of the New Zealand National Society for Earthquake Engineering, 26(3).

Proe, D. J., Bennetts, I. D., & Thomas, I. R. (1986). Simulation of the Fire Testing Structural Steel Elements by Calculation-Mechanical Response. Steel Construction, 19(4), 2-18.

Renner, A. (2005). The effect of strain-rate on the elevated-temeprature behaviour of structural steel. Research Dissertation. University of Sheffield.

Robinson, J. (1998). Fire - A Technical Challenge and A Market Opportunity. J. Construct. Steel Res, 46(1-3).

Robinson, T. R. (2014). Assessment of coseismic landsliding from an Alpine fault earthquake scenario, New Zealand. Doctoral Thesis, University of Canterbury.

Sabol, T. A., & Engelhardt, M. D. (1994). Steel Moment-Resisting Frame Connection Details and Geometry - A Discussion of Fundamental Issues. Proceedings of the Invitational Workshop on Steel Seismic Issues SAC 94-01, Los Angeles, California. Paper presented

at the Proceedings of the Invitational Workshop on Steel Seismic Issues SAC 94-01, Los Angeles, California.

Sarraj, M., Burgess, I. W., Davison, J. B., & Plank, R. J. (2007). Finite element modelling of steel fin plate connections in fire. Fire Safety Journal, 42(6–7), 408-415. doi: http://dx.doi.org/10.1016/j.firesaf.2007.01.007

Sarraj, M. (2007). The behaviour of steel fin plate connections in fire, PhD. Thesis, Department of Civil and Structural Engineering, University of Sheffield.

SCI. (1991). Investigation of Broadgate Phase 8 Fire

SCI. (2013). Joints in Steel Construction: Moment-Resisting Joints to Eurocode 3

SCI. (2014). Joints in Steel Construction: Simple Joints to Eurocode 3

SCNZ. (2008a). SCNZ 14.1: 2007 Structural Steelwork Connections Guide: Design Procedures

SCNZ. (2008b). SCNZ 14.2: 2007 Structural Steelwork Connections Guide: Connection Tables

Selamet, S., & Bolukbas, C. (2016). Fire resilience of shear connections in a composite floor: Numerical investigation. Fire Safety Journal, 81, 97-108. doi: http://dx.doi.org/10.1016/j.firesaf.2016.02.003

Selamet, S., & Garlock, M. E. (2014). Fire resistance of steel shear connections. Fire Safety Journal, 68, 52-60. doi: http://dx.doi.org/10.1016/j.firesaf.2014.05.016

Shepherd, P. G., & Burgess, I. W. (2011). On the buckling of axially restrained steel columns in fire. Engineering Structures, 33(10), 2832-2838. doi: https://doi.org/10.1016/j.engstruct.2011.06.007

Simões da Silva, L., & Santiago, A. (2005). Behaviour of steel joints under fire loading. Steel and Composite Structures, 5(6), 485-513.

Starossek, U. (2007). Typology of progressive collapse. Engineering Structures, 29(9), 2302-2207.

Steel Construction Institute. (1991). Investigation of Broadgate Phase 8 Fire. Structural Fire Engineering.

Sulong, N. H. R. (2005). Behaviour of Steel Connections Under Fire Conditions. Impreial College London.

Vegte, G. J. v. d. (2004). Numerical simulations of bolted connection: The implicit versus the explicit approach. Paper presented at the Connections in Steel Structures V, Amsterdam.

Wald, F., Simões da Silva, L., Moore, D., Lennon, T., Chladná, M., Santiago, A., Beneš, M., & Borges, L. (2005). Experimental behaviour of steel structure under natural fire. New Steel Construction, 13(3), 24-27.

Wang. Y., (2002). Steel and Composite Structures - Behaviour and Design for Fire Safety. London: Spon Press.

Wang, Y., Burgess, I., Wald, F., & Gillie, M. (2013). Performance-Based Fire Engineering of Structures. Boca Raton, Florida, U.S.A.: CRC Press.

Wang, Y., Burgess, I. W., Wald, F., & Gillie, M. (2012). Steel and composite joints Performance-Based Fire Engineering of Structures (pp. 233-276): CRC Press.

Wang, Y., Davison, J. B., Plank, R. J., Yu, H. X. D., X.H., , & Bailey, C. G. (2010). The safety of comon steel beam/column connectoins in fire. The Structural Engineer, 88(21).

Wang, Y. C., Dai, X. H., & Bailey, C. G. (2011). An experimental study of relative structural fire behaviour and robustness of different types of steel joint in restrained steel frames. Journal of Constructional Steel Research, 67(7), 1149-1163. doi: https://doi.org/10.1016/j.jcsr.2011.02.008

Welch, S., Jowsey, A., Deeny, S., Morgan, R., & Torero, J. L. (2007). BRE large compartment fire tests—Characterising post-flashover fires for model validation. Fire Safety Journal, 42(8), 548-567. doi: https://doi.org/10.1016/j.firesaf.2007.04.002

Yu, H.,, Burgess, I. W., Davison, J. B., & Plank, R. J. (2009a). Experimental investigation of the behaviour of fin plate connections in fire. Journal of Constructional Steel Research, 65(3), 723-736. doi: http://dx.doi.org/10.1016/j.jcsr.2008.02.015

Yu, H., Burgess, I. W., Davison, J. B., & Plank, R. J. (2009b). Tying capacity of web cleat connections in fire, Part 1: Test and finite element simulation. Engineering Structures, 31(3), 651-663. doi: http://dx.doi.org/10.1016/j.engstruct.2008.11.005

Yu, H., Burgess, I. W., Davison, J. B., & Plank, R. J. (2008). Numerical simulation of bolted steel connections in fire using explicit dynamic analysis. Journal of Constructional Steel Research, 64(5), 515-525. doi: http://dx.doi.org/10.1016/j.jcsr.2007.10.009

Yu, H., Burgess, I. W., Davison, J. B., & Plank, R. J. (2011). Experimental and Numerical Investigations of the Behavior of Flush End Plate Connections at Elevated Temperatures. Journal of Structural Engineering, 137(1), 80-87. doi: doi:10.1061/(ASCE)ST.1943-541X.0000277

Yu, H., Burgress, I. W., Davison, J. B., & R.J., P. (2008). Experimental investigation of the behaviour of flush endplate connections in fire. Paper presented at the Structures in Fire, 2008.

Appendix A – Flexible Endplate Calculations

FE1 – New Zealand Design (SCNZ, 2008a)

Design Forces: V* = 147 kN [0.3 x Shear Capacity of Connecting Beam (NZS3404)

					φR/R*
Bolt Group Strength Limits					
φV_b	=	740.8	Transverse shear	OK	5.0
Flexible End Plate Design Strength Limits					
φV_{bi}	=	1622.016	Bolt hole tranverse bearing	OK	11.0
φV_{tti}	=	1013.76	Bolt Hold transverse tearing	OK	6.9
φV_{gsi}	=	599.04	Gross shear yield	OK	4.1
φV_{bsi}	(max)	728.64 681.8688	Block shear of endplate	OK	5.0 4.6
Section Design Strength Limits					
φV_{wc}	=	420.146494	Web shear/Tension at top of cleat	OK	2.9
φV_{bsw}	(min)	404.1576 450.34704	Block Shear in Web	OK	2.7 3.1
φV_{gsw}	=	490.50036	Gross shear yield at top notch	OK	3.3
Support Design Strength Limits					
φV_{bsup}	=	1612.43136	bolt hole 1st bearing	OK	11.0
φV_{tsup}	=	1234.51776	bolt hole 1st tearing	OK	8.4

FE4 – U.K. Design (SCI, 2014)

Design Forces: V* = 146 kN

F_{ed} (BS EN 1991-1-7) = 233 kN

Bolt Strength Limits					**φR/R***
Shear of bolts $F_{v,RD}$	=	94			
Bearing endplate $F_{b,Rd}$	=	84			
If Fb,RD < 0.8 Fv,RD then FRd=nFb, RD If Fb,Rd > 0.8 Fv, Rd then FRd=0.8n(Fv,Rd)					
F_{Rd}=0.8n($F_{v,Rd}$)	=	602	kN	OK	4.1
Endplate Shear					
Gross Section $V_{Rd,\ g}$	=	725	kN	OK	5.0
Net section $V_{Rd,n}$	=	956	kN	OK	6.6
Block Tearing	=	691	kN	OK	4.7
Tying Resistance - Plate and Bolts					
Mode 1 - Yielding endplate $F_{RD,u,1}$	=	378	kN	OK	1.6
Mode 2 - Bolt Fail with yielding endplate	=	380	kN	OK	1.6
Mode3 - Bolt fail					
$F_{t,Rd,u}$	=	160			
$F_{rd,u,3}$	=	1282	kN	OK	5.5
Tying Resistance - Supported beam web					
$F_{Rd,u}$	=	917	kN	OK	3.9

Appendix B – Web Side Plate Calculations

New Zealand Design (SCNZ, 2008a)

Design Forces: V* = 147 kN [0.3 x Shear Capacity of Connecting Beam (NZS3404)

Bolt Group Strength						**φR/R***
φV_b	=	379	kN	Shear at eccentricity e	OK	2.6
φMb	=	28	kN	Seismic moment	OK	1.3
Web Plate Strength Limits						
φVbi	=	203	kN	Bolt hole 1st resultant bearing	OK	1.4
φV_{tti}	=	159	kN	Bolt hole 1st transverse tearing	OK	1.1
φVlti	=	686	kN	Bolt hole 1st longitudinal tearing	OK	4.7
φVgfi	=	809	kN	Cleat gross flexure yield	OK	5.5
φVnfi	=	632	kN	Cleat net flexure ultimate	OK	4.3
φVgsi	=	305	kN	Cleat gross shear yield	OK	2.1
φVnsi	=	336	kN	Cleat net shear ultimate	OK	2.3
Section Web Strength Limits						
φVbw	=	580	kN	Bolt hole 1st resultant bearing	OK	3.9
φVttw	=	802	kN	Bolt hole 1st transverse tearing	OK	5.4
φVltw	=	468	kN	Bolt hole 1st longitudinal tearing	OK	3.2
φVgsw	=	358	kN	Gross shear yield	OK	2.4

U.K. Design (SCI, 2014)

Design Forces: V* = 146 kN

F_{ed} (BS EN 1991-1-7) = 233 kN

					φR/R*
Bolt Shear					
$F_{V,RD}$	=	94	kN		
VD	=	219	kN	OK	1.5
Bolt bearing in fin plate					
V_{Rd}	=	265	kN	OK	1.8
Bolt bearing in supported beam web					
V_{Rd}	=	285	kN	OK	2.0
Supported beam - Fin plate					
Gross section shear					
$\mathbf{V_{RD,g}}$	=	325	kN	OK	2.2
Net section					
$\mathbf{V_{RD,n}}$	=	370	kN	OK	2.5
Block Shear					
$\mathbf{V_{Rd,b}}$	=	300	kN	OK	2.1
Bending					
$\mathbf{V_{Rd}}$	=	443	kN	OK	3.0
Lateral torsional buckling, short fin plate z<tp/0.15					
$\mathbf{V_{Rd}}$	=	443	kN	OK	3.0
Check 4 Supported beam - Web in shear					
$\mathbf{V_{pd,RD\ Gross\ section}}$	=	345	kN	OK	2.4
$\mathbf{V_{Rd,n\ Net\ Section}}$	=	1064	kN	OK	7.3
$\mathbf{M_{c,BC,Rd}+ V_{pl,AB,Rd(n1-1)p1}}$					
Resistance at Connection (M*)	=	27	kN	OK	3.1

Structural Integrity - Plate and Bolts **Tension Resistance of fin plate**					
$F_{Rd,b}$ Case 1	=	549	kN	OK	3.8
$F_{Rd,b}$ Case 2	=	738	kN	OK	5.1
Bolt Shear					
$F_{Rd.u}$	=	427	kN	OK	2.9
Bolt bearing in fin plate					
$F_{Rd,u}$	=	452	kN	OK	3.1
Structural integrity - supported beam web **Tension resistance of beam web**					
$F_{Rd,b}$ Case 1	=	470	kN	OK	3.2
$F_{Rd,b}$ Case 2	=	623	kN	OK	4.3
Bolt Bearing in beam web					
$F_{Rd,u}$	=	378	kN	OK	2.6